

Controlling morphology-structure of particles at different pulse rate, polarity and effect of photons on structure

Mubarak Ali^{1, *} and I-Nan Lin²

¹Department of Physics, COMSATS Institute of Information Technology, Islamabad 45550, Pakistan. *E-mail: mubarak74@comsats.edu.pk, mubarak74@mail.com

²Department of Physics, Tamkang University, Tamsui Dist., New Taipei City 25137, Taiwan (R.O.C.)

Abstract –Controlling morphology-structure of metallic colloids is an unusual phenomenon. Here, various shape-structure of colloidal particles are synthesized and are investigated for different process parameters. At solution surface, different tiny shaped particles of gold are developed where packets of nano shape energy converted monolayer assembly into their own shape depending on the ratio of bipolar pulse OFF to ON time. Tiny particles of joint triangular shape developed under the certain bipolar pulse time and are separated by themselves on exerting force of surface format at their perturbed axis between the points of connection. However, under unipolar pulse, triangular-shaped tiny particles developed directly as the placed packets of nano shape energy were in single triangle. Atoms of one-dimensional arrays of various tiny particles elongate as per available force where their developed structure of smooth elements deal dominating force at tip resulting into pack at common centre to develop particles of various anisotropy and geometry. When the ratio of bipolar pulse OFF to ON time is very large, the resulting particles are distorted while those developed at smaller values of this ratio reveal geometric anisotropic shapes. When the ratio of bipolar pulse OFF to ON time is 3, resulted particles reveal low aspect ratio to those developed at the inverse value of this ratio. At longer pulse ON time, tiny particles developed in structure of smooth elements having width less than inter-spacing distance where increased density of travelling photons at interface better align electrons of non-orientational stretching of

clamping energy knots in their atoms. When elongated atoms of tiny particles misaligned at an extended level, stretched energy knots clamped electrons which couldn't recover under the forcing energies of travelling photons where their structure is messed up. Shape-structure of particles is discussed.

Keywords: Pulse polarity; Nano shape energy; Triangular-shaped tiny particles; Morphology-structure; Geometric and distorted particles

Introduction:

New strategies in terms of material synthesis and designation process are prerequisite for obtaining the performance of materials in multi-dimensions and in diverse areas. Determining the performance of a material on the basis of understanding atomic structure is highly desirable. To design material at nanoscale for getting specific benefits has been the prime objective of scientific community. Controlling and understanding the atoms to design specific role and then investigating the effects of photons on the formation of their configurations are the challenges being faced today. Yet again, controlling the size and shape of metallic colloids is a hot topic. To structural matter, on length scale comparable or smaller to the subwavelength of light can deliver phenomenal optical properties [1, 2]. For catalytic applications, tiny metallic colloids have great potential [3, 4] owing to the enhanced performance as compared to the bulk [5, 6].

Several reports and articles are available in the literature explaining nanoparticles and particles in a variety of materials synthesized by various routes and some of the studies discussed the development mechanisms along with the implications on future technologies [7-17]. A tiny cluster behaves like a simple chemical compound and may find important applications in diverse areas [7]. Due to specific features of nanocrystals, they provide options to assemble into various materials, thus, providing opportunities to have better characteristics [8]. Ordered configurations of nanoparticles may give different properties to particles formed through their agglomeration [9]. The practical goal of nanocrystals is their coalescence [10]. Specific structure means to design a self-assembly [11]. Development of small devices is the long-term goal of nanoparticle

technology [12]. In the beginning, attempts should be to assemble the nanoparticles [13]. To organize tiny particles into specific structures is one of the recent challenges [14]. By having successful assembling of tiny particles, atoms and molecules will be materials of tomorrow [15]. A controlled assembly among nanoparticles will lead into the development of complex shapes [16]. A successful coalescence of nanocrystals will provide abundant options to synthesize materials having controlled features [17]. In several published studies, special emphasis remained on the size and shape of particles. It is challenging to be benefited by characteristics of nanoparticles in various catalytic, sensing and optoelectronic devices [18, 19] and specific geometry of particles can be a better choice for promising applications in waveguides [20-24]. Upto certain number of atoms, tiny particles form hcp structures and chemical properties of gold nanoparticles change with size [25, 26]. Geometry and entropy should also be used to explain structure and dynamics [27], and besides disordered jammed configuration, there are also ordered metrics which characterize the packing order [28].

Plasma solution processing technologies under various configurations have been employed for the synthesis of metallic colloids [29-35]. The gold nanoparticles are synthesized by employing plasma in contact to solution [35]. The fundamental process of formation of different gold tiny particles has been discussed elsewhere [36] and the process of formation of carbon tiny grains is also discussed [37, 38]. Developing various gold particles under varying precursor concentration are discussed elsewhere [39], formation of different tiny particles and particles while processing different precursors are also discussed [40] where nature of the precursor takes the edge in developing a tiny shaped particle. The mechanism of adjacent placement of electrons in atoms and their tiny particles has been discussed elsewhere [41]. A detailed study presented on formation of triangular shape monolayer tiny particle along with elongation behavior of atoms where converting structure to structure of smooth elements has been discussed [42]. Different mechanisms of binding atoms based on electron-dynamics in structure evolution of their different formats have been discussed elsewhere [43]. Atoms of electronic transition do not ionize, they either elongate or deform, whereas, inert gas atoms split under the application of photonic current [44]. Revealing the phenomena of

heat energy and photon energy on dealing matter at atomic level has been discussed elsewhere [45]. The different nature of atoms along with transition behaviors of state has been discussed elsewhere [46]. As it is critical to maintain nature of certain atoms in different environment and use of their tiny-sized particles as nanomedicine is to be in more planned ways [47].

The present work deals development of nanoparticles and particles of various shapes and structure under varying the ratios of bipolar pulse OFF to ON time. Different particles were also developed under unipolar pulse mode. This provides opportunities to obtain required properties of those on demand. This is the first ever study which reports the altering of morphology-structure of nanoparticles and particles under controlled varying process conditions. This study shows experimentally that all structural motifs of tiny particles, nanoparticles and particles are due to certain force-energy behaviors.

Materials and Method:

Gold (III) chloride trihydrate was purchased from Alfa Aesar and after mixing in DI water, different concentrations of solution were prepared. Symmetric-bipolar pulse mode was employed and was generated by the pulse DC power controller (SPIK2000A-20 MELEC GmbH Germany). A controlled pulse ON/OFF time was set while processing solution of each molar concentration. Different equal/unequal pulse ON/OFF times were chosen as given in Table S1 and Table S2 along with current and voltage, which were measured in ampere and volts, respectively. Two different precursor concentrations were chosen i.e., 0.20 mM and 0.40 mM. Total amount of solution prepared in each experiment was 100 ml. The set duration of each experiment was 20 minutes. Distance between the copper tube and graphite rod was set ~5 cm where amount of precursor concentration in each experiment was 0.40 mM (Figure S14a), whereas, distance between graphite rod and copper tube was set ~8 cm where the amount of precursor concentration in each experiment was 0.20 mM (Figure S14b). In planned set of experiments, temperature of the solution was recorded from the distance of one meter and for that purpose LASER-guided meter (CENTER, 350 Series) was used. Temperature of the solution at the start of process was ~22°C while it reached close to

50°C depending on the set pulse ON/OFF time. Further detail of the setup is given elsewhere [39]. To study the effect of pulse polarity, different solutions were also prepared to process for 15 minutes time duration where precursor concentration in each experiment was 0.30 mM. Approximate recorded values of voltage and current were 28 and 1.46, respectively, whereas, in the case of unipolar pulse polarity (a negative pulse polarity and a positive pulse polarity) approximate voltage and current values were recorded 18 and 1.46, respectively. In these three experiments, pulse ON/OFF time was set 10 μ sec in both unipolar pulse mode and bipolar pulse mode while other process parameters were kept constant as it is in the case of solutions processed for precursor concentrations 0.20 mM and 0.40 mM. Step-up transformer enhanced the running voltage approximately upto 40 times in each time of the processing solution. After processing solution in each experiment, a drop was poured on copper grid coated by carbon film and samples were placed in Photoplate degasser (JEOL EM-DSC30) for 24 hours to eliminate moisture. Bright field images of various gold nanoparticles and particles were taken by the transmission microscope known as TEM while high resolution images by high resolution transmission microscope known as HR-TEM (JEOL JEM2100F; operated at 200 kV). Structural information was captured by selected area photon reflection (SAPR) known as SAED.

Results and discussion:

Under the tuned input power where high density of photons characteristic current propagated through graphite rod (known as anode) transformed into energy on entering in solution where dissociated the gold atoms from precursor as discussed elsewhere [48]; the forcing energy of photons under set pulse ON/OFF time entering from bottom of copper capillary (known as cathode) uplifted atoms to solution surface under their reaction of entrance in solution. Uplifted atoms under suitable concentration of their precursor develop monolayer assembly around the light glow if the ratio of pulse OFF to ON time is appropriate. The placement of packets of nano shape energy over the assembly of gold atoms resulting into bind them when dealing certain transition state are discussed elsewhere [42].

At appropriate bipolar pulse OFF to ON time, the assembly of compact monolayer at solution surface developed tiny particles having shape-like joint triangles in each case as shown in Figure 1. Such tiny particles developed under the appropriate ratio of bipolar pulse OFF to ON time as controlling the dynamics of atoms for configuring their compact monolayer assembly at solution surface. Therefore, placing double-packets of nano shape energy utilized the gold atoms of monolayer assembly to isolate into tiny particles having shape identical to them. Under suitable bipolar pulse ON/OFF time, the shape of each packet of nano shape energy is in the shape of two joint triangles, thus, while placing over the surface of monolayer assembly of certain transition state gold atoms, they result into develop tiny particle of monolayer. Figure 1 (a) explains the formation mechanism of tiny particles developing in different geometric shapes depending on the ratio of bipolar pulse OFF to ON time; when the ratio of pulse OFF to ON time was very large, a large number of tiny particles were developed in ellipse, circle or triangle shape other than equilateral (a_1), and when this ratio was smaller (but greater than unity), many tiny particles were developed in the shape of two joint triangles for each case having low aspect ratio (a_2), and when this ratio was unity, many tiny particles were developed in the shape of two joint triangles for each case having moderate aspect ratio (a_3). At smaller value than the unity ratio (when pulse ON time was larger than pulse OFF time), many tiny particles were developed in the shape of two joint triangles for each case having very high aspect ratio as shown in Figure 1 (a_4).

Tiny particles of triangle shape were also developed under unipolar pulse mode where unity ratio of pulse OFF to ON time was chosen as shown in Figure 1 (b), however, the amount of precursor concentration in those experiments was 0.3 mM (instead of 0.4 mM), whereas, the processing time of each quantity of solution was 15 minutes; in unipolar pulse polarity when it is termed negative, the equilateral triangular-shaped tiny particles were developed directly as shown in Figure 1 (b_1). Again, under unipolar pulse polarity when it is termed positive, the similar shaped tiny particles were developed directly as shown in Figure 1 (b_2). When bipolar pulse polarity for unit ratio of pulse OFF to ON time under the same conditions of the process was employed as in the case of unipolar pulse modes, tiny particles were again developed in equilateral

triangle shape as shown in Figure 1 (b₃), but each tiny particle is again in the shape of two joint triangles as for the case of tiny particles developed in Figure 1 (a). In the case of certain ratio of bipolar pulse OFF to ON time where tiny particles developed in two joint triangles, they separated into two for each case while exerting the force of perturbed axis at the point of connection. Further detail of the mechanism of separation of jointly developed triangular-shaped tiny particles is discussed elsewhere [42].

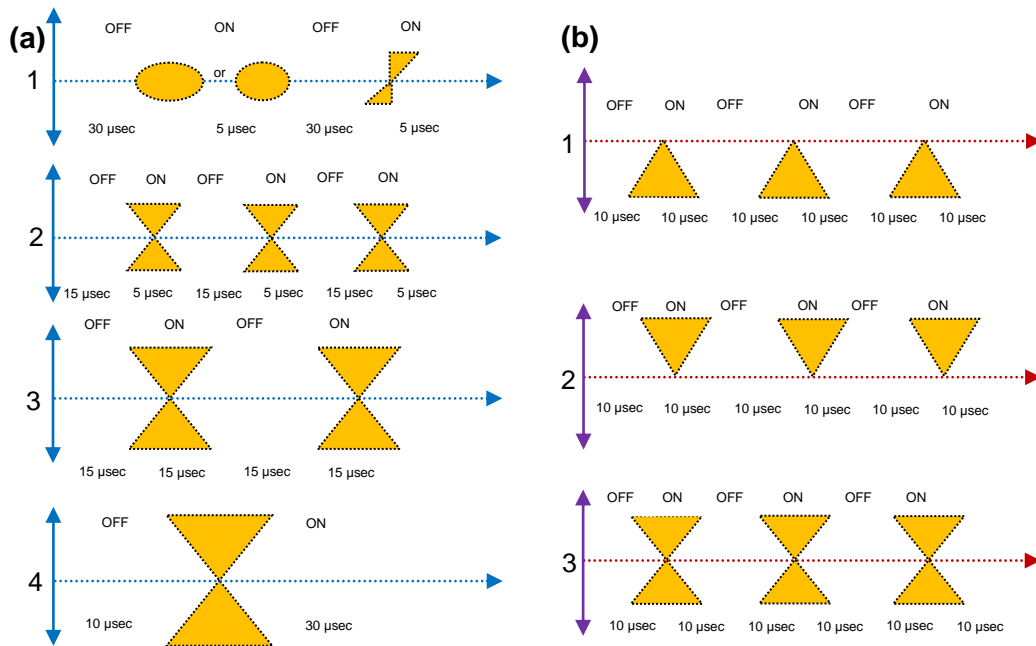


Figure 1: (a) tiny particles of different shape and size at varying ratio of bipolar pulse OFF to ON time; (a₁) pulse OFF time 30 μsec and pulse ON time 5 μsec, (a₂) pulse OFF time 15 μsec and pulse ON time 5 μsec, (a₃) pulse ON/OFF time 15 μsec and (a₄) pulse OFF time 10 μsec and pulse ON time 30 μsec, and (b) tiny particles at different pulse polarity where pulse ON/OFF time is 10 μsec; (b₁) unipolar pulse mode – a negative pulse polarity (b₂) unipolar pulse mode – a positive pulse polarity and (b₃) bipolar pulse

A tiny particle which was developed in the shape of two joint ellipses, circles or misfit triangles may also divide into two tiny particles if the force of perturbed axis exerting at point of their connection along different direction. However, such tiny particles are packed under exertion of non-uniform force where mixed behavior of the force resulted into develop their distorted particles. Further detail regarding the development mechanism of distorted particles is given elsewhere [39]. Where the tiny particles were developed in low aspect ratio of the shape of two joint triangles for each case, on

separation into two tiny particles, their packing also resulted into develop particles of low aspect ratio. Where the tiny particles were developed in moderate aspect ratio of the shape of two joint triangles for each case, on separation into two tiny particles, their packing also resulted into develop particles of moderate aspect ratio. Where the tiny particles were developed in high aspect ratio of the shape of two joint triangles for each case, on separation into two tiny particles, their packing also resulted into develop particles of high aspect ratio.

As shown in Figure 2, three triangular-shaped tiny particles positioned at $\sim 120^\circ$, $\sim 240^\circ$ and $\sim 360^\circ$ angles at solution surface. On elongating successively while dealing the immersing force, structure of their one-dimensional arrays of atoms develop into structure of smooth elements and when they just immobilize at centre of common point resulting into nucleate triangular-shaped particle. A separate study will discuss the packing hurdles of such tiny particles along with their packing to develop various geometric anisotropic shaped particles. A triangular-shaped tiny particle of monolayer assembly possesses three-dimensional structure of surface format prior to elongate, but on elongation of its each one-dimensional array, which is under exertion of surface format force develops, it develops into structure of smooth elements [42]. The consecutive packing of similar featured tiny particles for each mono layer resulted into develop triangular-shaped particle as shown in Figure 2. At top right corner in Figure 2, only light glow is shown where the central region of glow deals entering of very high forcing energy photons in solution, where against the reaction of their force, atoms uplifted to solution surface. Various geometric anisotropic shaped particles developed one at a time in the same manner as in Figure 2 except packing of tiny particles from different zones along with their certain numbers at instant of nucleating a certain shape of particle. Elongated monolayer tiny particles treated equally by the exerting force from the centre of each atom along opposite poles where their one-dimensional array further elongated while impinging electron streams of splitted argon atoms when going to pack at common centre. Further detail of developing different shapes of particles is given elsewhere [48]. Longer period to stay tiny particles at surface increase elongation rate of their atoms as they not only elongate due to exerting surface format force but also

under impinging electron streams as they carried the forcing energy as well. An electron when forced under certain length photon to strike to grounded certain state atom resulting into distort it at point of connect [45].

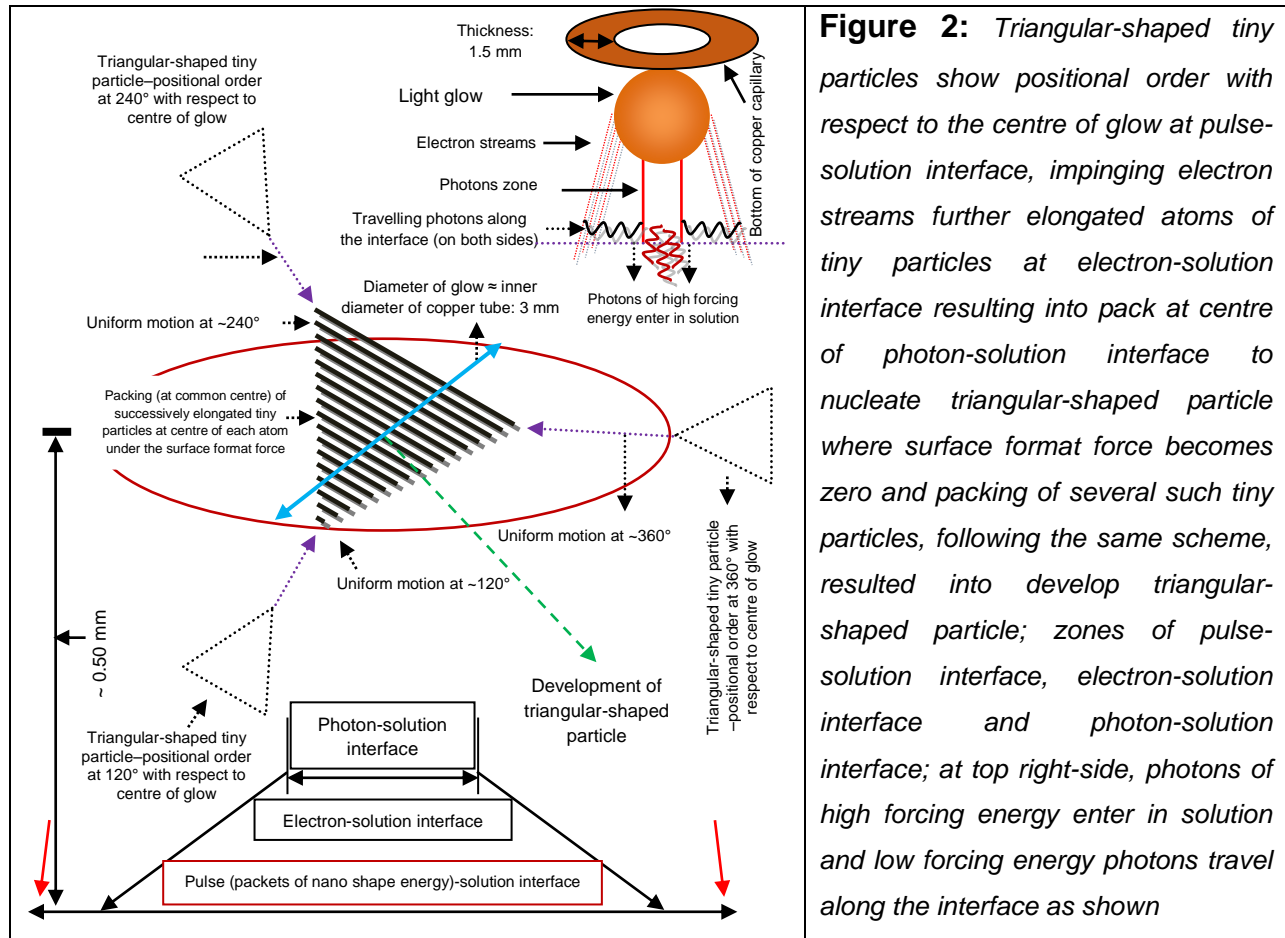


Figure 3 generalized the overall trend of developing particles of various aspect ratio depending on the set bipolar pulse OFF to ON time; when the ratio of pulse OFF to ON time is moderate, many low aspect ratio shaped particles are developed, when the ratio of pulse OFF to ON time is unity, many average aspect ratio shaped particles are developed and when the ratio of pulse OFF to ON time is very small (or unity under large pulse ON/OFF time), many high aspect ratio shaped particles are developed. The increase in the length of arrow in Figure 3 on increasing the pulse ON time (at fixed pulse OFF time) indicates the increase in the aspect ratio of geometric anisotropic shaped particles as well. These indicate that in addition to formation of tiny shaped

particles under the application of packets of nano shape energies placing at monolayer assembly of gold atoms at air-solution interface, the formation process of geometric anisotropic shaped particles is subjected to force behavior also. Figure 3 also shows distorted particles under very large ratio of bipolar pulse OFF to ON time; tiny particles developed in ellipse (in circle) shapes or in misfit triangle shapes under the application of small-sized packets of nano shape energies when very small pulse ON time selected as compared to pulse OFF time (indicated by red arrow). Again, the formation process of distorted particles may involve tiny shaped particles as well as tiny irregular-shaped particles where their mixed behaviours of motion under varying force are involved.

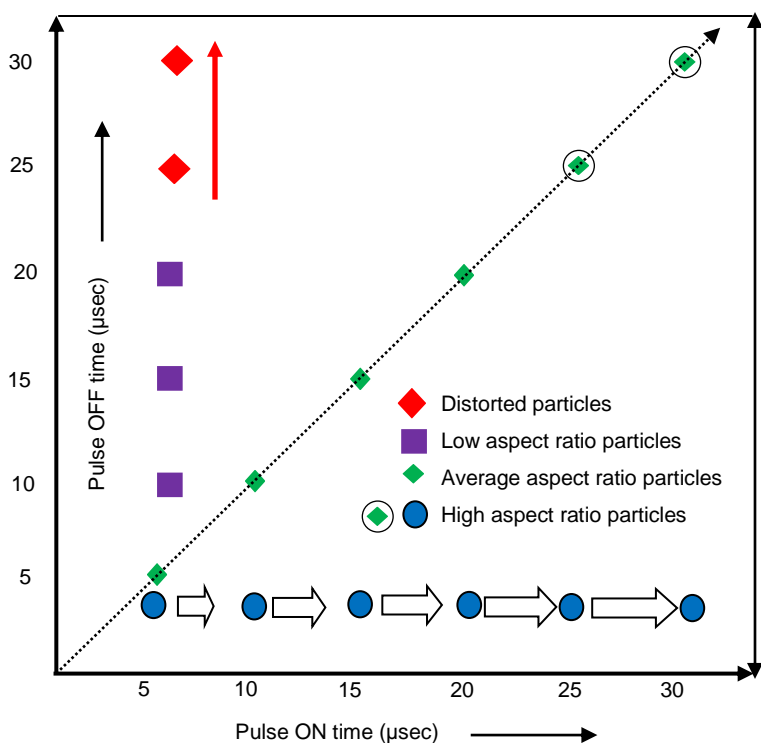


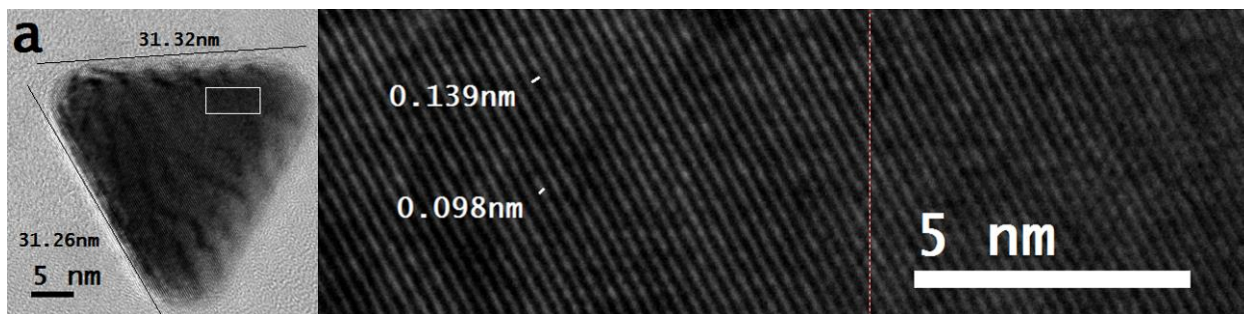
Figure 3: Plot of ratio of bipolar pulse OFF to ON time versus different aspect ratios gold particles

Overall, the set ratio of pulse ON/OFF time ratio controls the shape of tiny particles, thus, their packing was remained under uniform motion or variable motion; in the case of uniform motion, packing resulted into geometric anisotropic shaped particles. In the case of variable motion even for one tiny particle, packing resulted into distorted particle as in the case of Figure S1. In the case of bright field transmission microscope images

shown in Figure S1, the set ratio of bipolar pulse OFF to ON time was very large (= 6) resulting into develop ellipse (or circle) shaped tiny particles (or even scalene triangle), thus, they were packed under variable motion. When the ratio of pulse OFF to ON time is 3, the emerged dynamics of atoms manipulate the tiny particles largely in low aspect ratio of shape of the two joint triangles resulting into develop low aspect ratio particles also as shown in various bright field transmission microscope images of Figure S2 and Figure S13. At that instant, rate of more in-plane binding of mono layer tiny particles is decreased while the rate of more lateral binding of mono layer tiny particles is increased resulting into develop thicker nanoparticles and particles. In the development of such particles, the centre of dominating force is remained perturbed at the instant of packing tiny particles and such behaviours are pronounced in the case of nanoparticle and particles shown in Figure S13.

Depending on the rate of elongation of one-dimensional arrays of atoms of tiny particles, stretching rate of energy knots clamping electrons of atoms vary, so, in the case of overlapping to adjacent ones of one-dimensional arrays. This results into vary the width of structure of smooth elements and their inter-spacing distance as well. Under a very long period of pulse ON time, elongated atoms of tiny particles further elongated at electron-solution interface. On packing of such tiny particles at photon-solution interface, travelling photons along interface do not modify them to structure of perfect smooth elements as discernible in the large portion covered under rectangular-box of Figure S7 (a). The packing of such elongated structure of tiny particles messed up the structure of their developing particles as excess plastically-driven electron states doesn't get align to form structure of smooth elements. Thus, those cloudy atomic structures are not eligible to convert into structure of smooth elements despite of the travelling photons of adequate energy along the interface. However, it can be observed in the selective region shown in smaller rectangular-box of Figure S7 (a) where suitable elongation of atoms results into their conversion (modification) to structure of smooth elements. The structure of smooth element indicates (resembles) to elongated atoms of one-dimensional arrays where the contained well-pressed energy knots clamping electron states and appear to be straight like thread shape.

An equilateral triangular-shaped nanoparticle is shown in Figure 4 (a) where lengths of sides are almost equal. Magnified image of the marked region (pointed by rectangular-box) is shown at right-side in Figure 4 (a). In the magnified high-resolution image on the right-side portion to 'dotted line' in Figure 4 (a), the region related to structure of smooth elements appears to be blurred. However, in the magnified high-resolution image on the left-side to 'dotted line' in Figure 4 (a), equal width of each smooth element (~ 0.098 nm) and equal width of inter-spacing distance (~ 0.139 nm) are discernible. Such structural behaviours validate that elongated one-dimensional arrays of atoms in tiny particles are further elongated while impinging electron streams at electron-solution interface. Again, they may stay for longer time at solution surface resulting into deal exertion of surface format force for longer duration. At left-side in Figure 4 (b), a pentagonal-shaped nanoparticle is shown, and magnified image taken from the marked region (pointed by rectangular-box) is shown at right-side where width of structure of smooth element is measured ~ 0.120 nm, which is equal to inter-spacing distance of structure of smooth elements. However, while setting the same bipolar pulse ON time (15 μ sec) as in the case of triangular-shaped nanoparticle shown in Figure 4 (a), the structure of smooth elements of pentagonal-shaped nanoparticle shown in Figure 4 (b) is slightly different in width, which may be related to different pulse OFF time. Again pentagonal-shaped nanoparticle is shown in Figure 4 (b) where bipolar pulse mode was employed and packing of five triangular-shaped tiny particles at common centre didn't left any room to precede the packing, further.



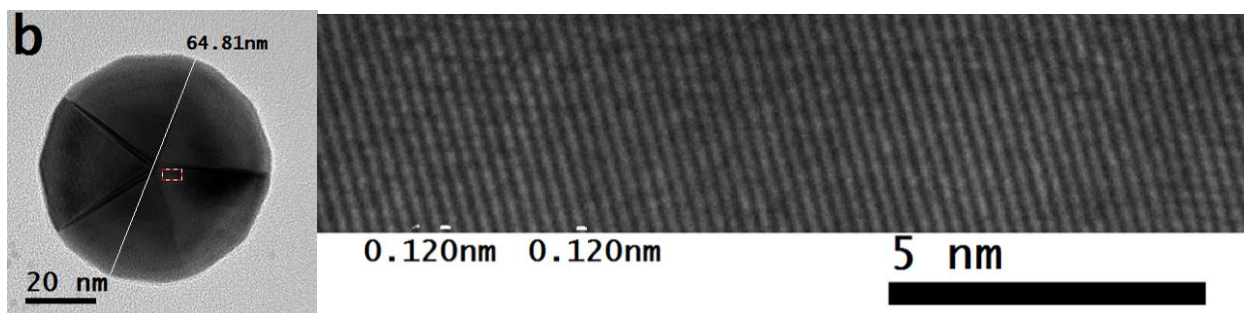


Figure 4: (a) high-resolution transmission microscope image of triangular-shaped nanoparticle is shown at left-side while magnified image taken from the marked region is shown at right-side (bipolar pulse ON/OFF time was 15 μ sec) and (b) high-resolution transmission microscope image of pentagonal-shaped nanoparticle is shown at left-side while magnified image taken from the marked region is shown at right-side (bipolar pulse ON time 15 μ sec & OFF time 5 μ sec); precursor concentration is 0.40 mM

Gold particles synthesized at varying ratios of bipolar pulse OFF to ON time where precursor concentration was 0.20 mM and 0.40 mM are shown in the supplementary material (Figures S1-S7 & Figures S9-S13 and color of processed solutions at 0.20 mM in Figure S8) along with synthesized nanoparticles and particles at different polarity of the pulse; in Figures S15 and S16 unipolar mode of pulse was employed while in Figure S17 bipolar mode of pulse was employed. Under both modes of unipolar pulse and bipolar pulse polarity, various gold nanoparticles and particles reveal identical features of morphology-structure. In Figure S12 (G), SAPR pattern of hexagonal-shaped particle measured distance \sim 0.24 nm between any two nearby intensity spots. In Figure S13 (A), the SAPR pattern of triangular-shaped particle also measured the same thickness of the structure of smooth element \sim 0.24 nm. However, in the case of SAPR pattern of rod-shaped particle (Figure S13B), the measured distance between parallel lines of intensity spots is \sim 0.27 nm. This difference in the width of structure of smooth element in the case of a particle having three-dimensional structure and a particle having one-dimensional structure has been discussed elsewhere [41]. A flow chart of whole process of formation of various geometric anisotropic shaped nanoparticles and particles along with distorted nanoparticles and particles is illustrated in Figure 5: on increasing the pulse ON time as compared to pulse OFF time (and when the ratio of pulse OFF to ON time was 1/3 or 1/6), mainly high aspect ratio equilateral triangular-shaped tiny particles were developed and their packing resulted into develop high aspect ratio geometric

anisotropic shaped particles also; at equal pulse ON time and pulse OFF time, mainly moderate aspect ratio equilateral triangle shape tiny particles were developed and their packing resulted into develop moderate aspect ratio geometric anisotropic shaped particles too; on decreasing the pulse ON time as compared to pulse OFF time and when the ratio of pulse OFF to pulse ON time was 3, mainly misfit (circle, ellipse, etc.) triangular-shaped tiny particles were developed; decreasing the pulse ON time as compared to pulse OFF time (the ratio of pulse OFF to pulse ON time = 6), tiny shaped particles of no specific shape were developed and they are in misfit triangular-shaped tiny particles where their packing also resulted into develop distorted particles.

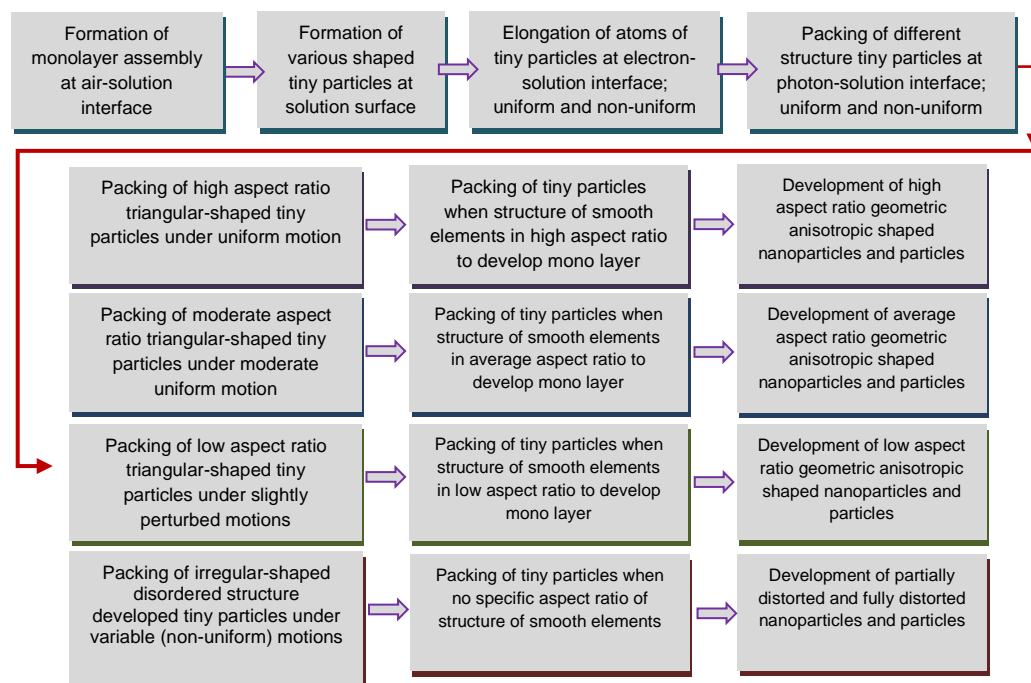


Figure 5: Flow chart highlighting major steps of development of various nanoparticles and particles; high aspect ratio geometric anisotropic shaped particles, average aspect ratio geometric anisotropic shaped particles, low aspect ratio geometric anisotropic shaped particles and distorted particles

Mainly, at short pulse ON time (5 μ sec or 10 μ sec) as compared to pulse OFF time (15 μ sec or 30 μ sec), in addition to slightly misfit triangular-shaped tiny particles, their perturbed common centre each time enabled slightly misfit packing and travelling photons aside to their surfaces do not enable their structure to shape into perfect structure of smooth elements while each layer of developing particle results into thick, dark and low aspect ratio features of particles. Also, when the pulse ON time was

mainly 5 μsec and pulse OFF time was mainly 15 μsec , the rate of packing of slightly misfit triangular-shaped tiny particles became faster as compared to the unity ratio of pulse OFF to ON time or smaller than unity ratio of pulse OFF to ON time; a greater number of amalgamated atoms (in monolayer assembly) are already available below smaller size packets of nano shape energy. When the pulse ON time was 5 μsec and pulse OFF time was 30 μsec , rate of amalgamation of atoms around electron-photon-solution interface further enhanced while the size of packets of nano shape energy remained the same resulting into develop irregular-shaped tiny particles. Thus, they pack under completely variable motion with more perturbed common centre and the level of disorder increased on increasing the number of packing of such tiny particles resulting into develop distorted particles.

All geometric anisotropic shaped particles are developed through the packing of tiny shaped particles in triangle shape but under their varying aspect ratio. The partially distorted or distorted particles are developed either under the packing of tiny particles shape like ellipse or circle or tiny particles which do not reveal any specific shape. In addition to individually attained dynamics of atoms under set ratios of pulse OFF to ON time, in certain zones, atoms might experience different dynamics under the process of synergy resulting into no specific shape of tiny particles. Such tiny particles have been discussed elsewhere [36]. Thus, variable motion of tiny particles along with those in uniform motion might result in develop partially distorted or distorted morphology-structure nanoparticle or particle. Again, uplift of atoms at suitable amount is not necessary all the time which developed the compact monolayer assembly at air-solution interface. Such tiny particles result into pack under slightly perturbed motions due to not letting them to deal the dominating force at single point of their tip, so, their packing results into either slightly distorted nanoparticle or distorted particle.

A tiny particle is a tiny sized particle which is developed on the first-hand amalgamation of atoms. A tiny particle can be related to certain shape (geometry) or can't be related to its certain shape depends on the mechanisms of its amalgamating atoms and their binding. When few such tiny particles assemble, they will develop a nanoparticle. When many such tiny particles assembled (coalesced or packed), they

developed a large sized particle. If in the case of assembling of certain shape of tiny particles, they may result into develop a shaped particle. In other way, a distorted particle develops.

Varying the ratio of pulse OFF to ON time provides option for not only altering the morphology-structure of tiny particles but also of particles. In this context, the morphology-structure of metallic colloids brings huge consequences not only in the on-going research efforts but also in practical demonstrations at the forefronts of photonics, ultra-high-speed applications, catalytic and many others. More specifically, high aspect ratio geometrical shapes are expected to be strong candidates for photonics applications and ultra-high-speed devices, whereas, the low aspect ratio and distorted shapes are considered to be the strong candidates for various catalytic activities. The geometrical shapes are expected to perform as per geometry of the particle.

Conclusions:

All structural motifs of tiny particles, nanoparticles and particles are subjected to force and energy behaviours where in few microseconds-controlled dynamics of the process control structure under the application of force-energy behaviors, hence, their morphology (shape). In pulse-based electron-photon-solution interface process, emerged dynamics of ratio of pulse OFF to ON time control the geometry of tiny particle. Under unity ratio of bipolar pulse OFF to ON time (or when this ratio is smaller than unity), many tiny particles develop in the shape of two joint triangles for each case, when this ratio is larger than unity ($= 3$) many tiny particles develop in low aspect ratio of the shape of two joint triangles for each case, when the ratio is very large ($= 6$), many tiny particles develop in ellipse or circle or misfit triangle shape. The tiny particles developed in the shape of two joint triangles divide into two under the exerting force of surface format at perturbed axis at point of connection, but under the unity ratio of unipolar pulse OFF to ON time, the tiny particles straight-forward develop in equilateral triangular-shaped tiny particles.

Depending on pulse ON/OFF time, nanoparticles and particles of different morphology-structure developed at centre of photon-solution interface; high aspect ratio

shapes of particles develop on packing of high aspect ratio tiny particles, average aspect ratio shapes of particles develop on packing of average aspect ratio tiny particles and low aspect ratio shapes of particles develop on packing of low aspect ratio tiny particles. Distorted shapes of particles develop on packing of ellipse or circle or misfit triangle tiny particles. However, when nano shape energy of set bipolar pulse ON/OFF time is not in triangle shape, the resulting tiny particles also do not develop in triangle shape. When the pulse OFF time is three times greater than pulse ON time, the in-plane binding of mono layer tiny particles is decreased as compared to their lateral binding as per arisen dynamics of set ratio pulse. Under bipolar and unipolar pulse modes the morphology-structure of particles remains nearly the same.

At 5 μsec pulse ON time and 30 μsec pulse OFF time, amalgamation of atoms around electronphoton-solution interface don't results into triangle shape of tiny particles as longer pulse OFF time results into develop disordering of atoms where circle or ellipse or non-regular triangle shape tiny particles develop. When the pulse ON time is 5 μsec and pulse OFF time is 15 μsec , the amalgamation of atoms is in less disordering, thus, develop the partially misfit tiny shaped particles and partially fit tiny shaped particles resulting into the low aspect ratio of shapes of particles, largely.

Depending on the ratio of pulse OFF to ON time, stretching of energy knots clamping electrons vary resulting into varying the width of structure of smooth elements along with their inter-spacing distance. At 30 μsec pulse ON time and 5 μsec pulse OFF time, inter-spacing distance of structure of smooth elements is greater (~ 0.14 nm) than individual width (~ 0.10 nm) and under opposite conditions, the widths of structure of smooth elements also get reverse. In the case of adequate wavelength photons travelling where atomic structure is messed up due to miscellaneous causes, their structures don't modify to structure of perfect smooth elements. Different colors of solutions are due to different sizes and shapes of particles (as per set ratio of bipolar pulse OFF to ON time) depending on the overall modes of refraction and reflection of travelling light and, so, the pronounced effects of the colors are under sunlight.

Clearly, the present study enlightens us to find ways and means to control tiny particles in different aspect ratio of shape, so, their packing into diversifying class of

morphology-structure along with identifying effects of travelling photons on the structure. Present strategies explore multi-dimension routes to cope with ever-increasing demands of emerging and applied materials in any shape and size along with their aspect ratio which not only shed light on the materials science, physics, and nanoscience but also develop new knowledge in the diversified areas of science and technology.

Acknowledgements

Mubarak Ali sincerely thanks to the National Science Council (now MOST) Taiwan (R.O.C.) for awarding postdoctorship: NSC-102-2811-M-032-008 (August 2013- July 2014). Authors thank to Mr. Chien-Jui Yeh for helping in transmission microscope operation. Mubarak Ali greatly appreciates useful suggestions of Dr. M. Ashraf Atta.

References:

1. J. Kim, Y. Lee, S. Sun. Structurally ordered FePt nanoparticles and their enhanced catalysis for oxygen reduction reaction. *J. Am. Chem. Soc.* **132**, 4996-4997 (2010).
2. K. Kusada, *et al.* Discovery of face-centered-cubic ruthenium nanoparticles: facile size-controlled synthesis using the chemical reduction method. *J. Am. Chem. Soc.* **135**, 5493-5496 (2013).
3. J. Zhang, G. Chen, M. Chaker, F. Rosei, D. Ma. Gold nanoparticle decorated ceria nanotubes with significantly high catalytic activity for the reduction of nitrophenol and mechanism study. *Appl. Catal. B: Environ.* **132/133**, 107-115 (2013).
4. Z. Xu, *et al.* Harvesting Lost Photons: Plasmon and Upconversion Enhanced Broadband Photocatalytic Activity in Core@Shell Microspheres Based on Lanthanide-Doped NaYF₄, TiO₂, and Au. *Adv. Funct. Mater.* **25**, 2950-2960 (2015).
5. Y. Liu, X. Zhang. Metamaterials: a new frontier of science and technology. *Chem. Soc. Rev.* **40**, 2494-2507 (2011).
6. A. Kuzyk, *et al.* DNA-based self-assembly of chiral plasmonic nanostructures with tailored optical response. *Nature* **483**, 311-314 (2012).

7. M. Brust, M. Walker, D. Bethell, D. J. Schiffrin, R. Whyman. Synthesis of Thiol-derivatised Gold Nanoparticles in a Two-phase Liquid-Liquid System. *J. Chem. Soc., Chem. Commun.* 801-802 (1994).
8. R. L. Whetten, *et al.* Nanocrystal Gold Molecules. *Adv. Mater.* **8**, 428-433 (1996).
9. S. Link, M. A. El-Sayed. Shape and size dependence of radiative, nonradiative and photothermal properties of gold nanocrystals. *Inter. Rev. Phys. Chem.* **19**, 409- 453 (2002).
10. L. O. Brown, J. E. Hutchison. Formation and Electron Diffraction Studies of Ordered 2-D and 3-D Superlattices of Amine-Stabilized Gold Nanocrystals. *J. Phys. Chem. B* **105**, 8911-8916 (2001).
11. G. M. Whitesides, M. Boncheva. Beyond molecules: Self-assembly of mesoscopic and macroscopic components. *Proc. Natl. Acad. Sci. U.S.A.* **99**, 4769-4774 (2002).
12. M. Brust, C. J. Kiely. Some recent advances in nanostructure preparation from gold and silver particles: a short topical review. *Colloids and Surfaces A: Physicochem. Eng. Aspects* **202**, 175-186 (2002).
13. J. Huang, F. Kim, A. R. Tao, S. Connor, P. Yang. Spontaneous formation of nanoparticle stripe patterns through dewetting. *Nat. Mater.* **4**, 896-900 (2005).
14. S. C. Glotzer, *et al.* Self-assembly of anisotropic tethered nanoparticle shape amphiphiles. *Curr. Opin. Colloid Interface Sci.* **10**, 287-295 (2005).
15. S. C. Glotzer, M. J. Solomon. Anisotropy of building blocks and their assembly into complex structures. *Nature Mater.* **6**, 557-562 (2007).
16. C. P. Shaw, D. G. Fernig, R. Lévy. Gold nanoparticles as advanced building blocks for nanoscale self-assembled systems. *J. Mater. Chem.* **21**, 12181-12187 (2011).
17. D. Vanmaekelbergh. Self-assembly of colloidal nanocrystals as route to novel classes of nanostructured materials. *Nano Today* **6**, 419-437 (2011).
18. N. Liu, M. L. Tang, M. Hentschel, H. Giessen, A. P. Alivisatos. Nanoantenna-enhanced gas sensing in a single tailored nanofocus. *Nat. Mater.* **10**, 631-637 (2011).
19. N. Li, P. Zhao, D. Astruc. Anisotropic Gold Nanoparticles: Synthesis, Properties, Applications, and Toxicity. *Angew. Chem. Int. Ed.* **53**, 1756-1789 (2014).

20. M. L. Brongersma, N. J. Halas, P. Nordlander. Plasmon-induced hot carrier science and technology. *Nature Nanotechnol.* **10**, 25-34 (2015).
21. P. Dombi, *et al.* Ultrafast strong-field photoemission from plasmonic nanoparticles. *Nano Lett.* **13**, 674-678 (2013).
22. S. Yang, *et al.* Feedback-driven self-assembly of symmetry-breaking optical metamaterials in solution. *Nature Nanotechnol.* **9**, 1002-1006 (2014).
23. N. Zeng, A. B. Murphy. Heat generation by optically and thermally interacting aggregates of gold nanoparticles under illumination. *Nanotechnology* **20**, 375702-09 (2009).
24. M. Mecklenburg, *et al.* Nanoscale temperature mapping in operating microelectronic devices. *Science* **347**, 629-632 (2015).
25. Y. Negishi, *et al.* A Critical Size for Emergence of Nonbulk Electronic and Geometric Structures in Dodecanethiolate-Protected Au Clusters. *J. Am. Chem. Soc.* **137**, 1206-1212 (2015).
26. A. Moscatelli. Gold nanoparticles: Metallic up to a point. *Nature Nanotechnol.* (2015) DOI:10.1038/nnano.2015.16.
27. V. N. Manoharan. Colloidal matter: Packing, geometry, and entropy. *Science* **349**, 1253751 (2015).
28. S. Atkinson, F. H. Stillinger, S. Torquato. Existence of isostatic, maximally random jammed monodisperse hard-disk packings. *Proc. Natl. Acad. Sci. U.S.A.* **111**, 18436-18441 (2015).
29. D. Mariotti, J. Patel, V. Švrček, P. Maguire. Plasma –Liquid Interactions at Atmospheric Pressure for Nanomaterials Synthesis and Surface Engineering. *Plasma Process. Polym.* **9**, 1074-1085 (2012).
30. J. Patel, L. Němcová, P. Maguire, W. G. Graham, D. Mariotti. Synthesis of surfactant-free electrostatically stabilized gold nanoparticles by plasma –induced liquid Chemistry. *Nanotechnology* **24**, 245604-14 (2013).
31. X. Huang, Y. Li, X. Zhong. Effect of experimental conditions on size control of Au nanoparticles synthesized by atmospheric microplasma electrochemistry. *Nanoscale Research Lett.* **9**, 572-578 (2014).

32. N. Shirai, S. Uchida, F. Tochikubo. Synthesis of metal nanoparticles by dual plasma electrolysis using atmospheric dc glow discharge in contact with liquid. *Jpn. J. Appl. Phys.* **53**, 046202-07 (2014).
33. J. Hieda, N. Saito, O. Takai. Exotic shapes of gold nanoparticles synthesized using plasma in aqueous solution. *J. Vac. Sci. Technol. A* **26**, 854-856 (2008).
34. N. Saito, J. Hieda, O. Takai. Synthesis process of gold nanoparticles in solution plasma. *Thin Solid Films* **518**, 912-917 (2009).
35. K. Furuya, Y. Hirowatari, T. Ishioka, A. Harata. Protective Agent-free Preparation of Gold Nanoplates and Nanorods in Aqueous H_{AuCl}₄ Solutions Using Gas–Liquid Interface Discharge. *Chem. Lett.* **36**, 1088-1089 (2007).
36. M. Ali, I –N. Lin. The effect of the Electronic Structure, Phase Transition, and Localized Dynamics of Atoms in the formation of Tiny Particles of Gold. <http://arxiv.org/abs/1604.07144>.
37. M. Ali, I –N. Lin. Phase transitions and critical phenomena of tiny grains carbon films synthesized in microwave-based vapor deposition system. <http://arXiv.org/abs/1604.07152>.
38. M. Ali, M. Ürgen. Switching dynamics of morphology-structure in chemically deposited carbon films –A new insight. *Carbon* **122**, (2017) 653-663.
39. M. Ali, I –N. Lin. Development of gold particles at varying precursor concentration. <http://arXiv.org/abs/1604.07508>.
40. M. Ali, I –N. Lin. Tapping opportunity of tiny shaped particles and role of precursor in developing shaped particles. <http://arxiv.org/abs/1605.02296>.
41. M. Ali, I –N. Lin. Formation of tiny particles and their extended shapes -Origin of physics and chemistry of materials. <http://arxiv.org/abs/1605.09123>.
42. M. Ali. The study of tiny shaped particle dealing localized gravity at solution surface. <http://arxiv.org/abs/1609.08047>.
43. M. Ali. Structure evolution in atoms of solid state dealing electron transitions. <http://arxiv.org/abs/1611.01255>.
44. M. Ali. Atoms of electronic transition deform or elongate but do not ionize while inert gas atoms split. <http://arxiv.org/abs/1611.05392>.

45. M. Ali. Revealing the Phenomena of Heat and Photon Energy on Dealing Matter at Atomic level. <https://www.preprints.org/manuscript/201701.0028/v10>.
46. M. Ali. Why atoms of some elements are in gas state and some in solid state, but carbon works on either side (2018). <https://www.preprints.org/manuscript/201803.0092/v1>
47. M. Ali. Nanoparticles-Photons: Effective or Defective Nanomedicine. J. Nanomed. Res. **5**, (2017) 00139.
48. M. Ali, I –N. Lin, C. –J. Yeh. Predictor packing in developing unprecedented shaped colloidal particles. <https://www.preprints.org/manuscript/201801.0039/v2>

Authors' biography:



Mubarak Ali graduated from University of the Punjab with B.Sc. (Phys& Maths) in 1996 and M.Sc. Materials Science with distinction at Bahauddin Zakariya University, Multan, Pakistan (1998); thesis work completed at Quaid-i-Azam University Islamabad. He gained Ph.D. in Mechanical Engineering from Universiti Teknologi Malaysia under the award of Malaysian Technical Cooperation Programme (MTCPC;2004-07) and postdoc in advanced surface technologies at Istanbul Technical University under the foreign fellowship of The Scientific and Technological Research Council of Turkey (TÜBİTAK; 2010). He completed another postdoc in the field of nanotechnology at Tamkang University Taipei (2013-2014) sponsored by National Science Council now M/o Science and Technology, Taiwan (R.O.C.). Presently, he is working as Assistant Professor on tenure track at COMSATS Institute of Information Technology, Islamabad campus, Pakistan (since May 2008) and prior to that worked as assistant director/deputy director at M/o Science & Technology (Pakistan Council of Renewable Energy Technologies, Islamabad; 2000-2008). He was invited by Institute for Materials Research (IMR), Tohoku University, Japan to deliver scientific talk on growth of synthetic diamond without seeding treatment and synthesis of tantalum carbide. He gave several scientific talks in various countries. His core area of research includes materials science, physics & nanotechnology. He was also offered the merit scholarship (for PhD study) by the Government of Pakistan but he couldn't avail. He is author of several articles published in various periodicals (<https://scholar.google.com.pk/citations?hl=en&user=UYjvhDwAAAAJ>).



I-Nan Lin is a senior professor at Tamkang University, Taiwan. He received the Bachelor degree in physics from National Taiwan Normal University, Taiwan, M.S. from National Tsing-Hua University, Taiwan, and the Ph.D. degree in Materials Science from U. C. Berkeley in 1979, U.S.A. He worked as senior researcher in Materials Science Centre in Tsing-Hua University for several years and now is faculty in Department of Physics, Tamkang University. Professor Lin has more than 200 referred journal publications and holds top position in his university in terms of research productivity. Professor I-Nan Lin supervised several PhD and Postdoc candidates around the world. He is involved in research on the development of high conductivity diamond films and on the transmission microscopy of materials.

Supplementary Materials:

Controlling morphology-structure of particles at different pulse rate, polarity and effect of photons on structure

Mubarak Ali^{1, *} and I-Nan Lin²

¹Department of Physics, COMSATS Institute of Information Technology, Islamabad 45550, Pakistan. *E-mail: mubarak74@comsats.edu.pk, mubarak74@mail.com

²Department of Physics, Tamkang University, Tamsui Dist., New Taipei City 25137, Taiwan (R.O.C.)

In Figure S1, bright field transmission microscope images (a-h) show different sort of distorted nanoparticles. The smallest size of the nanoparticle is 7.14 nm (tiny-sized particle in Figure S1c) and the biggest is 60.34 nm (in Figure S1e). In Figure S2, bright field transmission microscope images (a-j) show nanoparticles of various geometric anisotropic shape. Size of the similar geometric anisotropic shape is different within the same process as triangular-shaped nanoparticles in Figure S2 (i) have bigger size as compared to nanoparticle in Figure S2 (j). Similarly, a triangular-shaped nanoparticle in Figure S2 (e) is bigger as compared to those shown in Figure S2 (i) and Figure S2 (j). Again, in Figure S3, different bright field transmission microscope images (a-l) show various geometric anisotropic shaped nanoparticles where they reveal the same trend of morphology-structure as in the case of nanoparticles in Figure S2. In various bright field transmission microscope images of Figure S4 and Figure S5, the morphological-structural features of nanoparticles and particles are almost identical to ones shown in various bright field transmission microscope images of Figure S2 and Figure S3, however, their atoms deal different behavior of elongation and deformation. Again, in Figure S1, various bright field transmission microscope images show distorted nanoparticles and reveal development under the packing of tiny particles shapes like

ellipse, circle or misfit triangle. When the electron streams remained OFF for 30 μsec and ON for 5 μsec (in each pulse cycle), then the arisen dynamics of the process were altered largely, and tiny particles of misfit packing were developed. As an evidence, in Figure S1 (c) such nanoparticles (tiny-sized particles) can be observed; in Figure S1 (f) and Figure S1 (g), geometry of tiny particle is more-like in ellipse shape or circle shape. However, many tiny particles developed in the joint triangles when the ratio of pulse OFF to ON time was 3 as several geometric anisotropic shaped particles developed on packing of triangular-shaped tiny particles (Figure S2). In Figure S2, the packets of nano shape energy under set pulse ON/OFF time developed tiny particles shape like two joint triangles for each case. From the physical observation of various geometric anisotropic shaped particles shown in bright field transmission microscope images of Figures S2 to S5, apparently no significant difference is evident. However, in Figure S4 set pulse ON/OFF time developed tiny particles in joint triangles for each case along with greater elongation rate of atoms of tiny particles as longer period of pulse ON time.

A distorted nanoparticle is shown in Figure S6 (a) where the important portions are labelled; area under larger rectangular-box shows less elongation of atoms of tiny particles, area under smaller rectangular-box shows atoms neither having specific orientation nor compact configuration and area under square-box shows elongation of atoms in different orientations (indicated by arrow lines). Magnified high-resolution transmission microscope images of regions marked with larger and smaller circles are shown in Figure S6 (b) and Figure S6 (c), respectively. In Figure S6 (b), inter-spacing distance of structure of smooth elements is ~ 0.099 nm, which is less than the width of a structure of smooth element (~ 0.143 nm). However, in Figure S6 (c), magnified high-resolution transmission microscope image reveals non-compact configuration of atoms along with their deformation under the non-orientational stretching of energy knots clamping electrons. Obviously, their tiny particles packed in the last stage of developing that particle. When the pulse ON time is very long as compared to pulse OFF time, the atoms of tiny particle get more elongated where also stretching of energy knots clamping electrons was more as well. Figure S7 (a) shows half part of the pentagonal-shaped nanoparticle which is divided into three important regions. Region covered

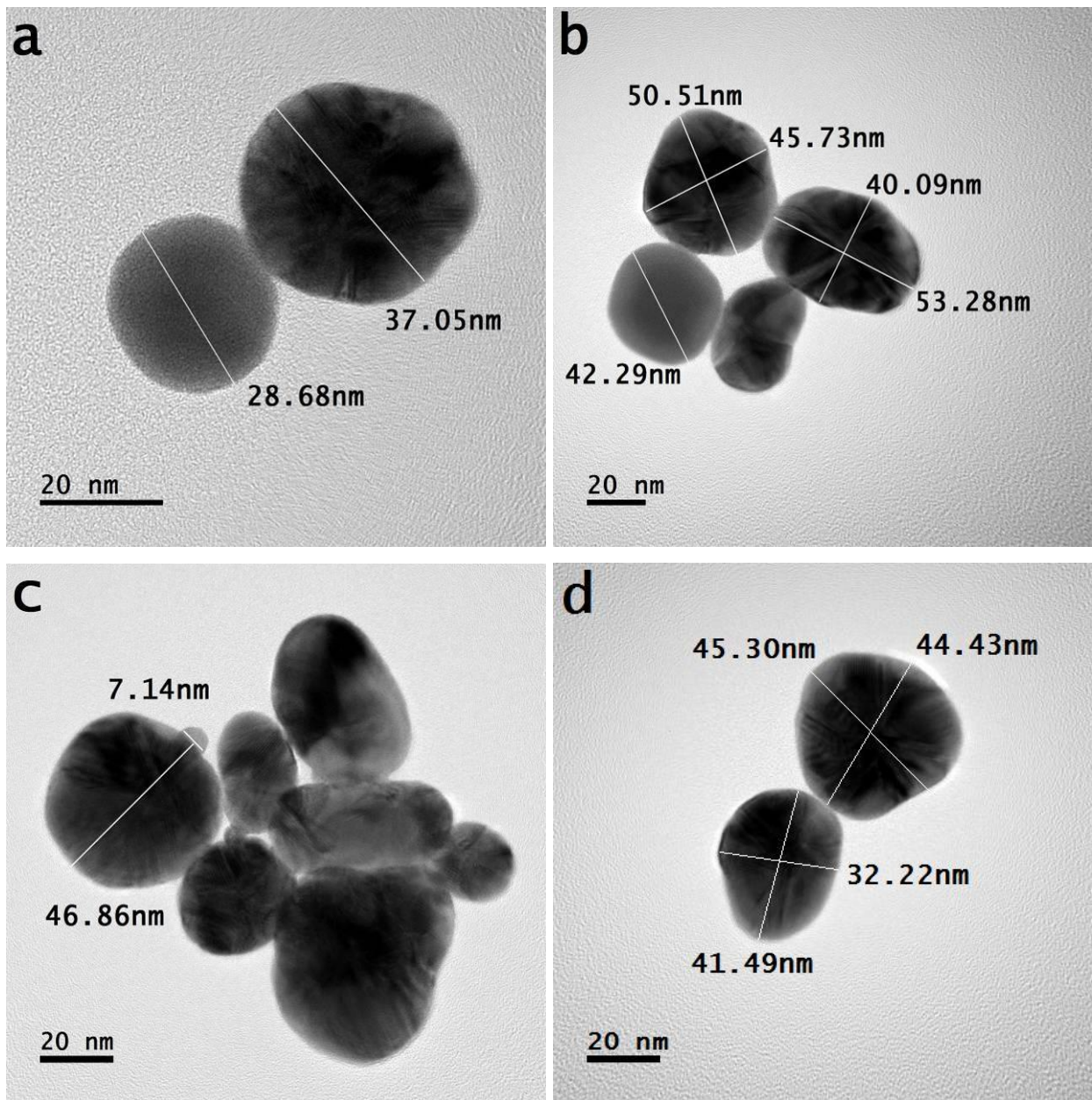
under the square-box is shown in Figure S7 (b) where magnified image of structure of smooth elements reveals increased inter-spacing distance (~ 0.143 nm) and width of each structure of smooth element is only ~ 0.097 nm. These widths have values that are opposite to what is observed in Figure S6 (b) indicating greater elongation rate of atoms of their tiny particles. In Figure S7 (a), the area of pentagonal-shaped nanoparticle marked by bigger sized rectangular-box indicates that elongated atoms of tiny particles didn't modify structure to structure of smooth elements as their structures are appeared to be messed up, most probably due to an extended level stretching of energy knots clamping electrons in atoms and their capability to align into smooth elements under photons of adequate forcing energy also diminished. As in the case of Figure S6 (b), atoms of tiny particles elongated less and travelling photons modified the structure having width of inter-spacing distance of structure of smooth elements only 0.099 nm, which is less than the width of a structure of smooth element (0.143 nm). However, in Figure S7 (b), the elongation of atoms of packed tiny particle was more, so inter-spacing distance of structure of smooth elements (0.143 nm) is greater than the width of a structure of smooth element (0.097 nm). Less or more elongation of atoms of tiny particles is mainly related to the set ratio of pulse OFF to ON time.

Under varying ratios of pulse OFF to ON time, the colors of resulted solutions are different as shown in Figure S8 indicating the various morphological-structural changes of nanoparticles and particles. Quite a large difference in the color of solutions observed where processed at pulse ON time 5 μsec OFF time 30 μsec and pulse ON time 30 μsec OFF time 5 μsec ; it is related to large variation in the morphology-structure of size and shape of particles. At equal pulse ON/OFF time or less difference in pulse ON and OFF time, the difference in the color of resulted solutions is not so pronounced as evident in Figure S8 (both under sunlight and in the absence of sunlight). While placing those processed solutions in front of glass window, their colors varied significantly under sunlight and in the absence of sunlight as shown in Figure S8 (a) and Figure S8 (b), respectively. The difference in the color of the solution is under the overall modes of refraction and reflection of travelling light to differently processed colloids; different set pulse ON/OFF time.

On increasing the precursor concentration from 0.20 mM to 0.40 mM, the average size of tiny particles increased resulting in the increase of the size of particles as shown in various bright field transmission microscope images of Figures S9 to S13. Bright field transmission microscope images (a-g) of various particles at pulse ON/OFF time 5 μ sec are shown in Figure S9. SAPR patterns of bar- and rod- shaped particles are shown in Figure S9 (A-C) along with distance between two parallel printed intensity lines. Several geometric anisotropic shaped nanoparticles and particles are shown in bright field transmission microscope images (a-h) of Figure S10 along with some distorted nanoparticles and particles, which were developed at pulse ON/OFF time 15 μ sec. Some of the nanoparticles' shapes were very small and developed at later stage of the process as total process duration was 20 minutes (in bright field transmission microscope images (d-h) of Figure S10). A range of nanoparticles and particles chosen from the solution was processed at pulse ON/OFF time 30 μ sec and their bright field transmission microscope images ('a' to 'p') are shown in Figure S11. The particles reveal the same trend as discussed above (and in many ways like those discussed in the case of precursor concentration 0.20 mM). A tiny spherical-shaped particle in Figure S11 (d) indicates that it didn't pack, timely, due to geometrical limitation. In Figure S11 (i), Figure S11 (j) and Figure S11 (o), very small triangular-shaped nanoparticles are observed, which were developed on packing of equilateral triangular-shaped tiny particles.

When the ratio of pulse OFF to ON time was large, particles were developed in lower aspect ratio (various bright field transmission microscope images (a-p) in Figure S13) and the trend of morphology-structure was different to that which was observed for smaller ratio pulse OFF to ON time as shown in various bright field transmission microscope images (a-g) of Figure S12. In Figure S13, due to longer pulse OFF time to pulse ON time, the size of nano shape energy became shorter and packing of tiny particles resulted into lower aspect ratio shapes as compared to ones shown in Figure S12. In Figure S12 (G), the distance between two intensity spots is approx. 0.24 nm and the same distance is measured in the case of SAPR pattern shown in Figure S13 (A), however, more distance between printed intensity spots is measured in one-

dimensional shape (Figure S13B) which is related to different rate of elongation of atoms as compared to particles of three-dimensional shapes as discussed elsewhere [41]. The identical morphological-structural shapes of particles were resulted under unipolar pulse modes known as negative unipolar pulse and positive unipolar pulse as shown in Figure S15 and Figure S16, respectively. Various bright field images of particles shown in Figure S17 were developed under bipolar pulse revealing the same shapes as in negative pulse polarity and positive pulse polarity.



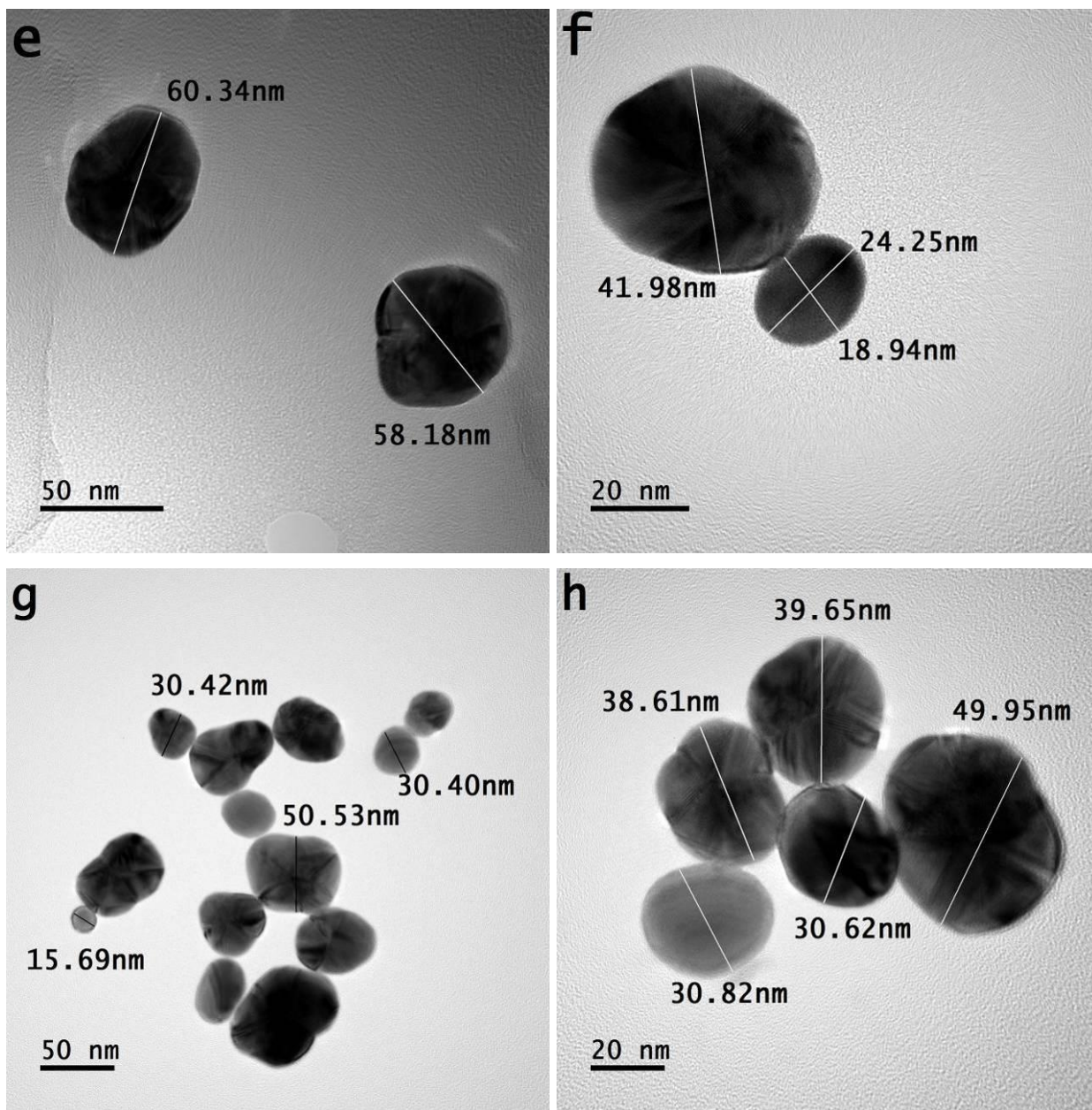
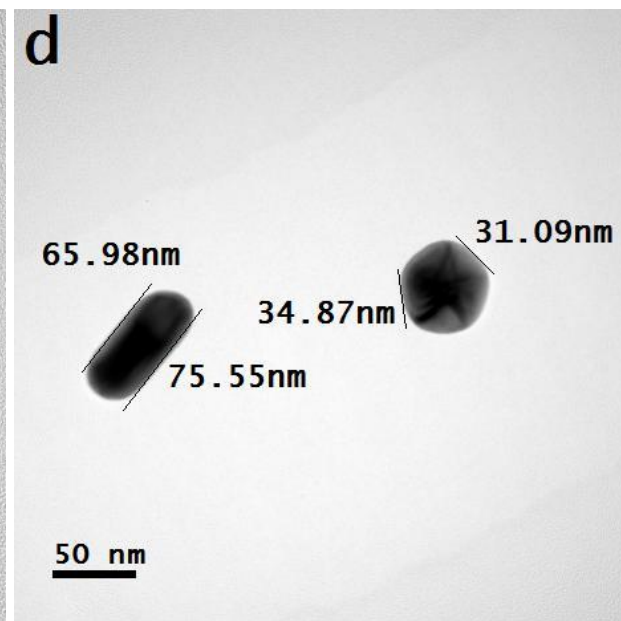
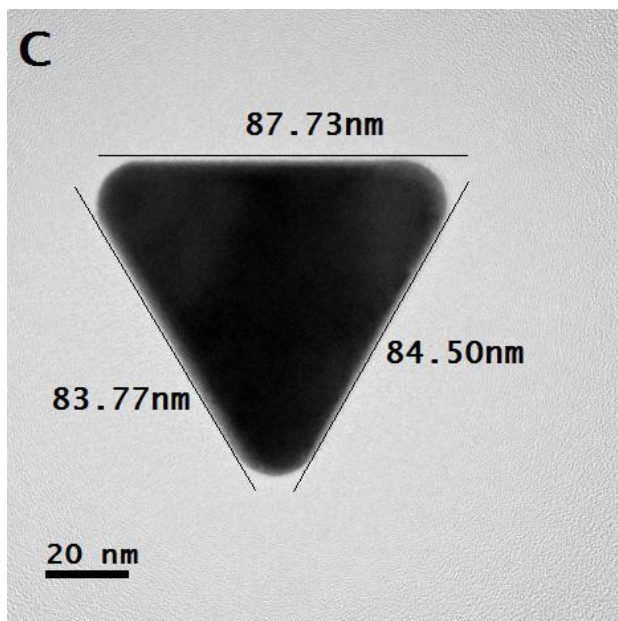
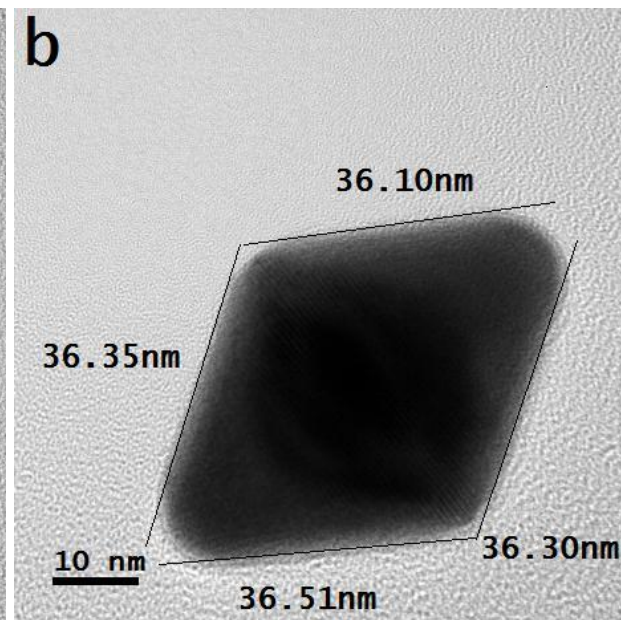
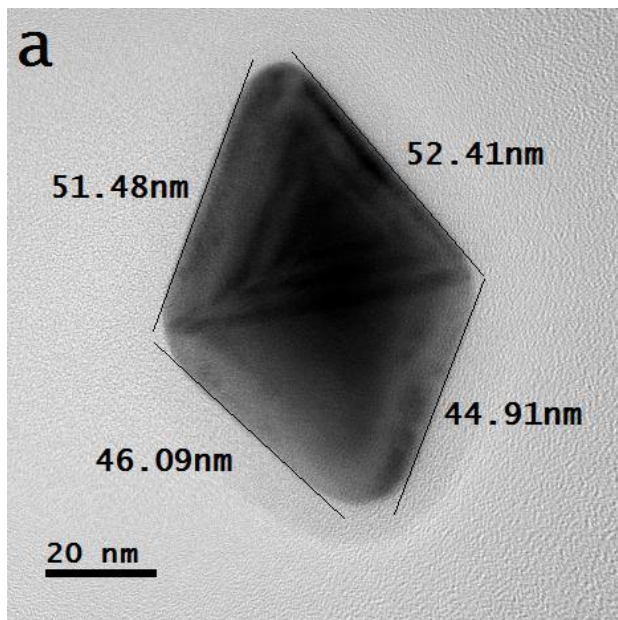
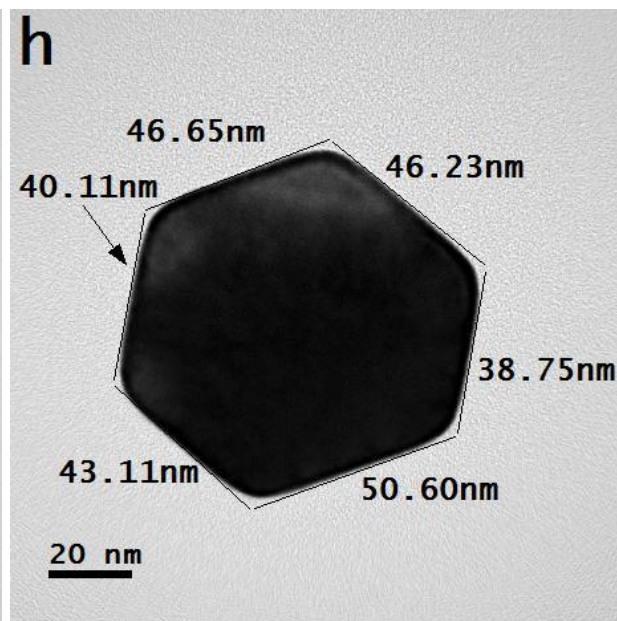
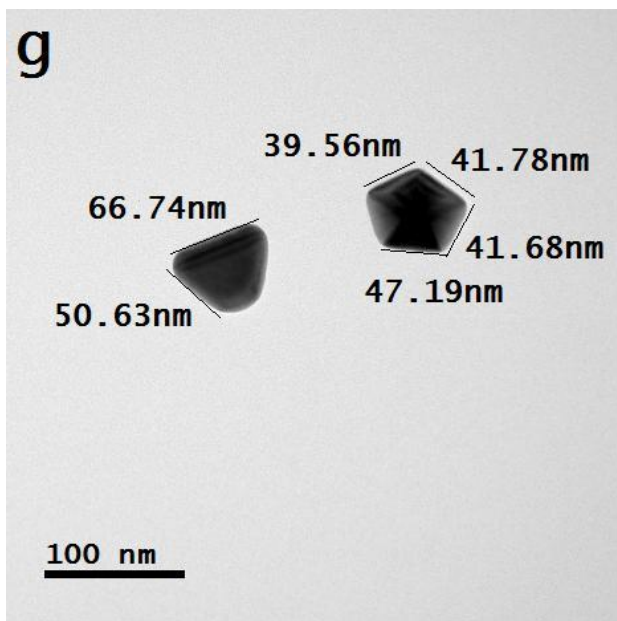
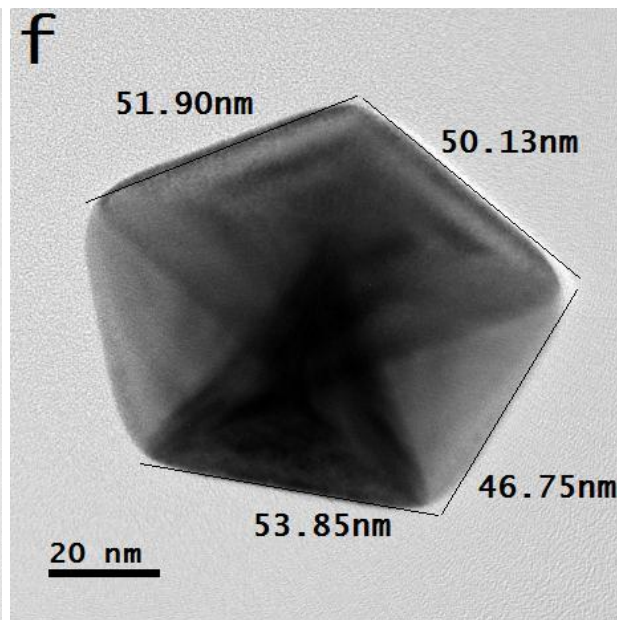
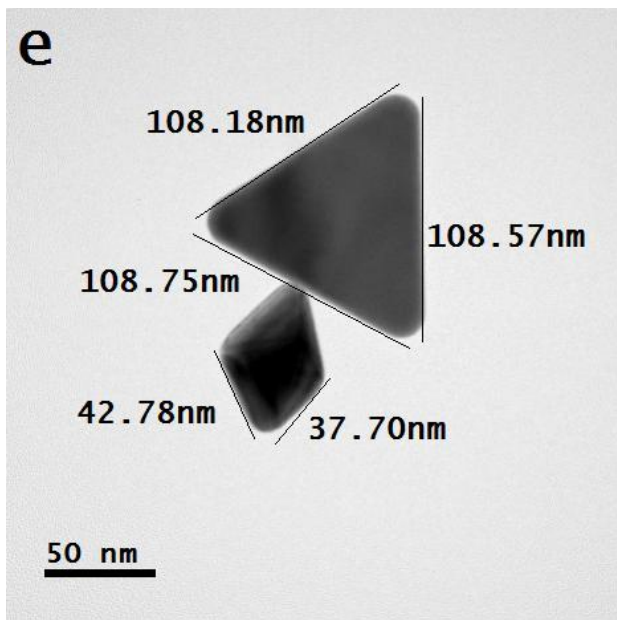


Figure S1: (a-h) bright field transmission microscope images of various distorted nanoparticles and particles; pulse ON time 5 μ sec and pulse OFF time 30 μ sec and precursor concentration 0.20 mM.





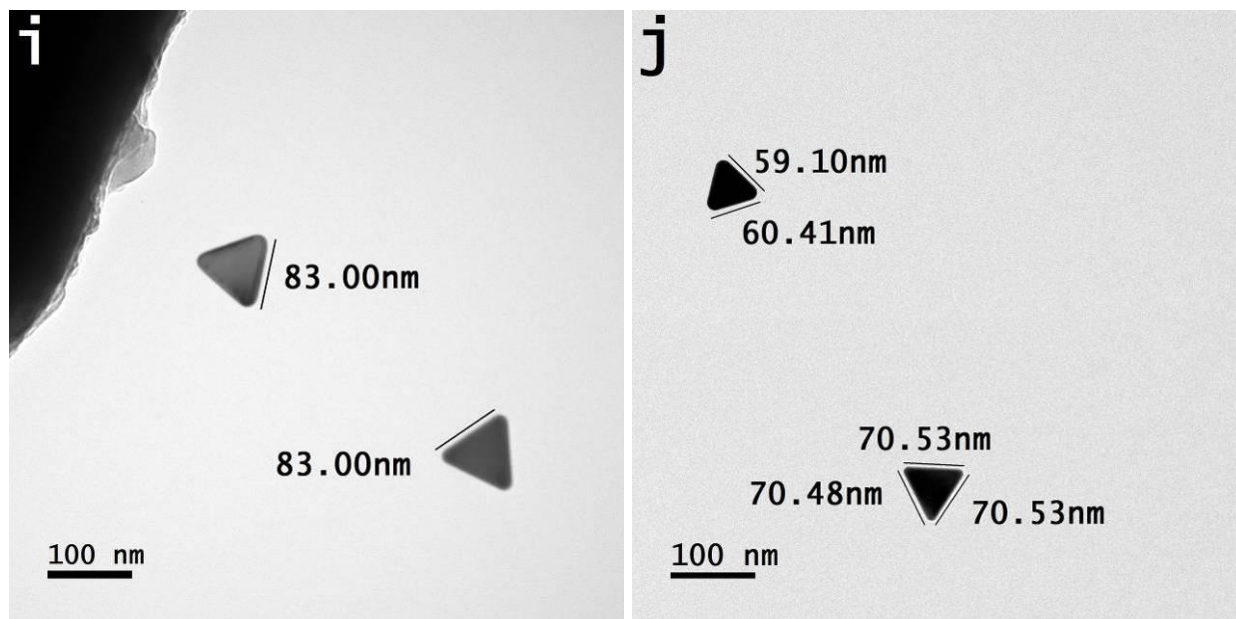
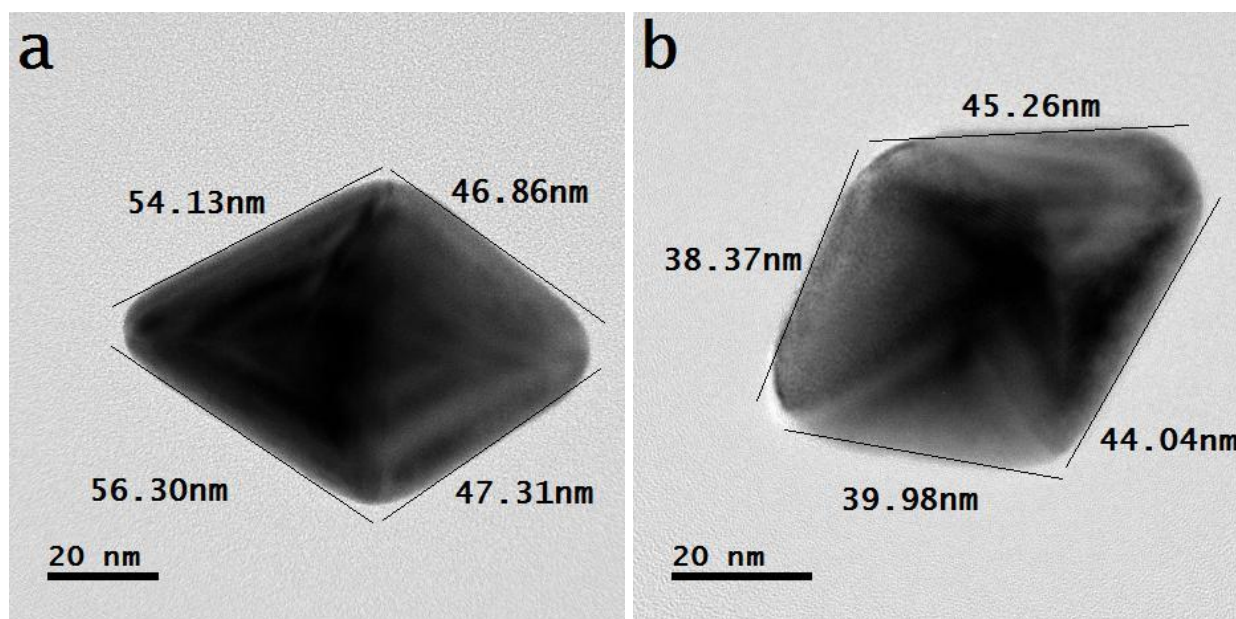
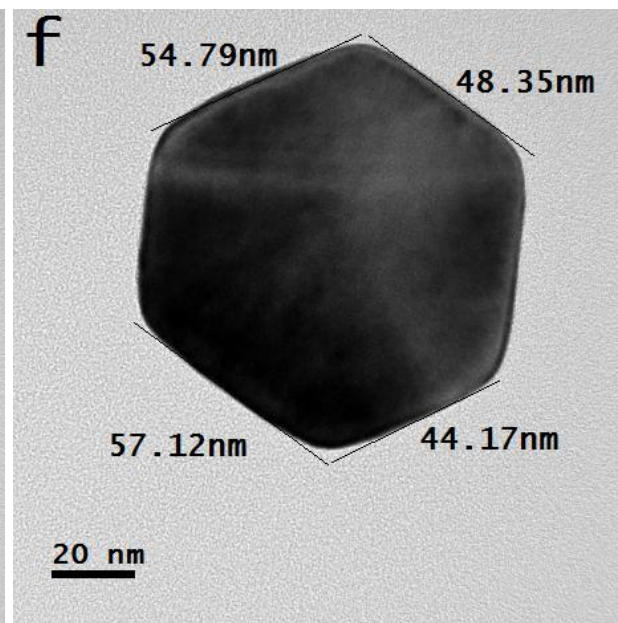
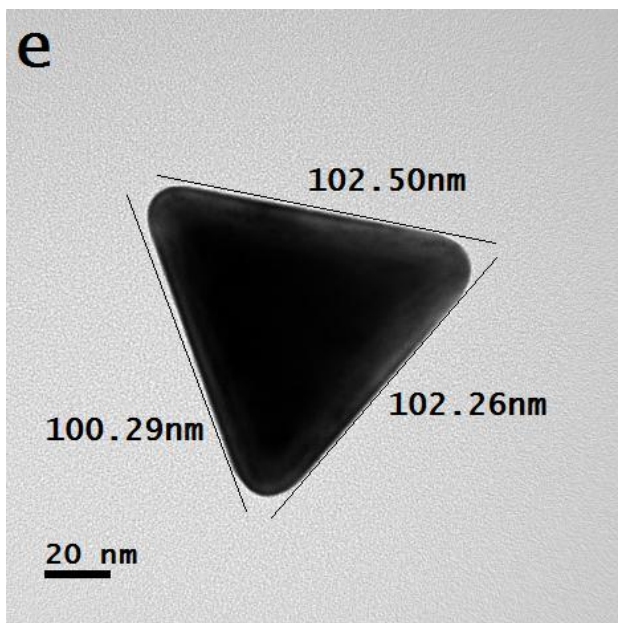
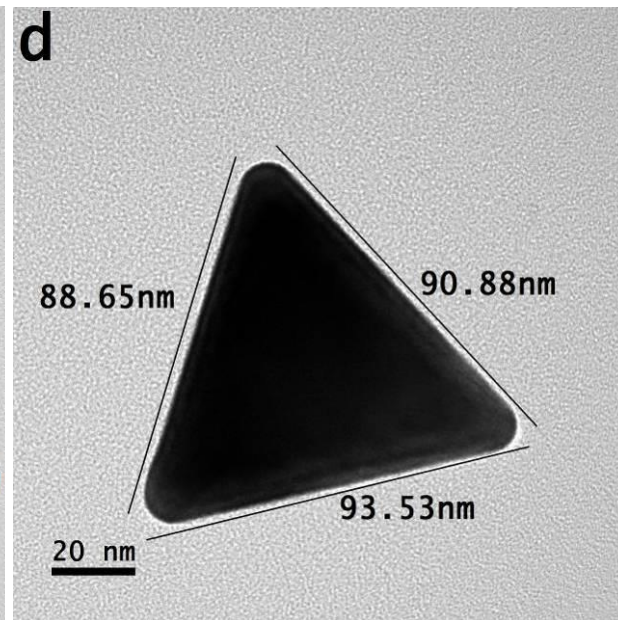
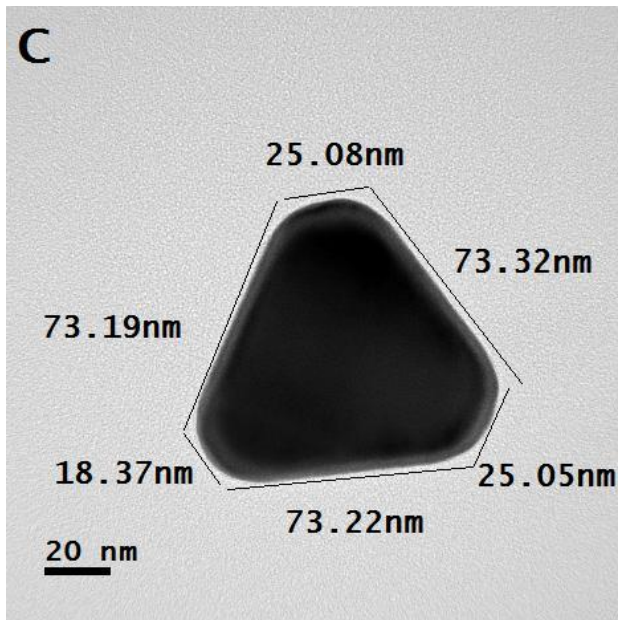
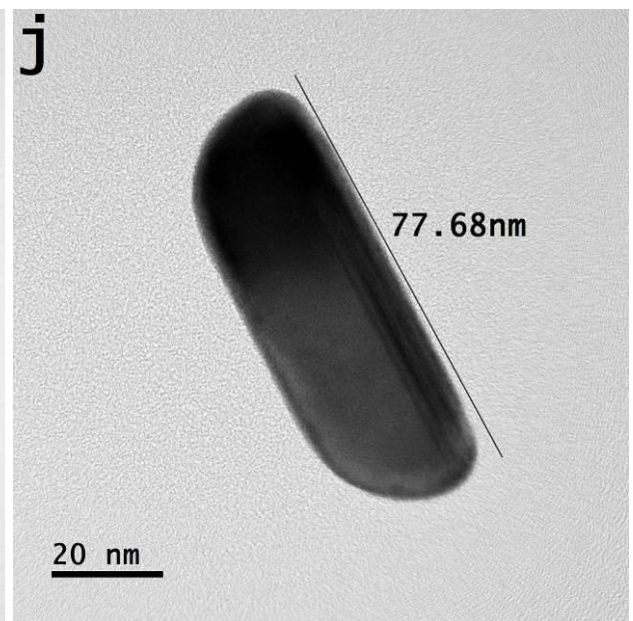
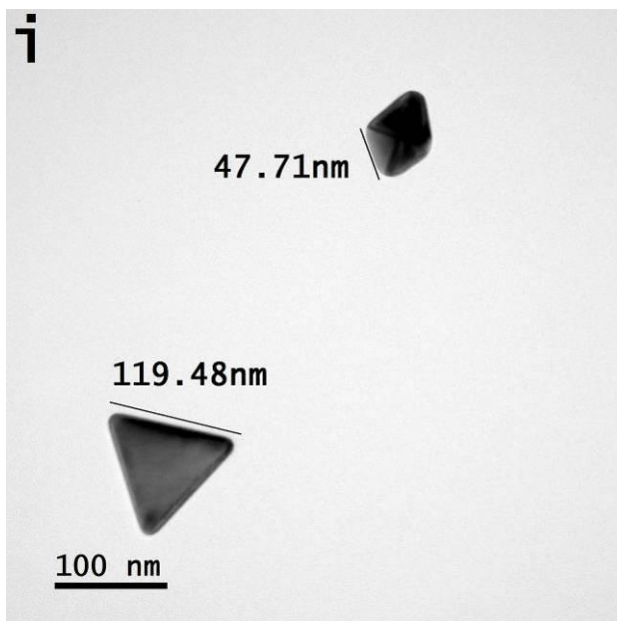
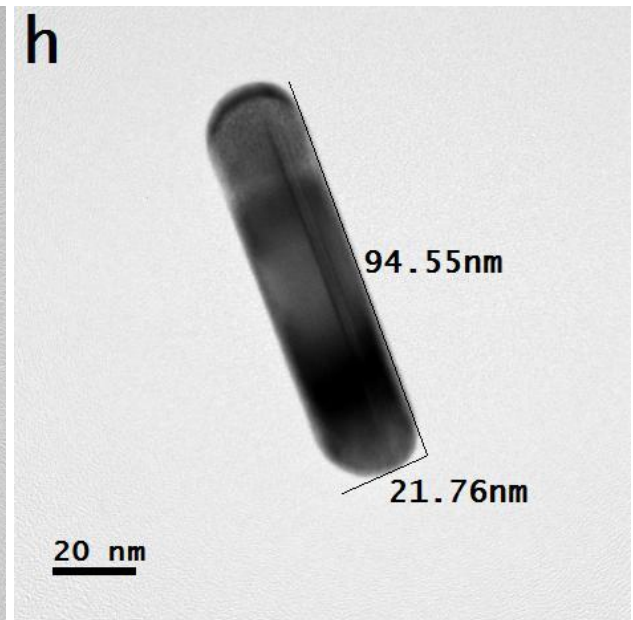
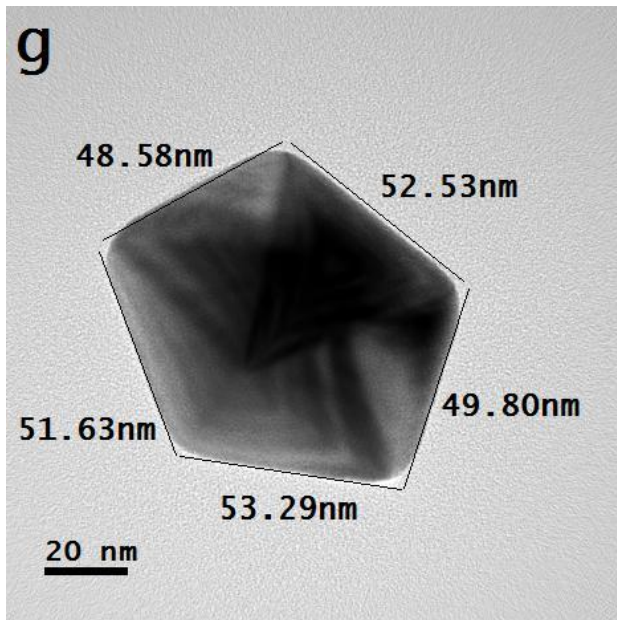


Figure S2: (a-j) bright field transmission microscope images of various geometric anisotropic shaped nanoparticles and particles; pulse ON time 10 μ sec and pulse OFF time 30 μ sec and precursor concentration 0.20 mM.







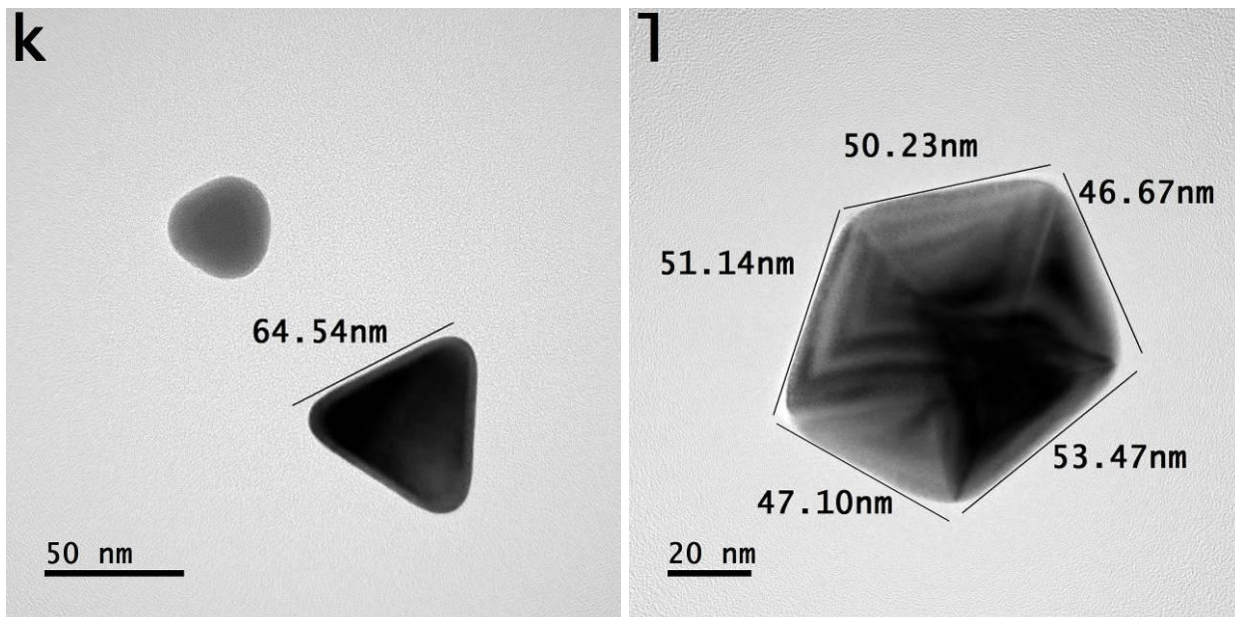
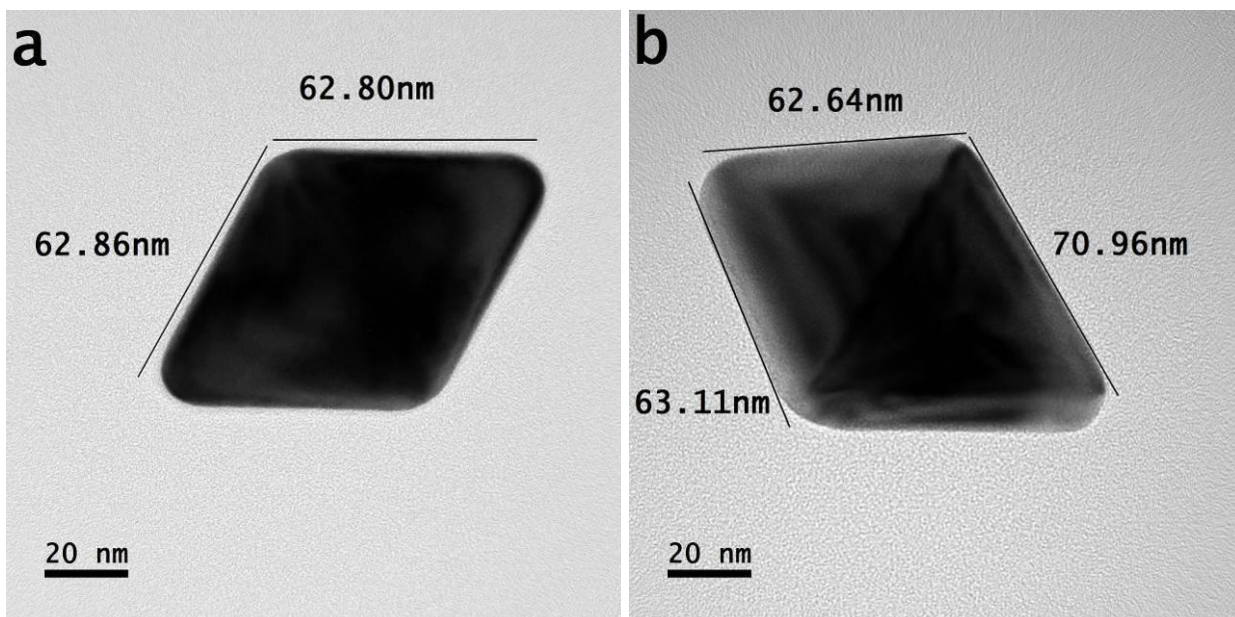
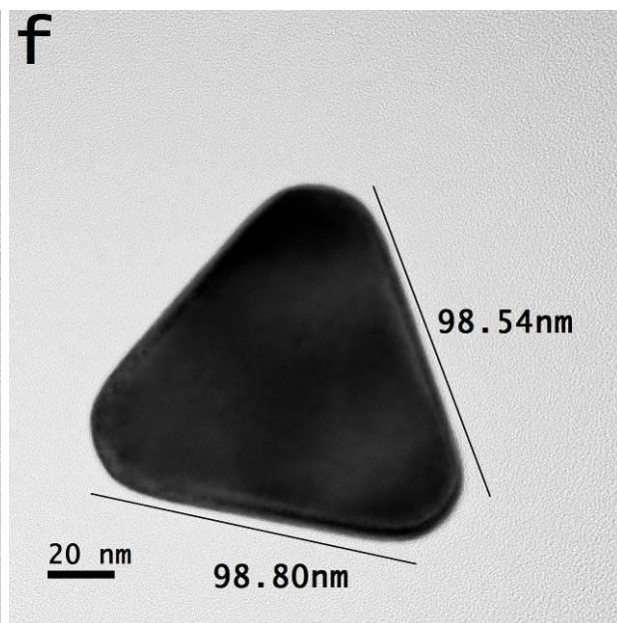
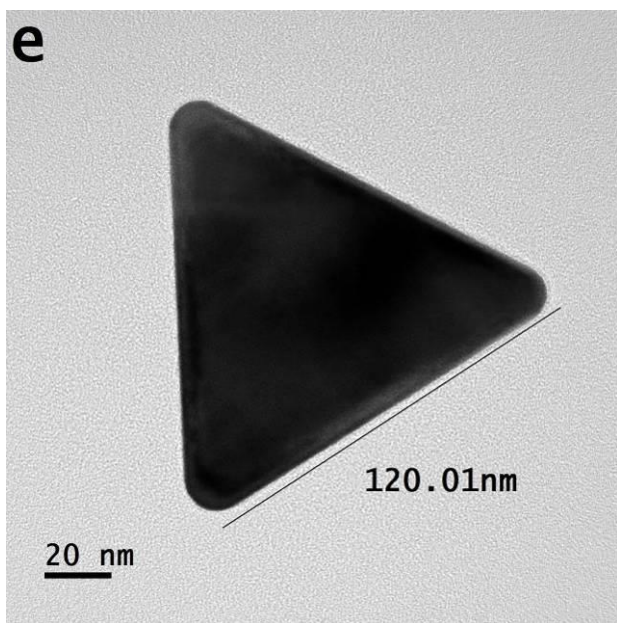
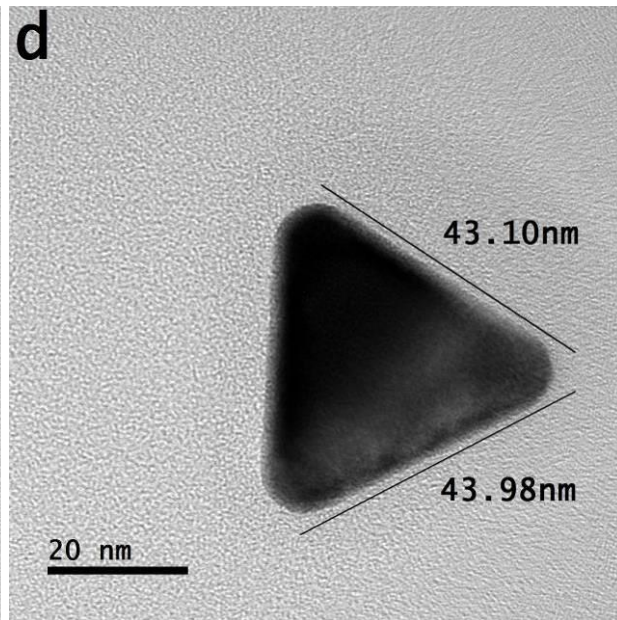
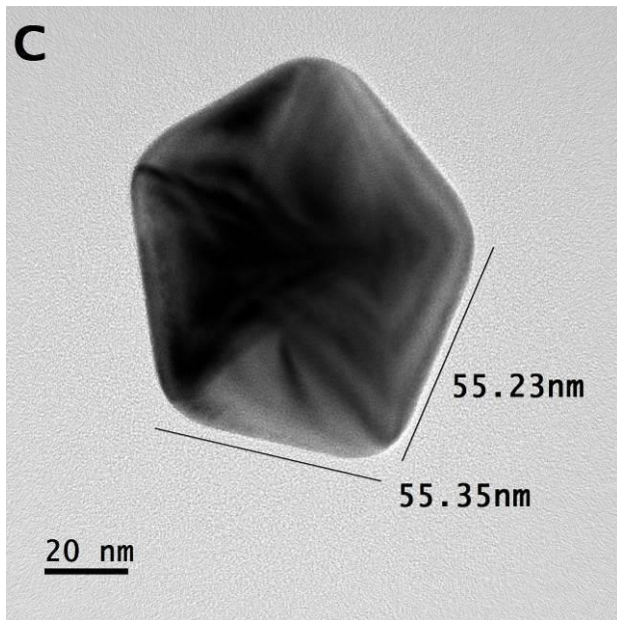


Figure S3: (a-l) bright field transmission microscope images of various geometric anisotropic shaped nanoparticles and particles; pulse ON time 15 μ sec and pulse OFF time 15 μ sec and precursor concentration 0.20 mM.





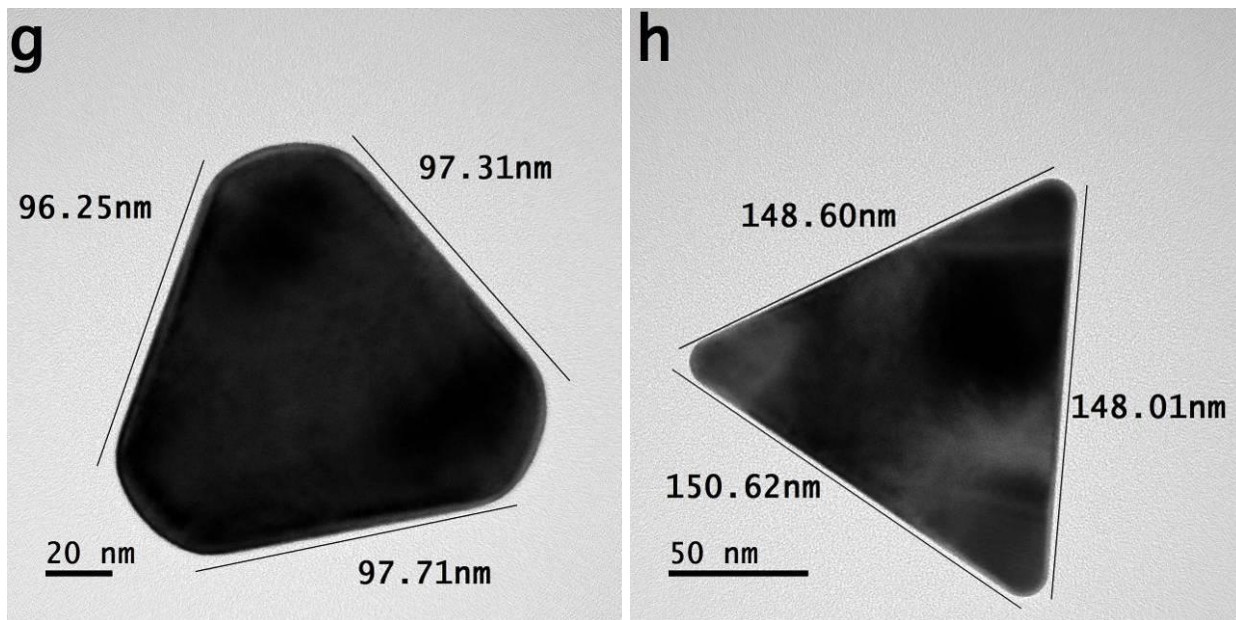
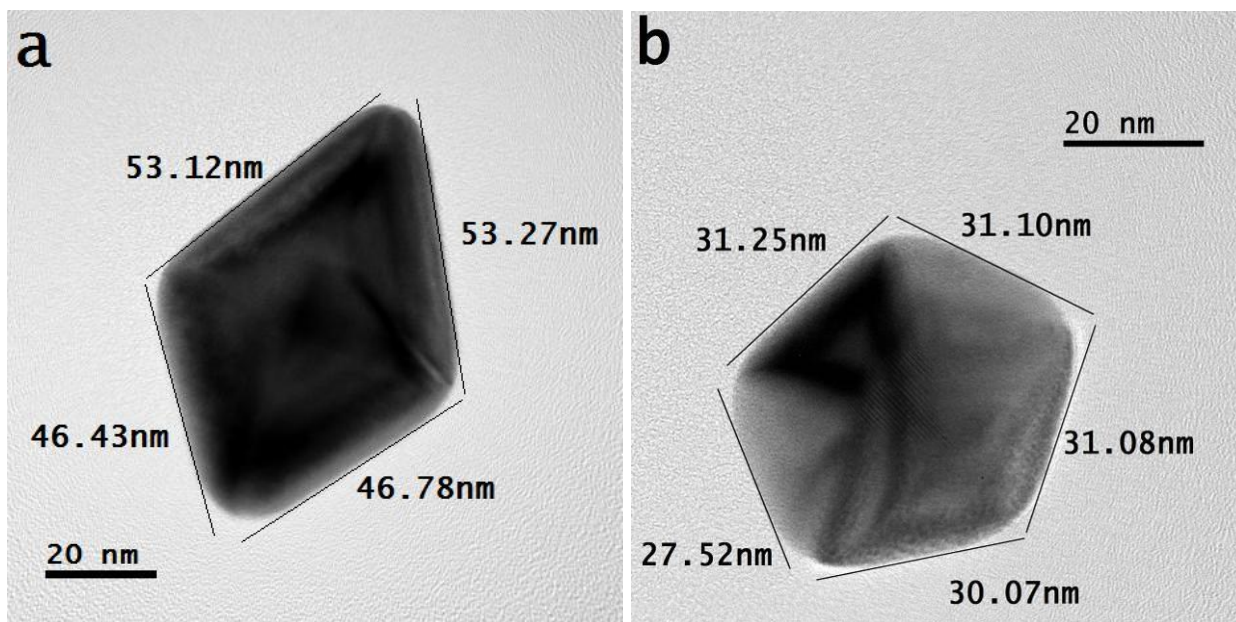
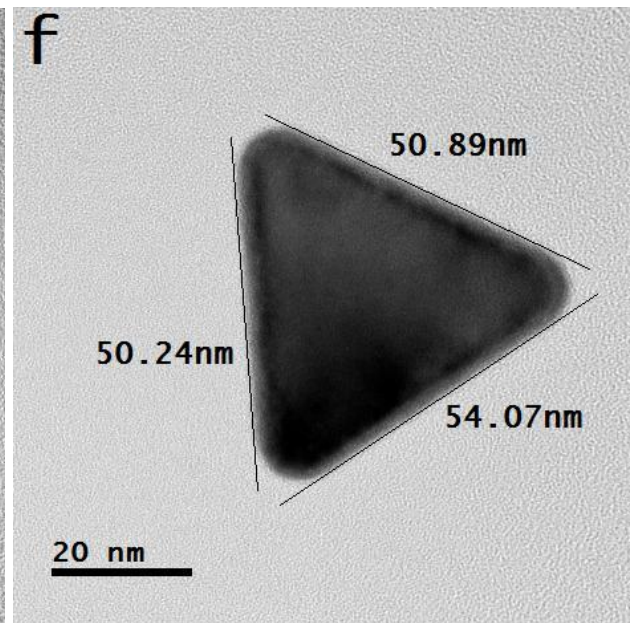
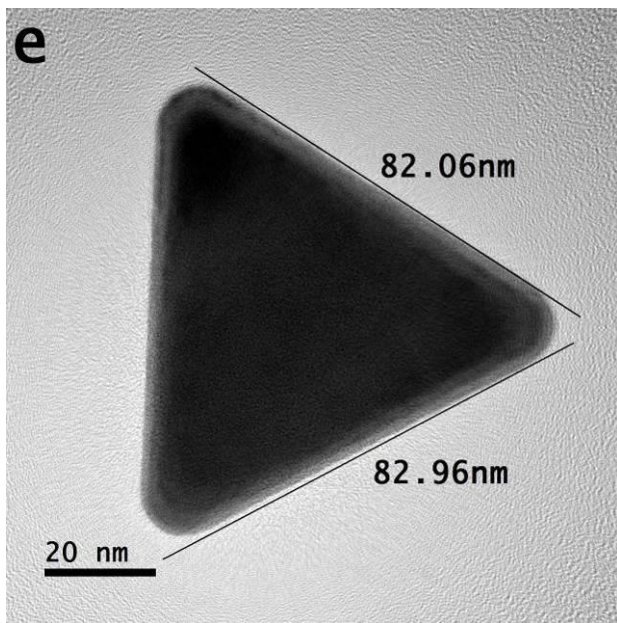
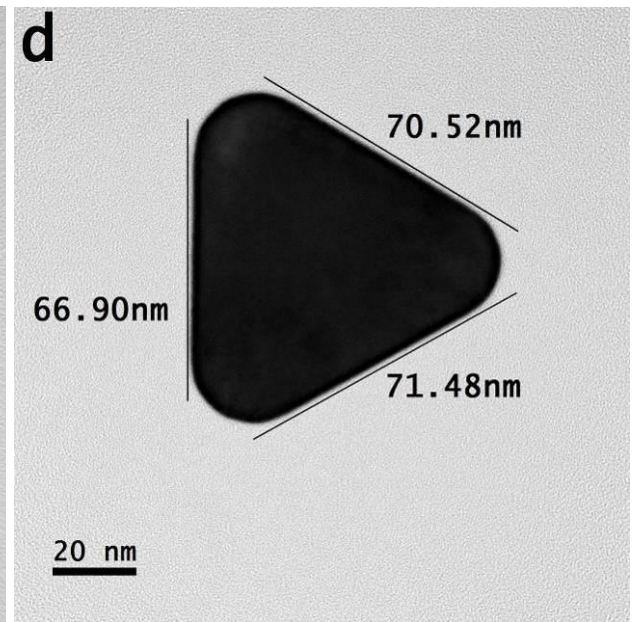
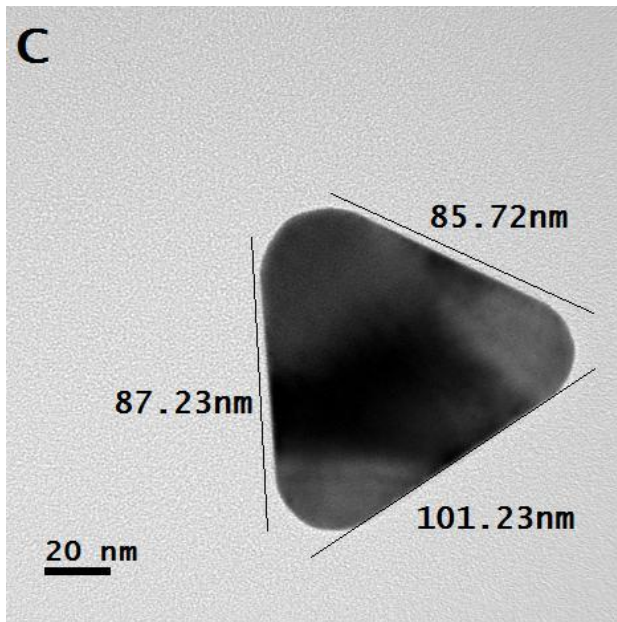


Figure S4: (a-h) bright field transmission microscope images of various geometric anisotropic shaped nanoparticles and particles; pulse ON time 30 μ sec and pulse OFF time 5 μ sec and precursor concentration 0.20 mM.





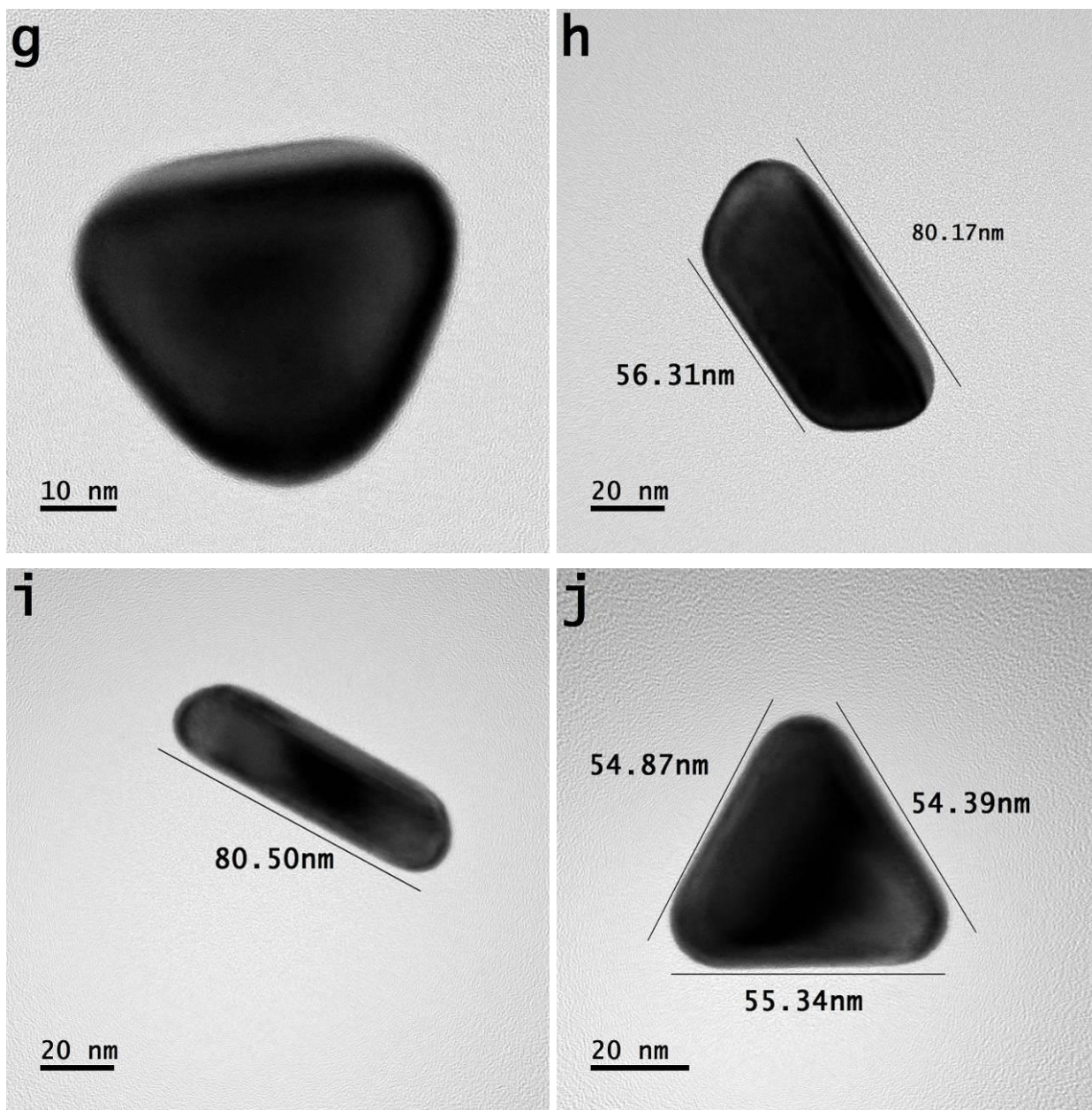


Figure S5: (a-j) bright field transmission microscope images of various geometric anisotropic shaped nanoparticles and particles; pulse ON time 30 μ sec and pulse OFF time 15 μ sec and precursor concentration 0.20 mM.

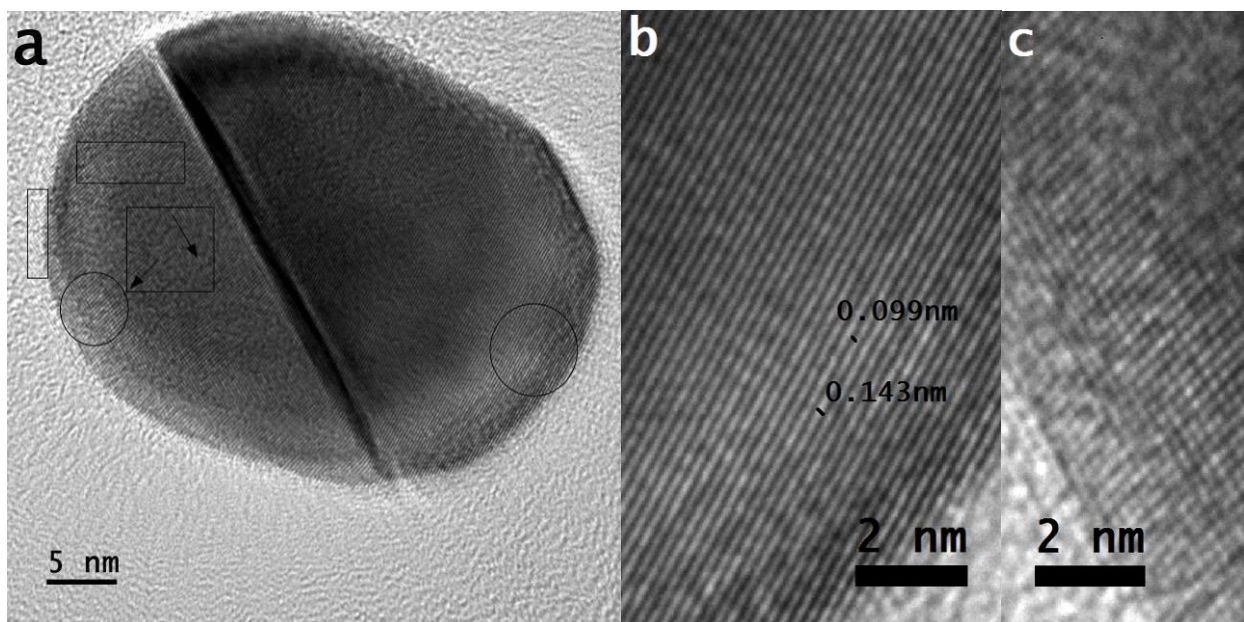


Figure S6: (a) high-resolution transmission microscope image of distorted nanoparticle, (b) magnified image of the region covered under large circle in 'a' and (c) magnified image of the region covered under smaller circle in 'a'; pulse ON time 5 μ sec and pulse OFF time 30 μ sec and precursor concentration 0.20 mM.

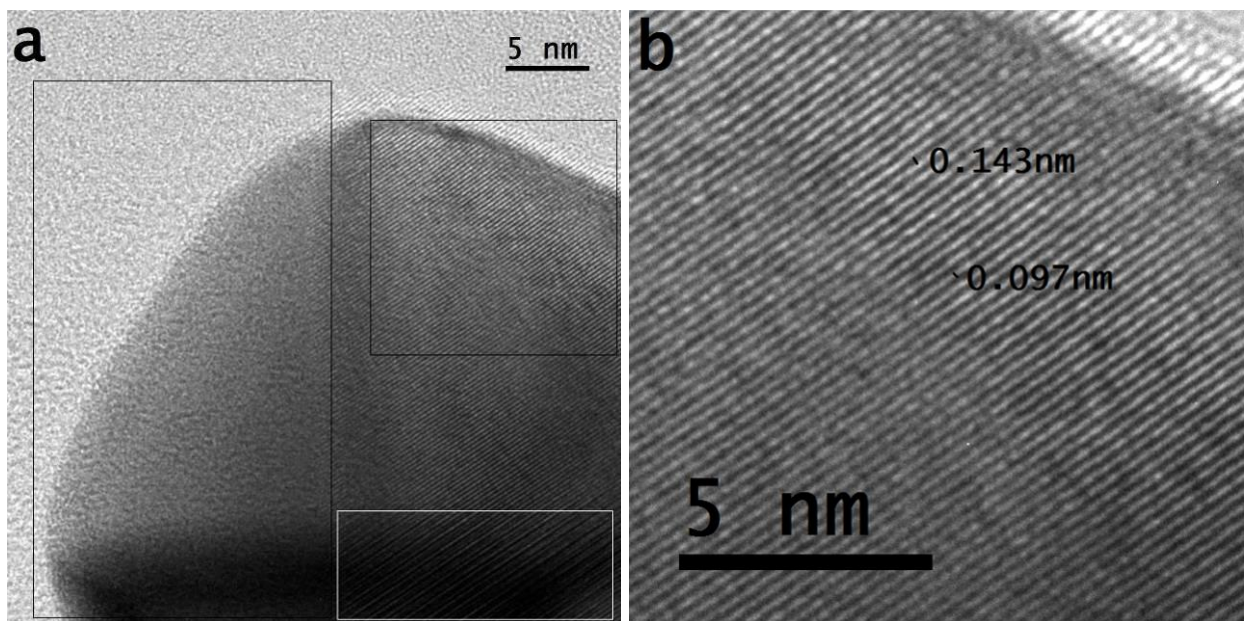


Figure S7: (a) high-resolution transmission microscope image of pentagonal-shaped nanoparticle and (b) magnified image of the region covered under square in 'a'; pulse ON time 30 μ sec and pulse OFF time 5 μ sec and precursor concentration 0.20 mM.

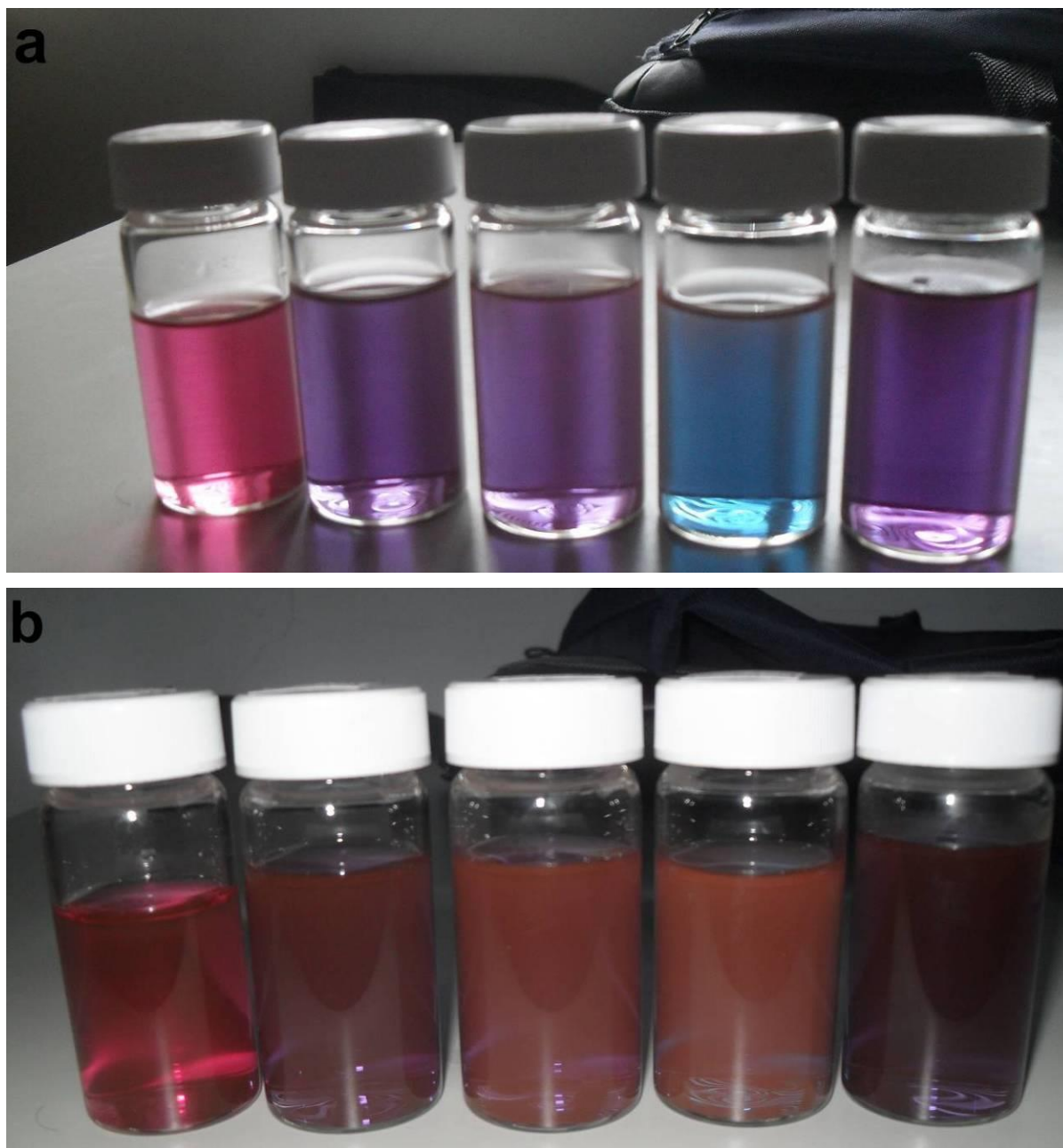
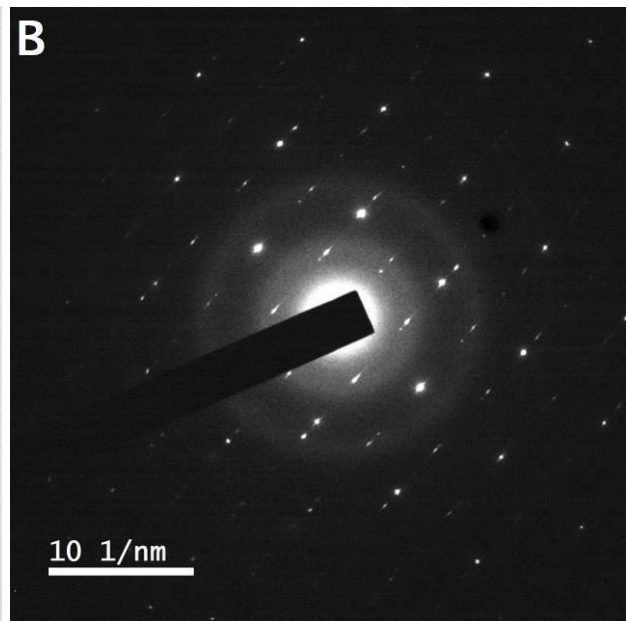
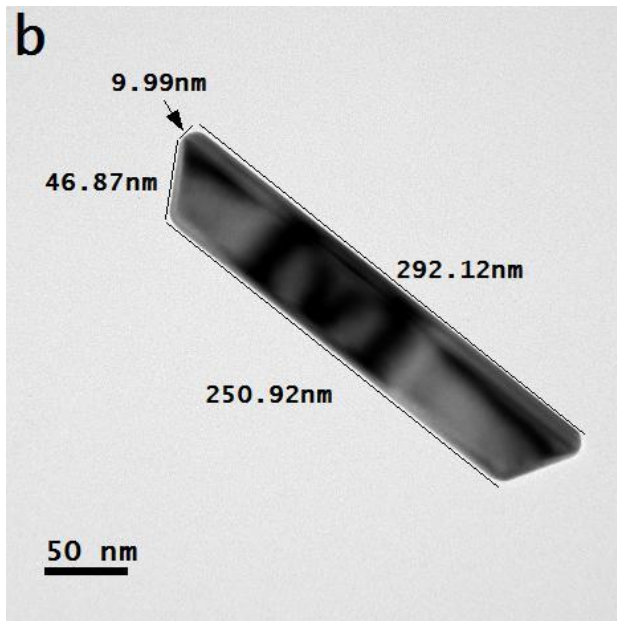
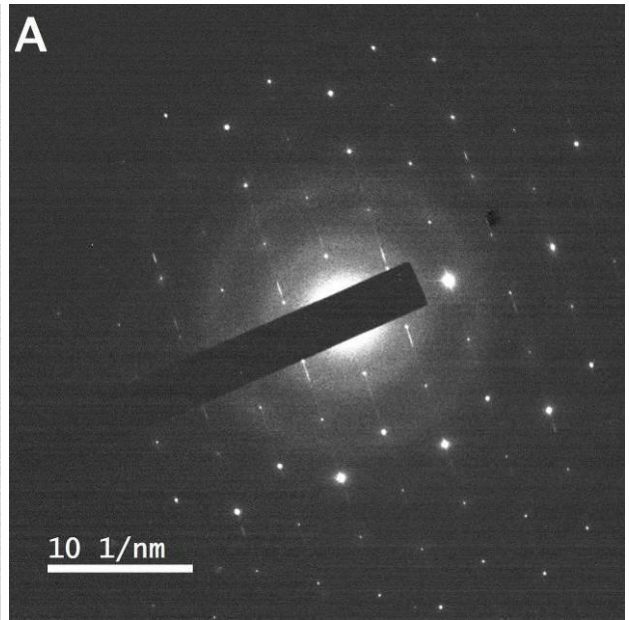
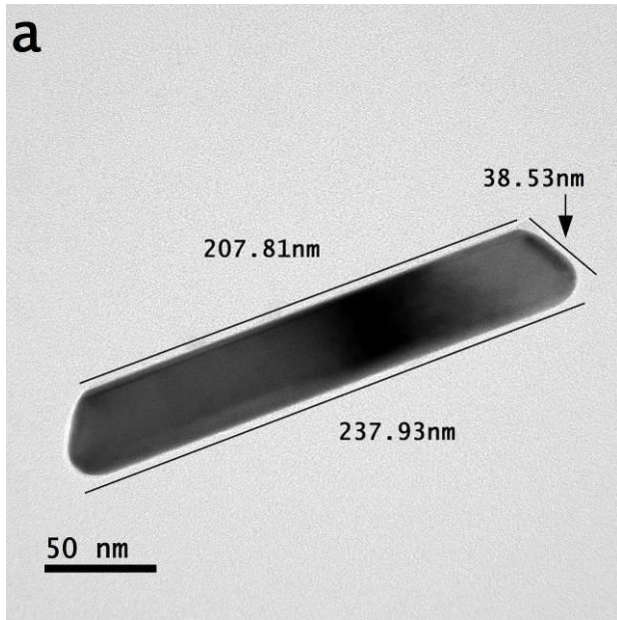
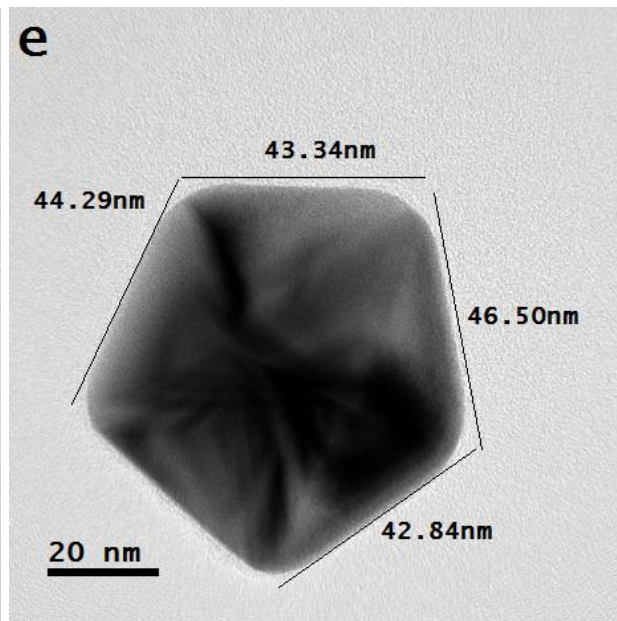
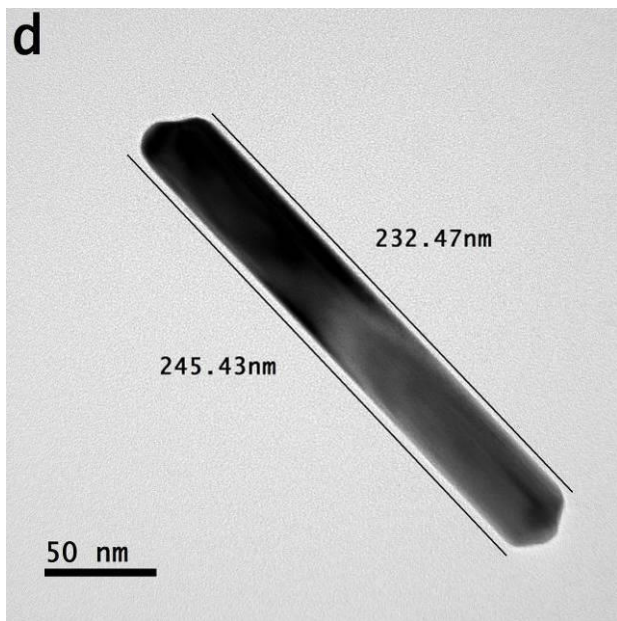
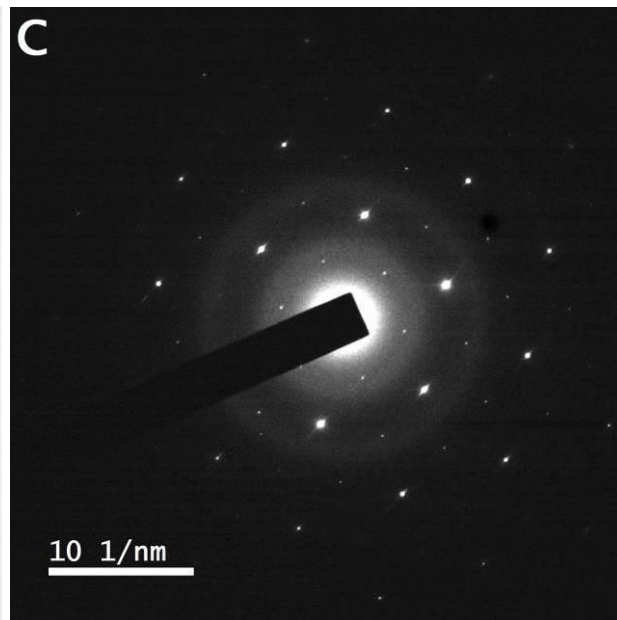
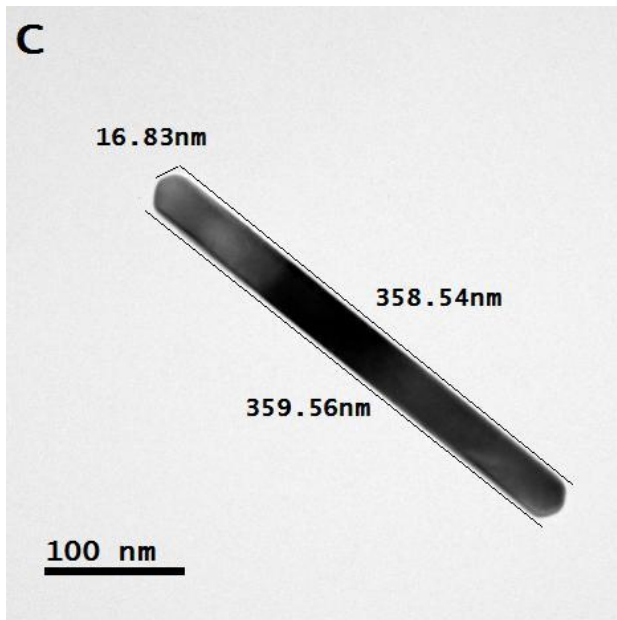


Figure S8: Color of processed solutions at different pulse ON/OFF time (a) in the sunlight and (b) in the absence of sunlight; (left to right) pulse ON time 5 μsec and pulse OFF time 30 μsec , pulse ON time 10 μsec and pulse OFF time 30 μsec , pulse ON time 15 μsec and pulse OFF time 15 μsec , pulse ON time 30 μsec and pulse OFF time 5 μsec , and pulse ON time 30 μsec and pulse OFF time 15 μsec (precursor concentration 0.20 mM).





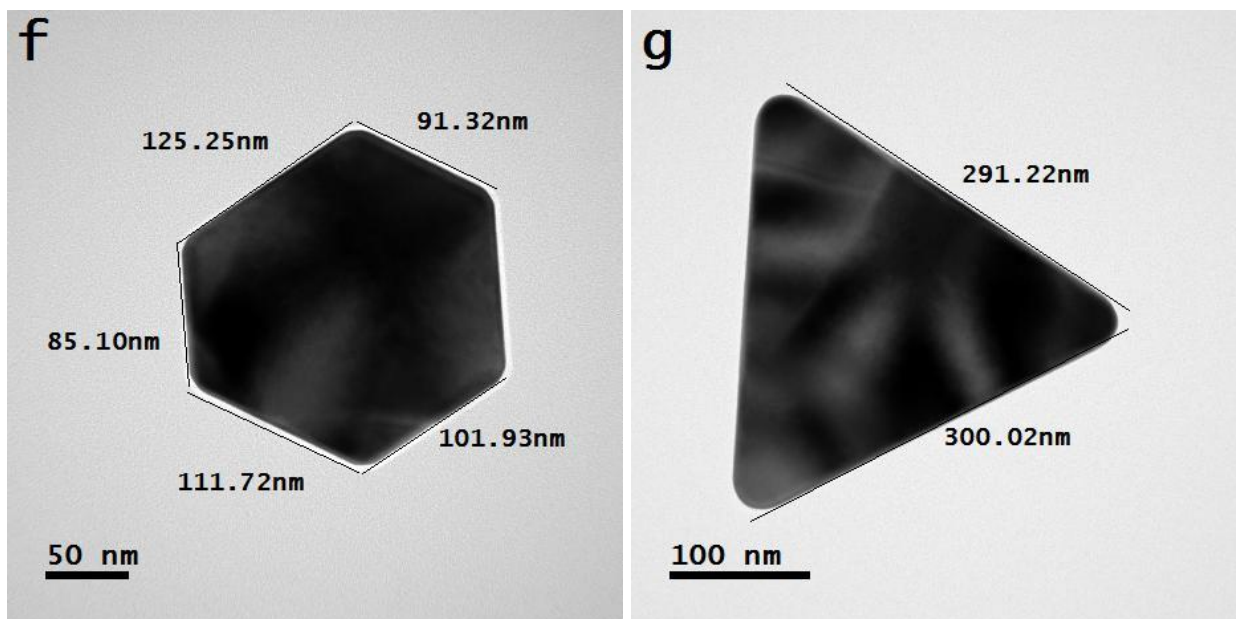
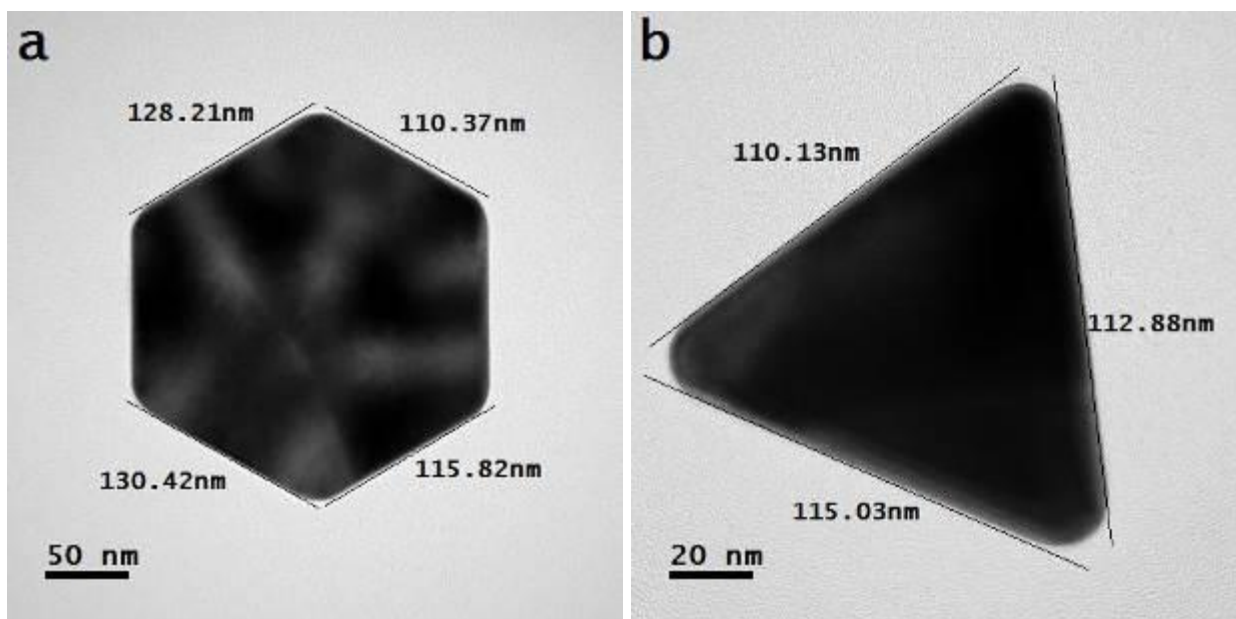
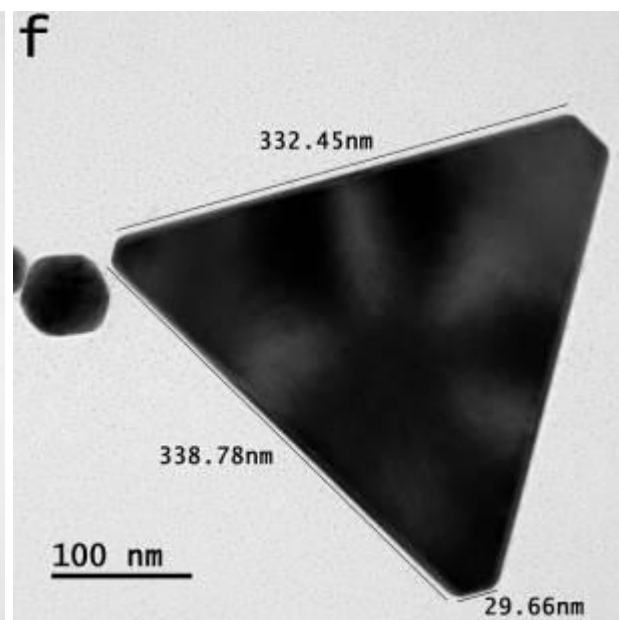
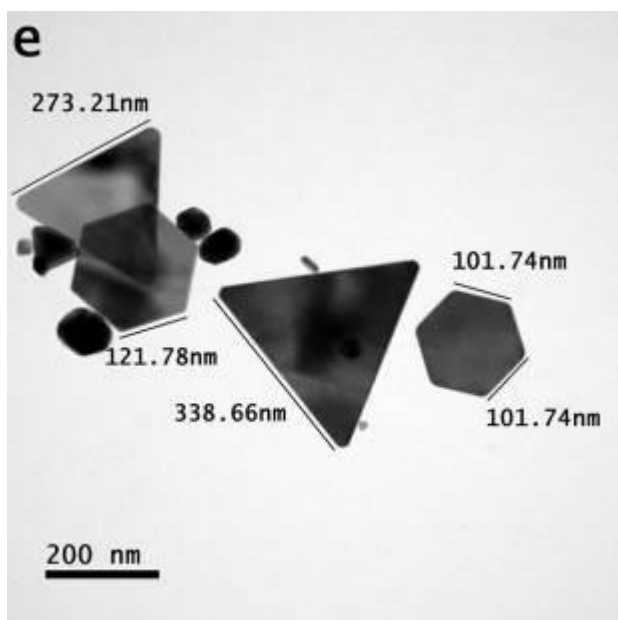
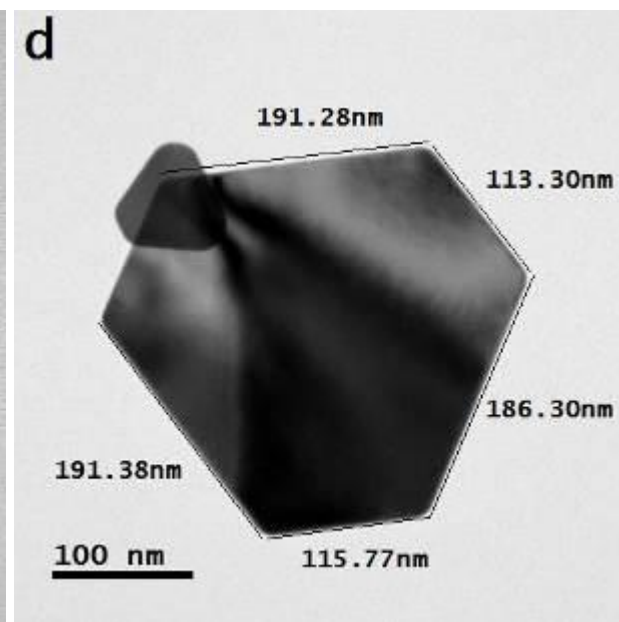
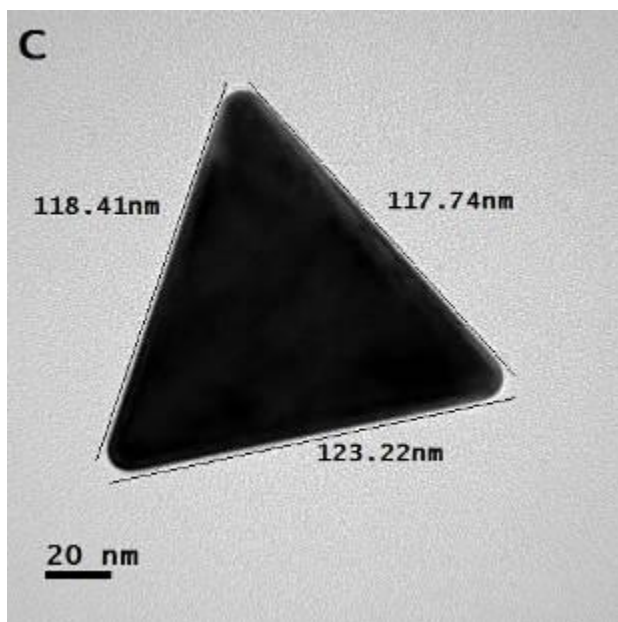


Figure S9: (a-g) bright field transmission microscope images of bar-, rod-, pentagon-, hexagon- and triangle-shaped particles/ (A-C) SAPR patterns of bar-/rod-shaped particles; pulse ON/OFF time 5 μ sec and precursor concentration 0.40 mM.





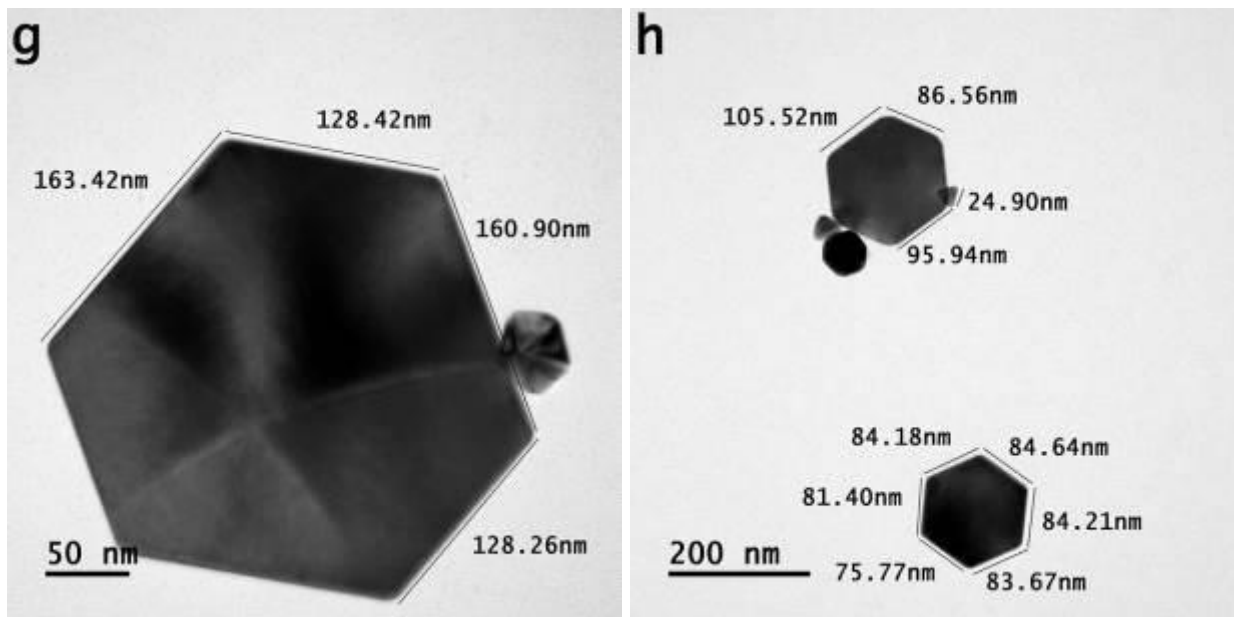
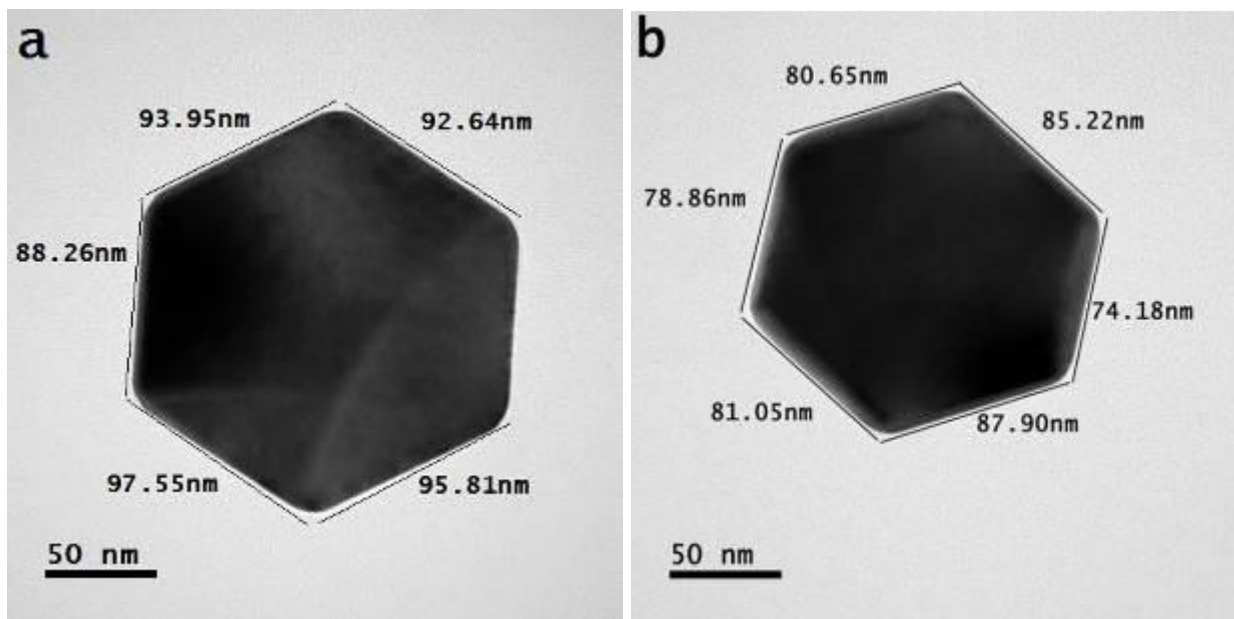
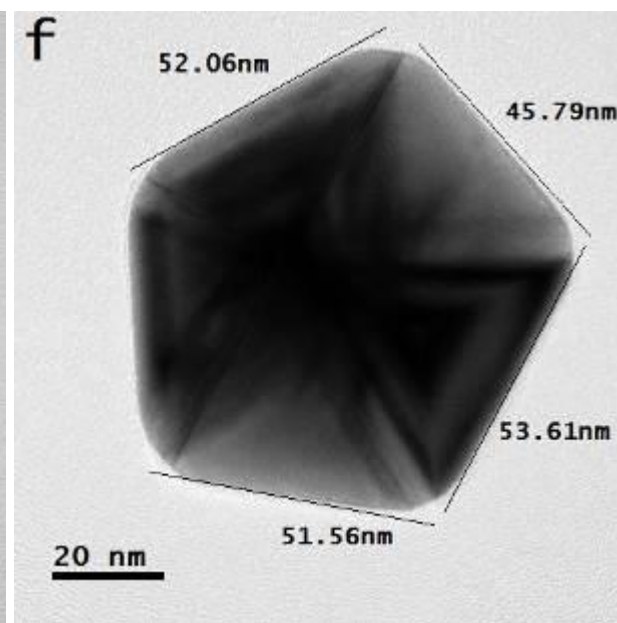
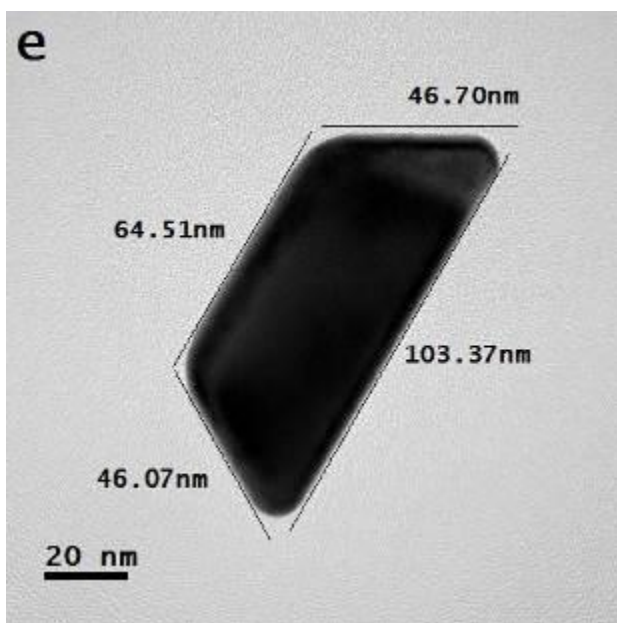
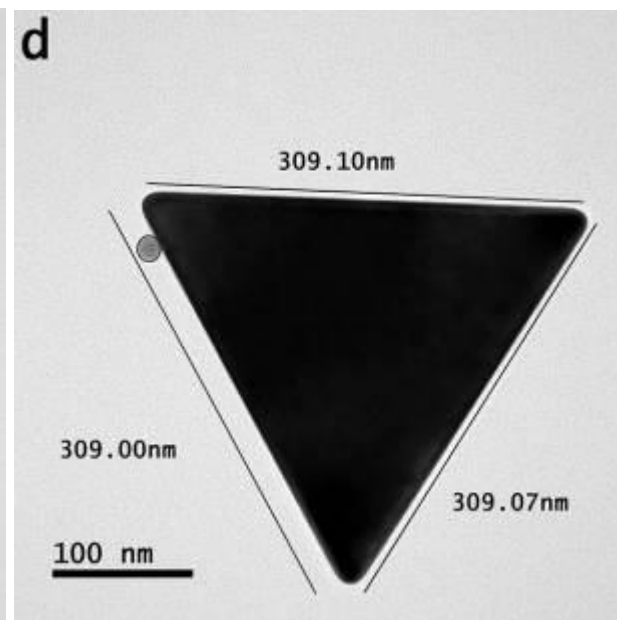
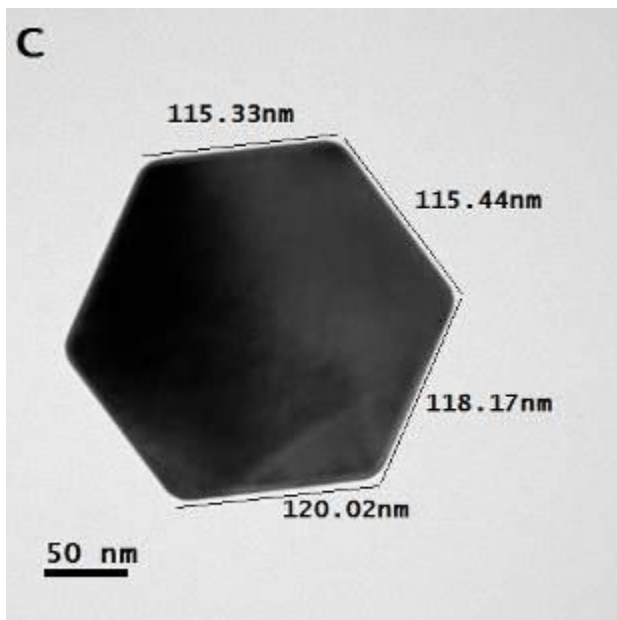
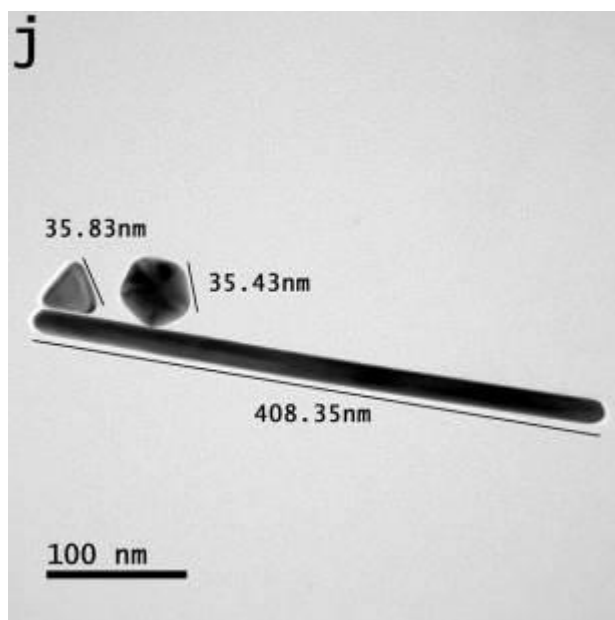
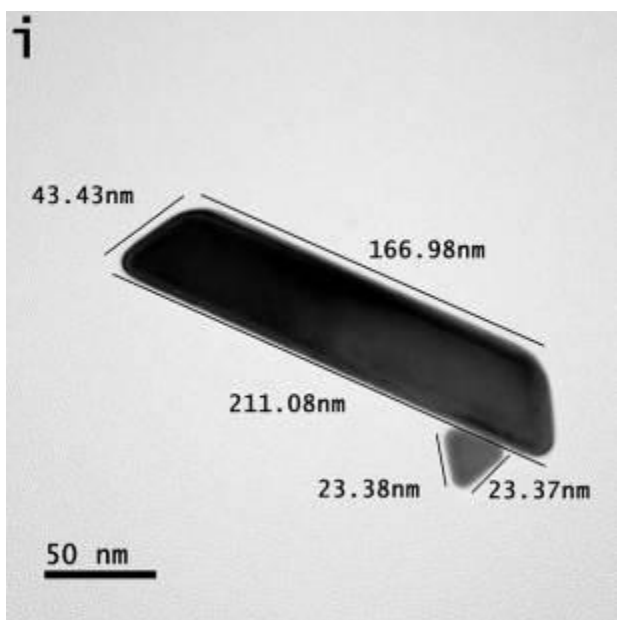
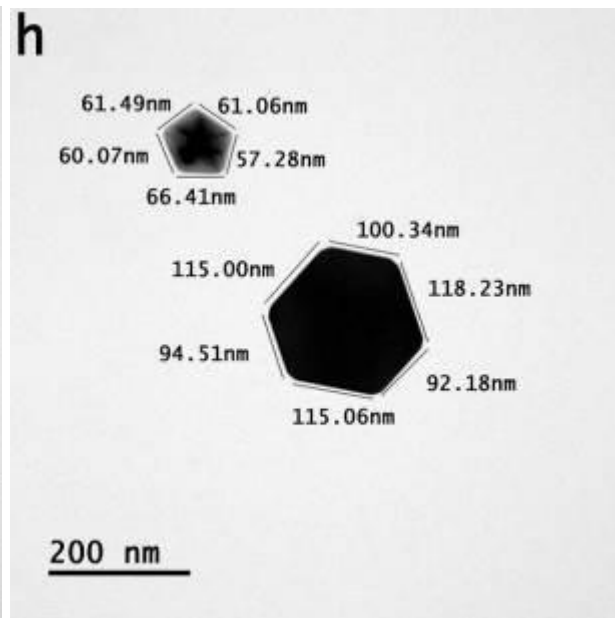
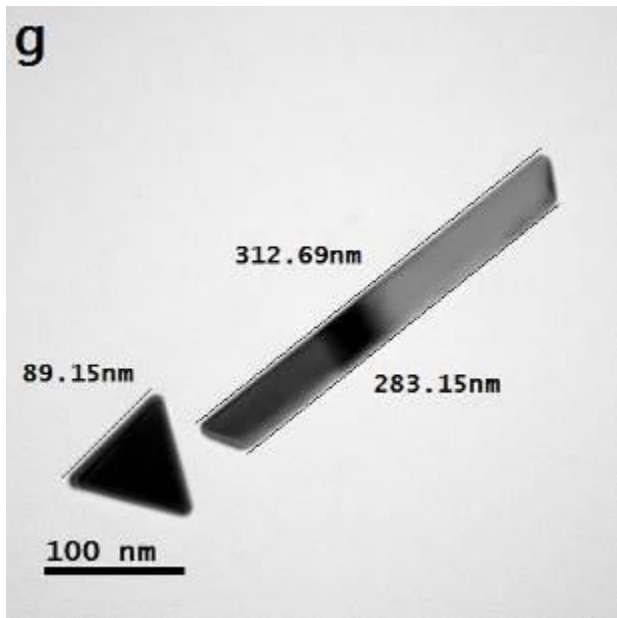
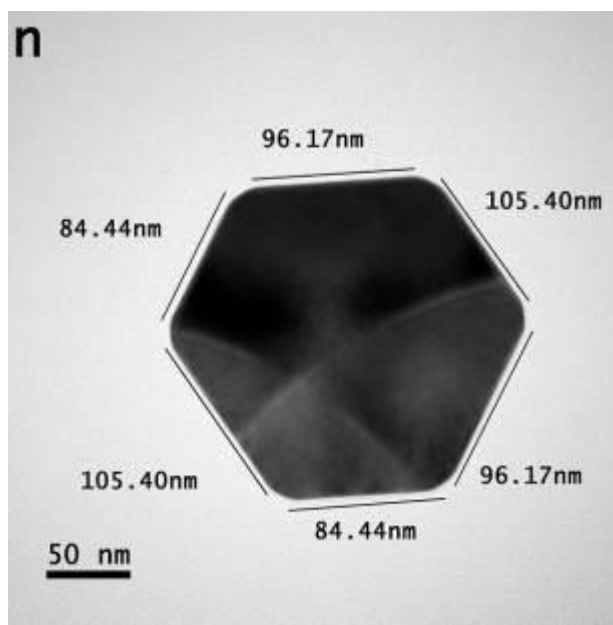
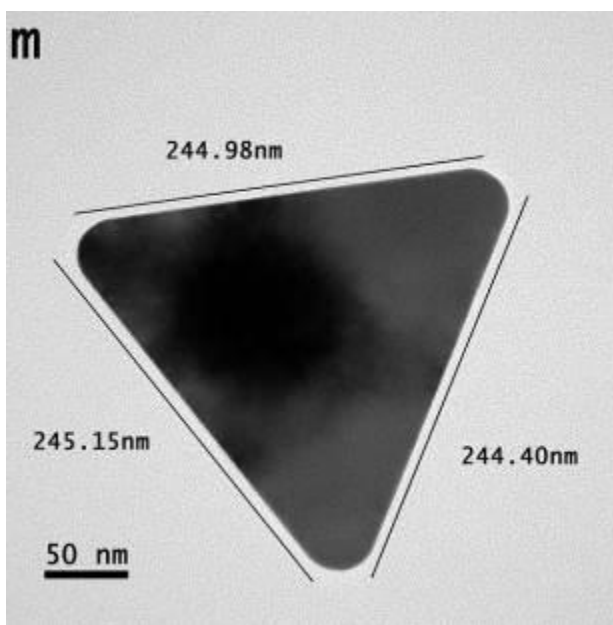
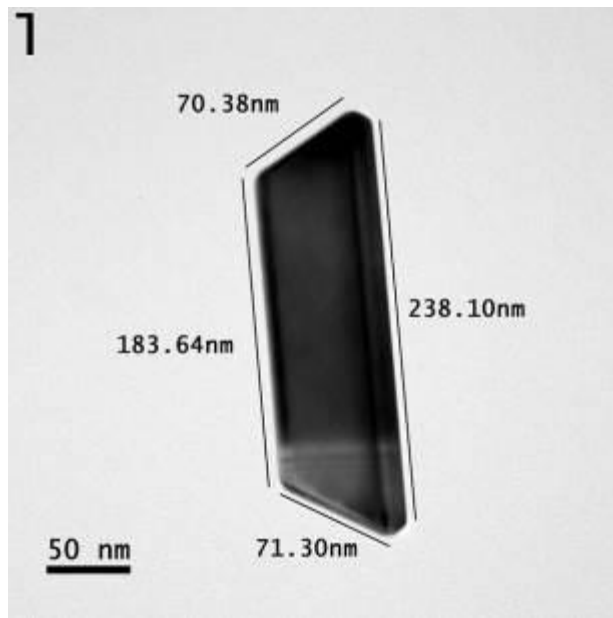
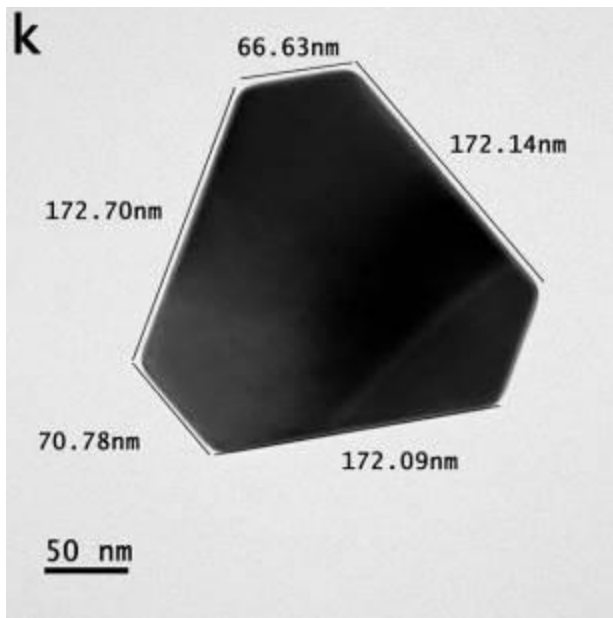


Figure S10: (a-h) bright field transmission microscope images of various nanoparticles and particles; pulse ON/OFF time 15 μ sec and precursor concentration 0.40 mM.









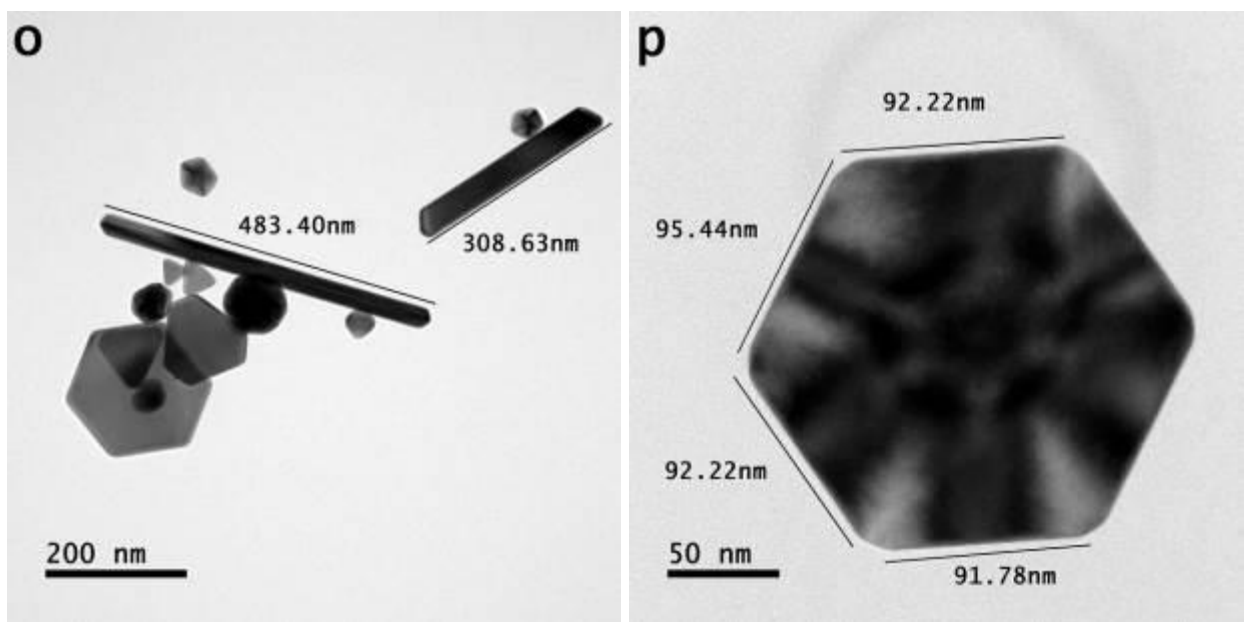
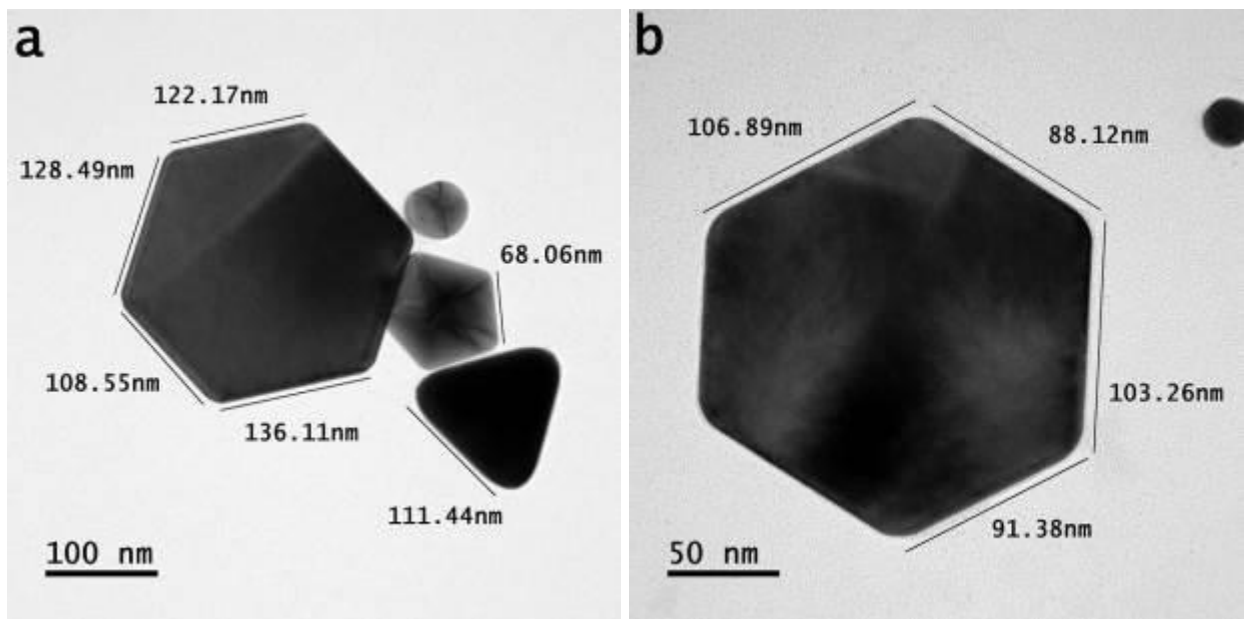
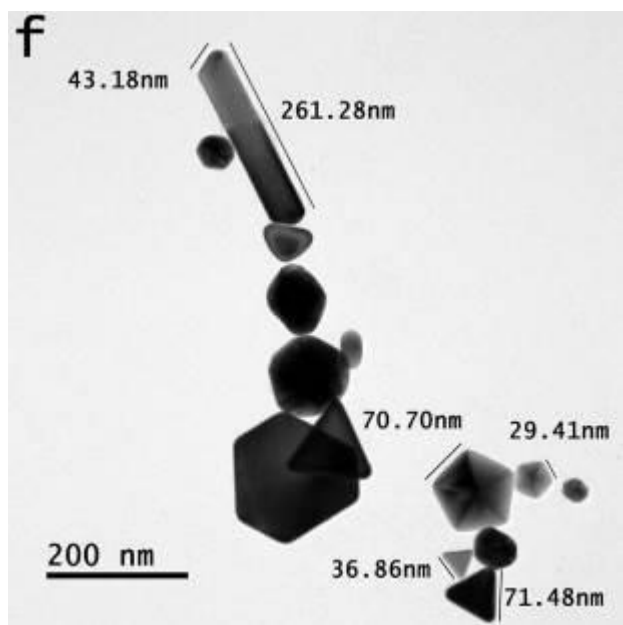
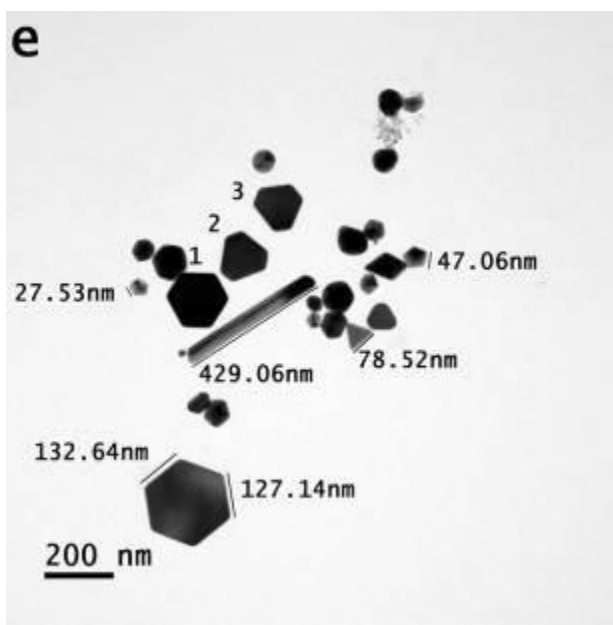
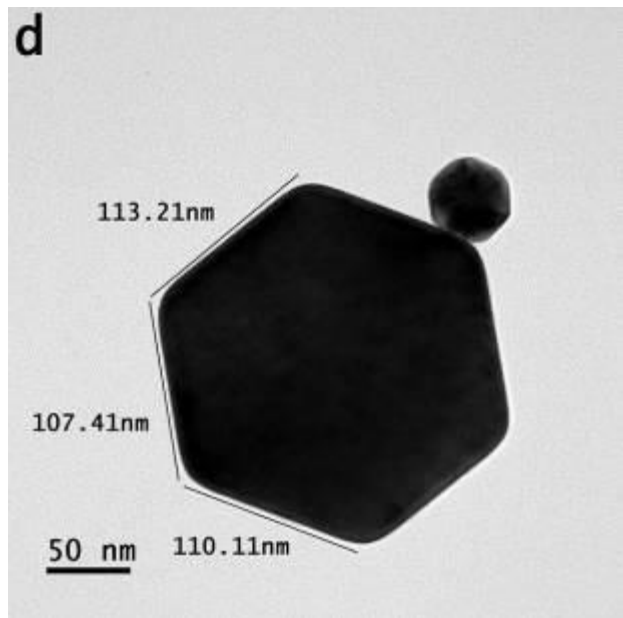
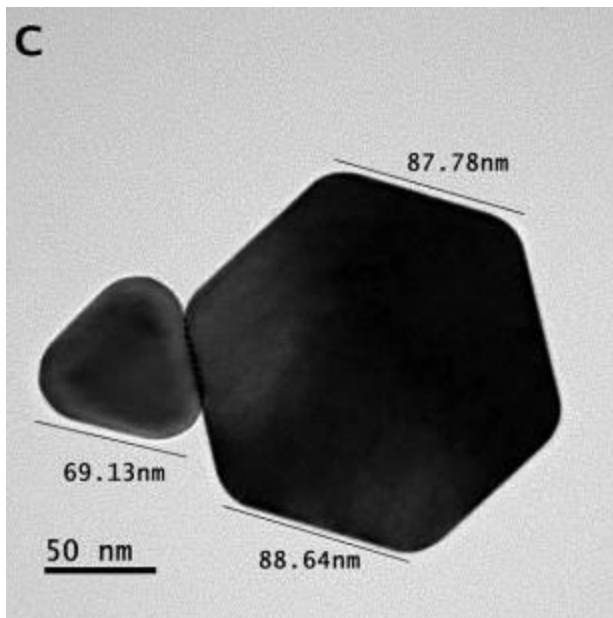


Figure S11: (a-p) bright field transmission microscope images of various nanoparticles and particles; pulse ON/OFF time 30 μ sec and precursor concentration 0.40 mM.





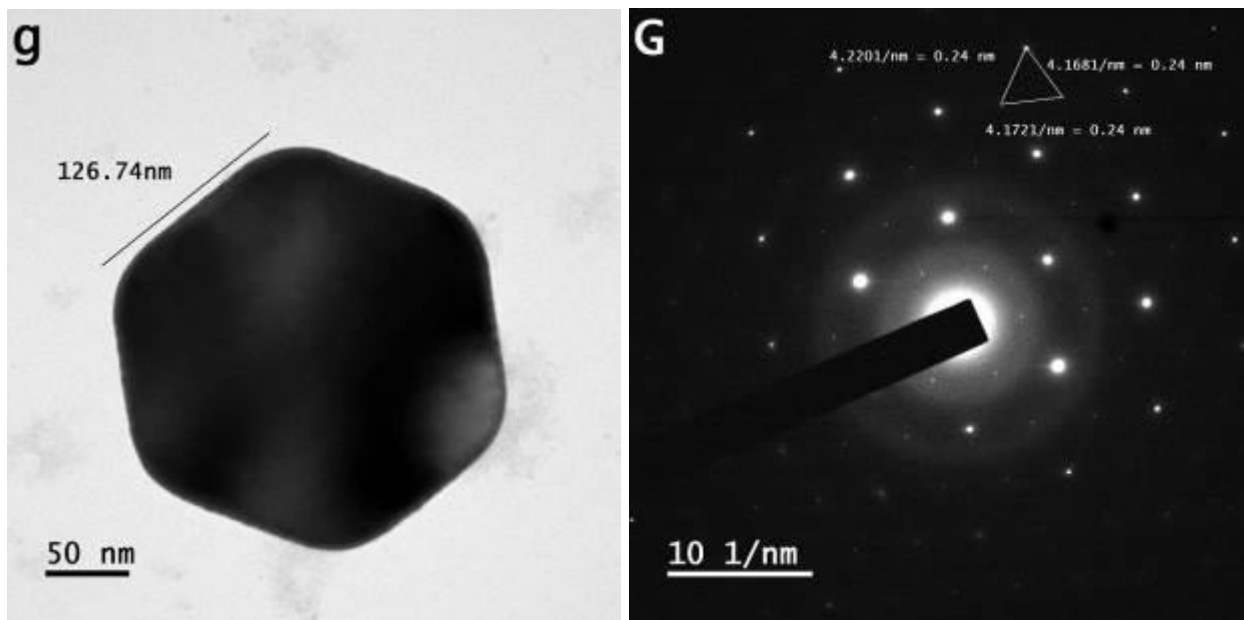
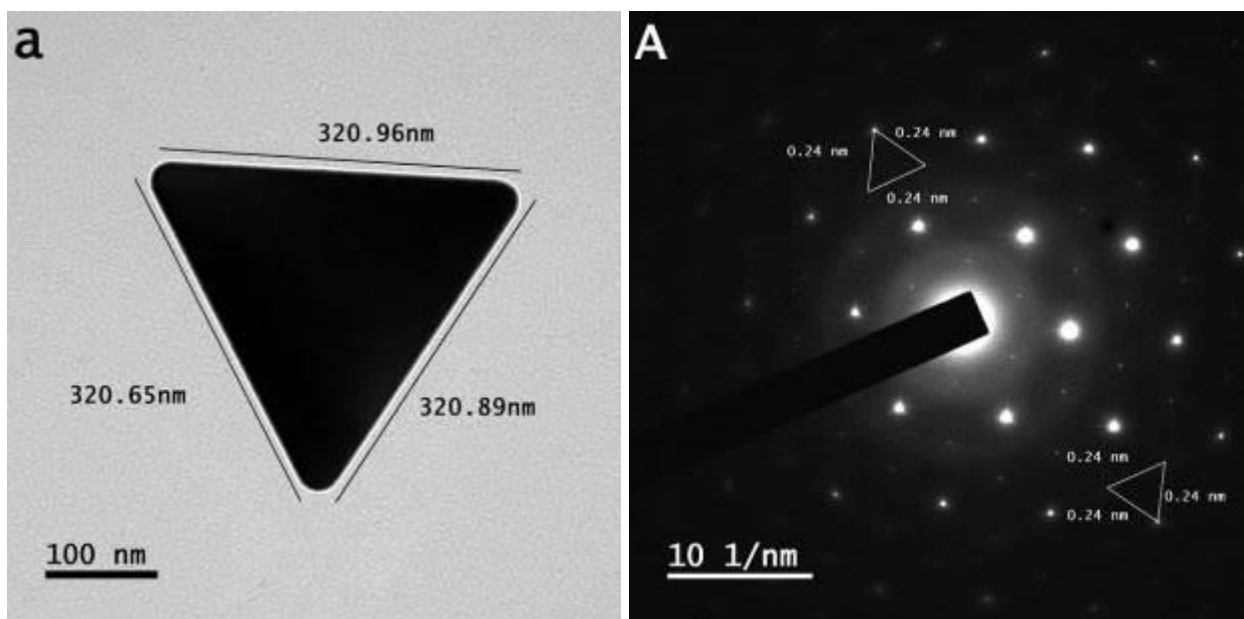
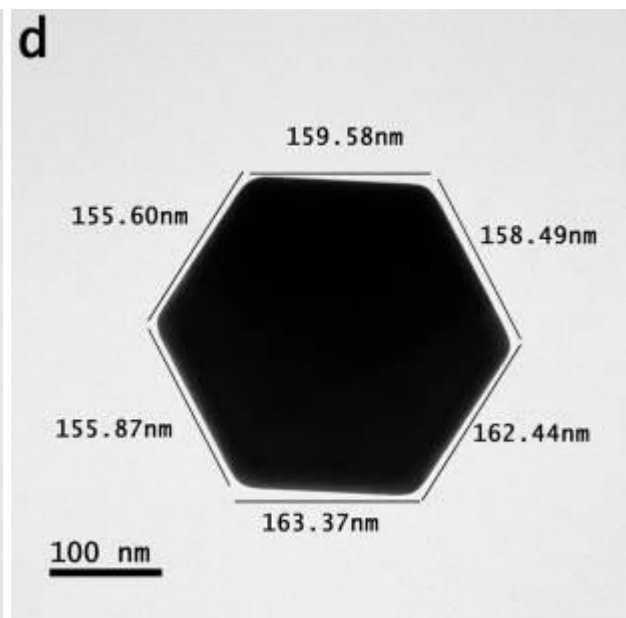
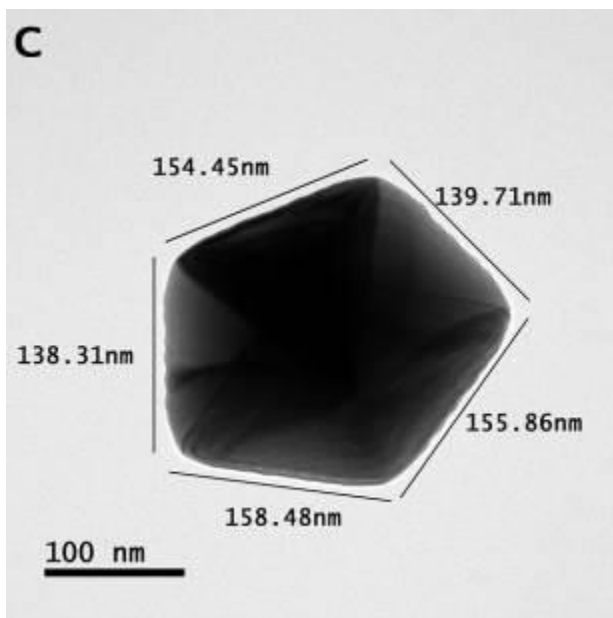
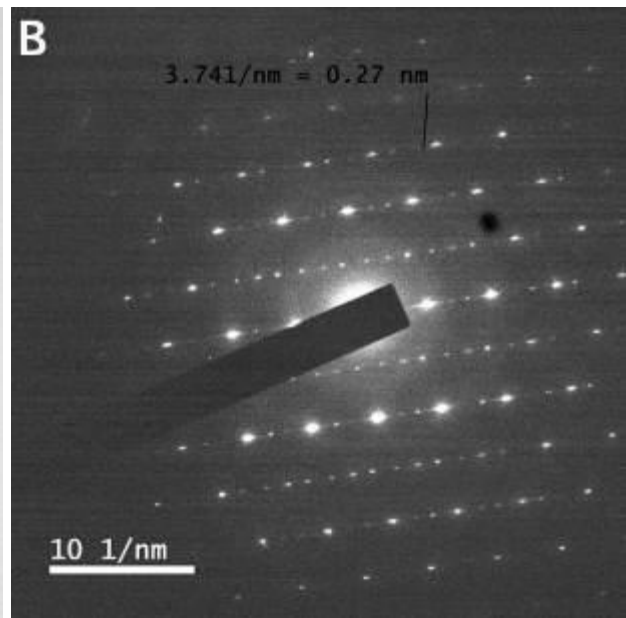
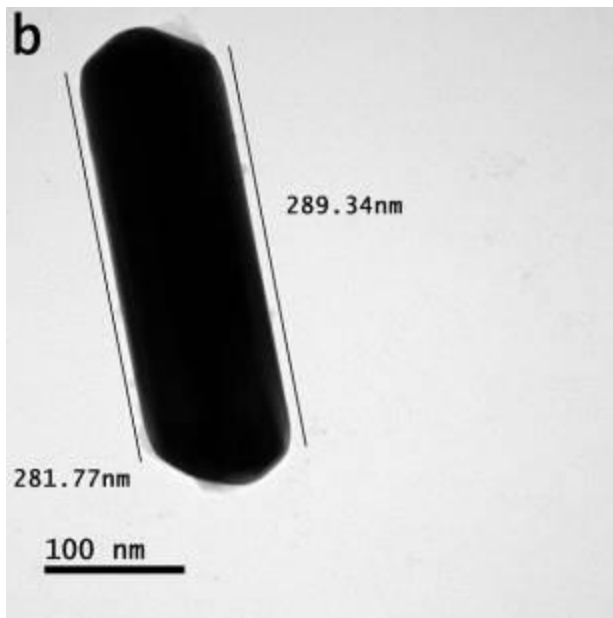
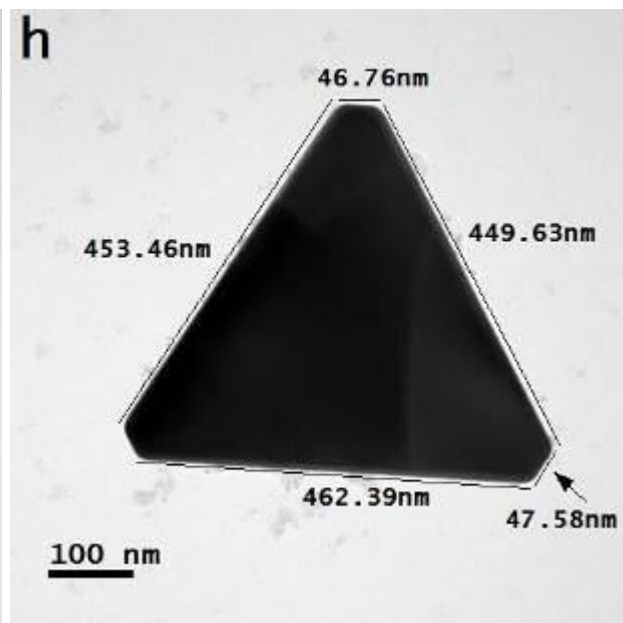
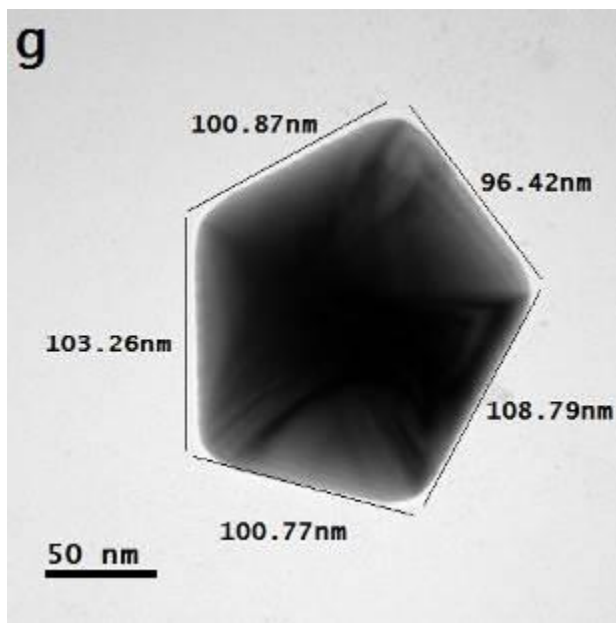
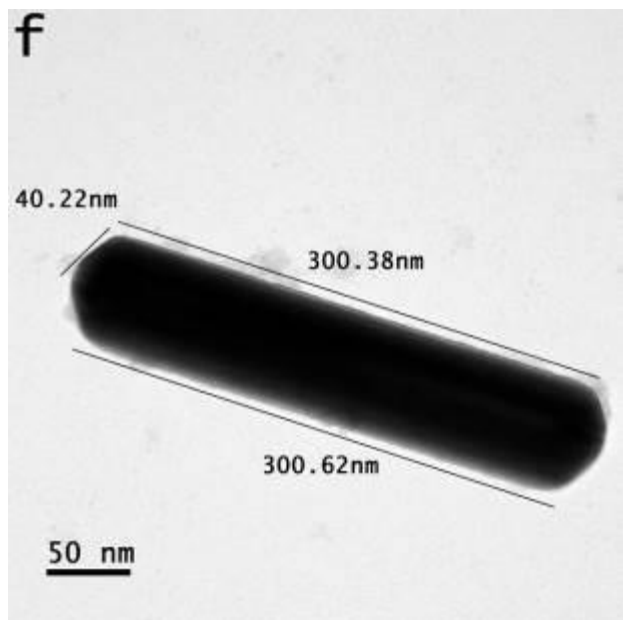
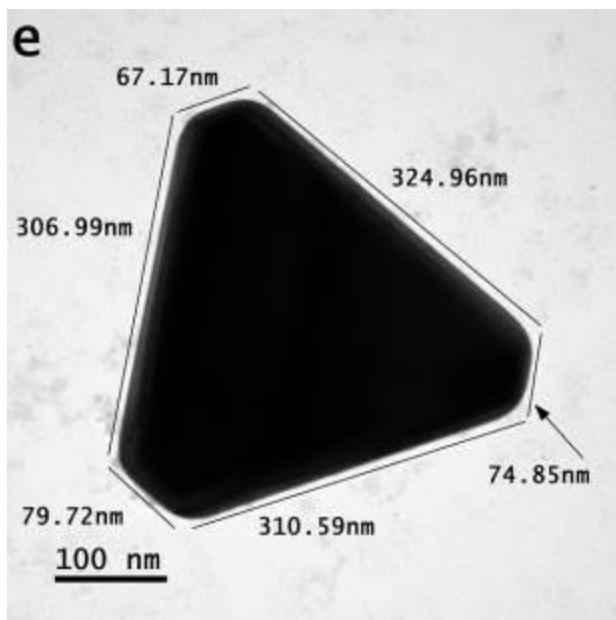
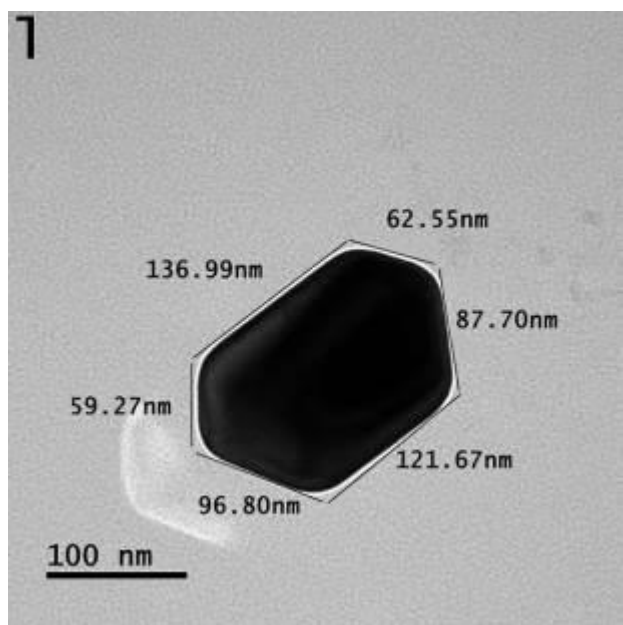
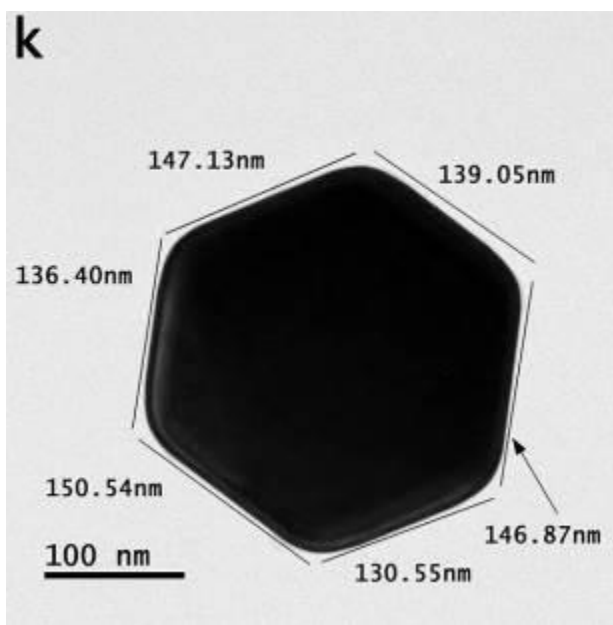
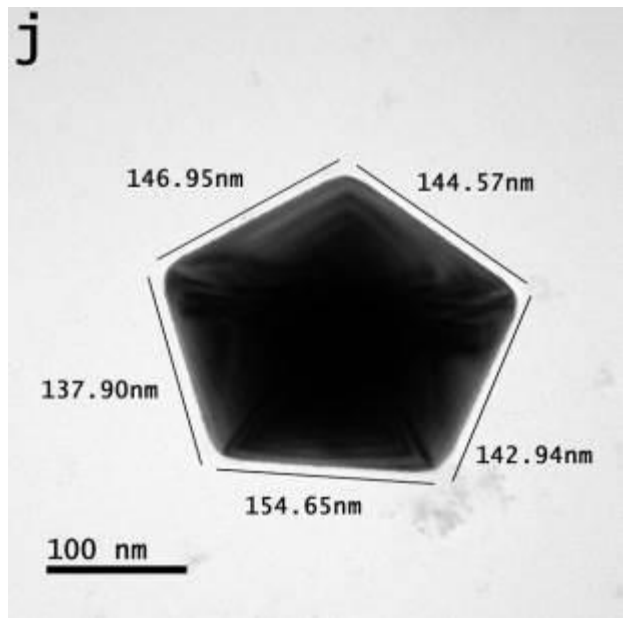
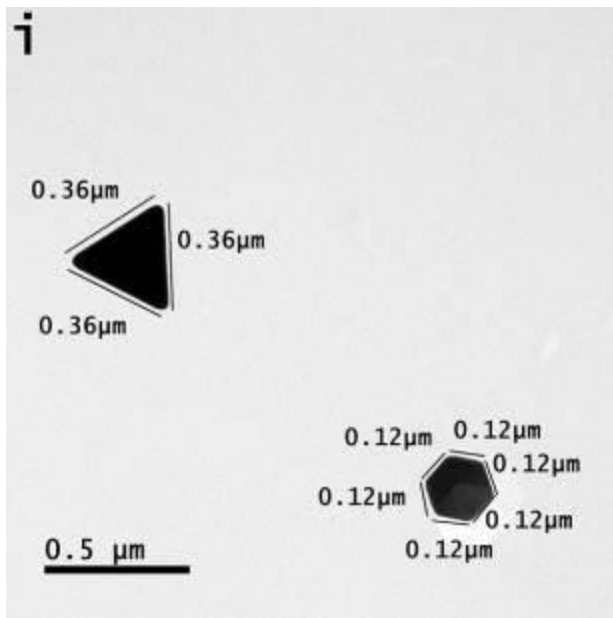


Figure S12: (a-g) bright field transmission microscope images of various nanoparticles and particles and (G) SAPR pattern of hexagonal-shaped particle; pulse ON time 15 μ sec pulse OFF time 5 μ sec and precursor concentration 0.40 mM.









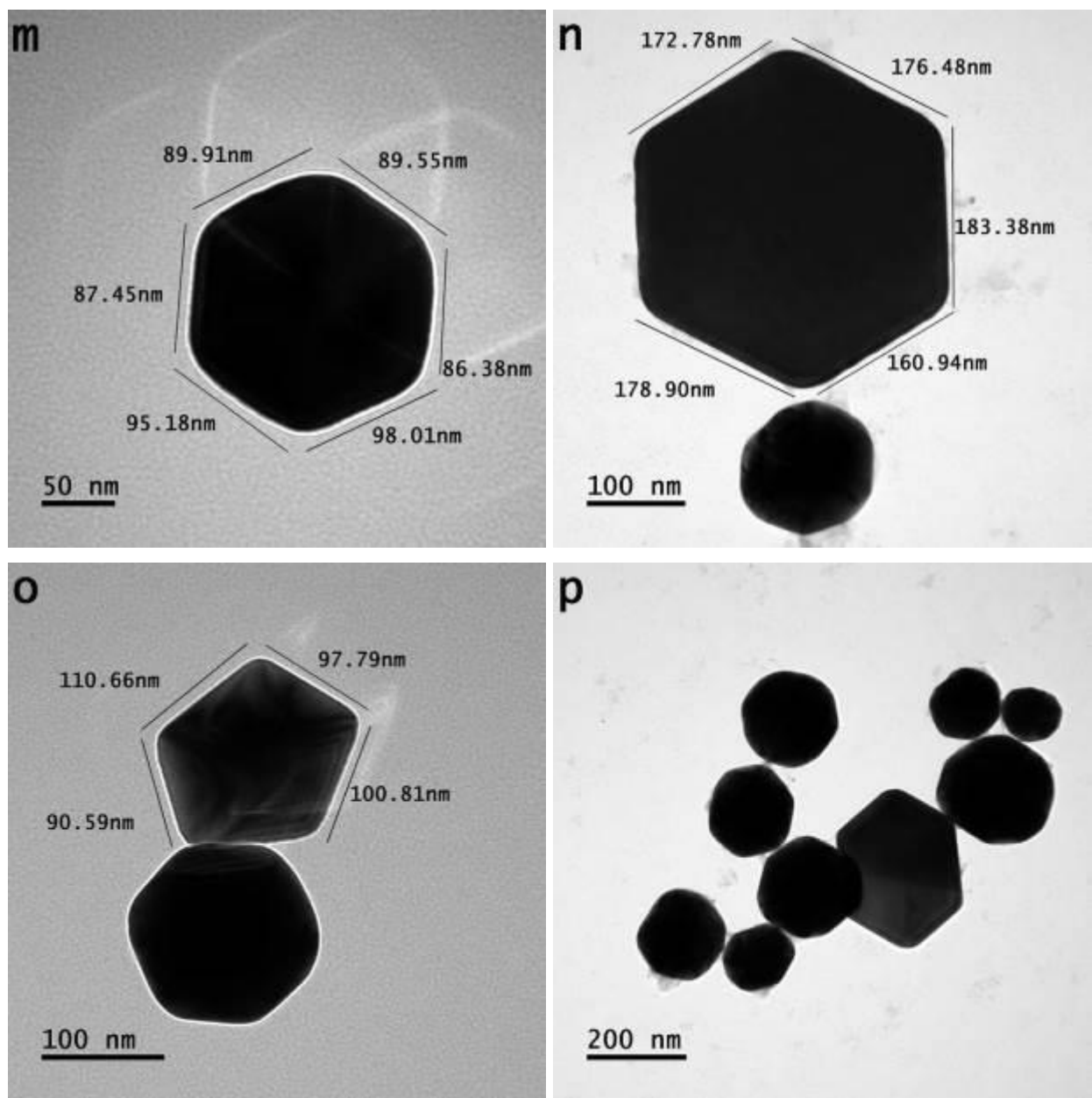


Figure S13: (a-p) bright field transmission microscope images of various particles/ (A & B) SAPR patterns of triangular-shaped and rod-shaped particles; pulse ON time 5 μ sec pulse OFF time 15 μ sec and precursor concentration 0.40 mM.

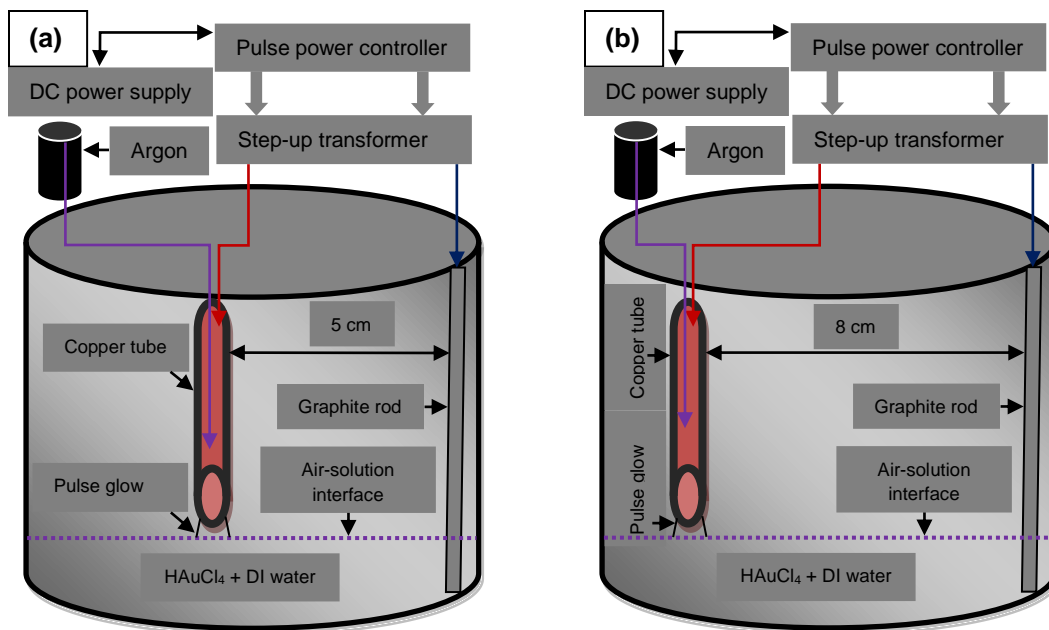
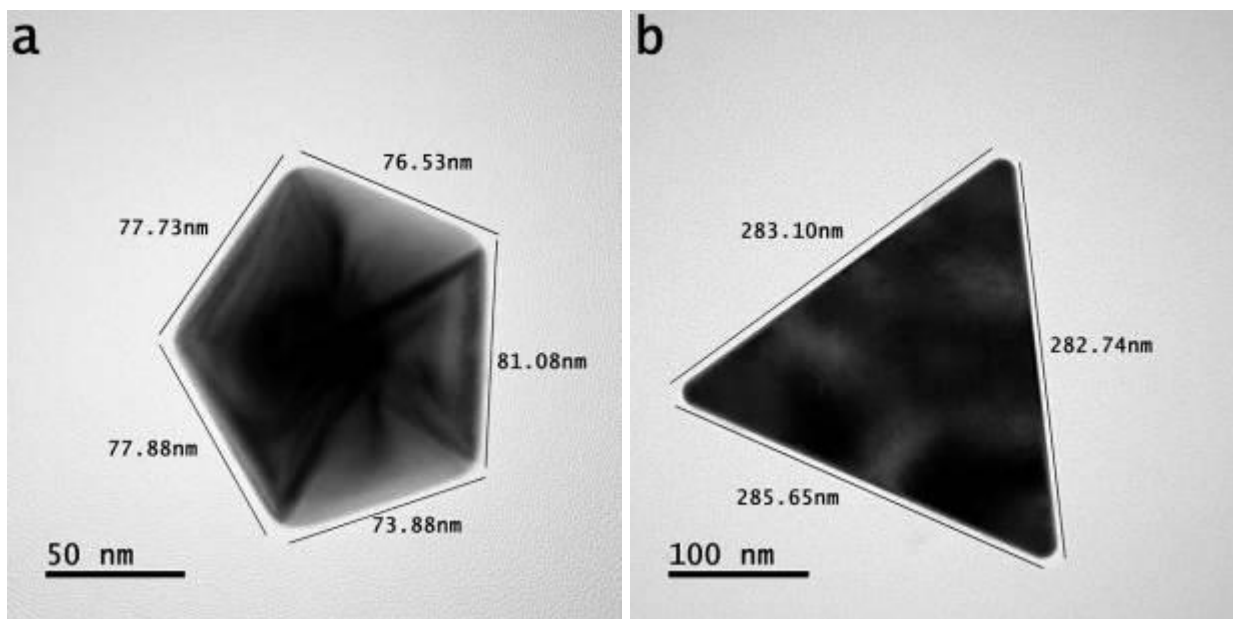
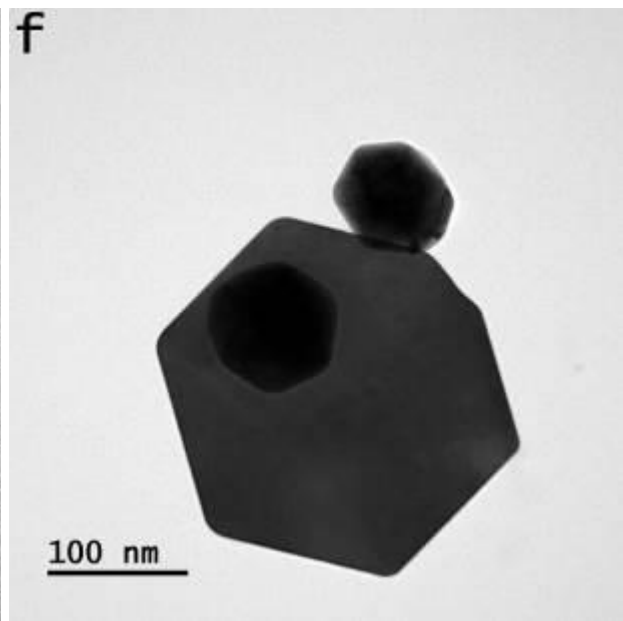
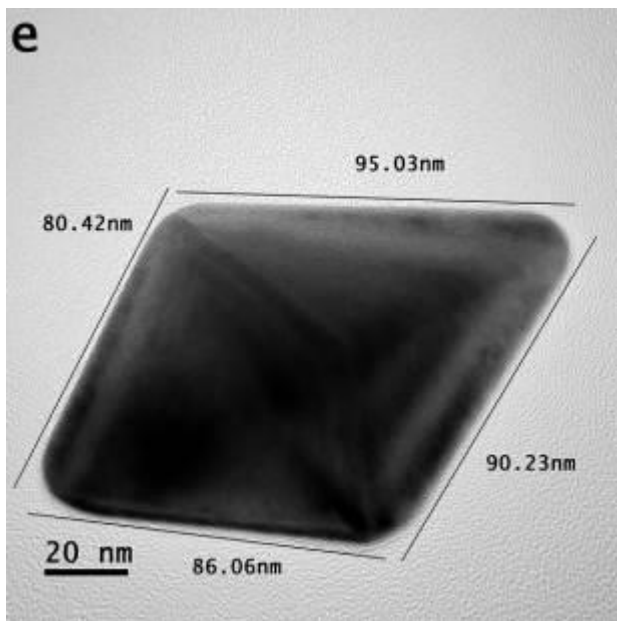
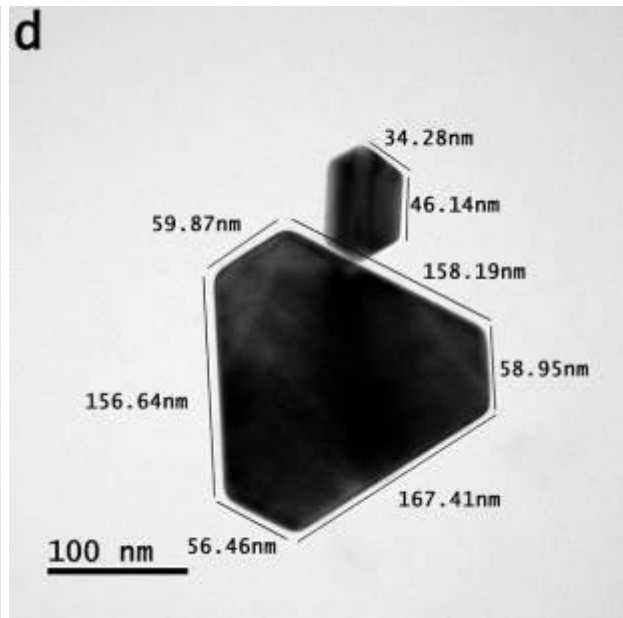
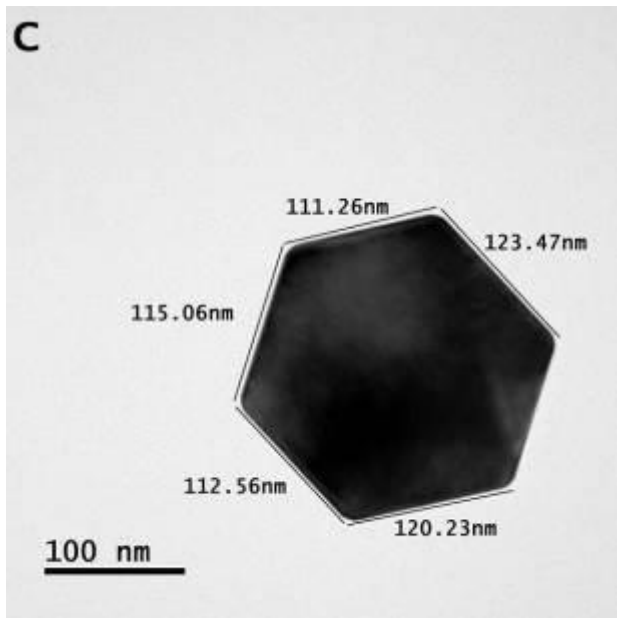


Figure S14: pulse-based electronphoton-solution interface setup (a) distance between graphite rod and copper tube: 5 cm and (b) distance between graphite rod and copper tube: 8 cm.





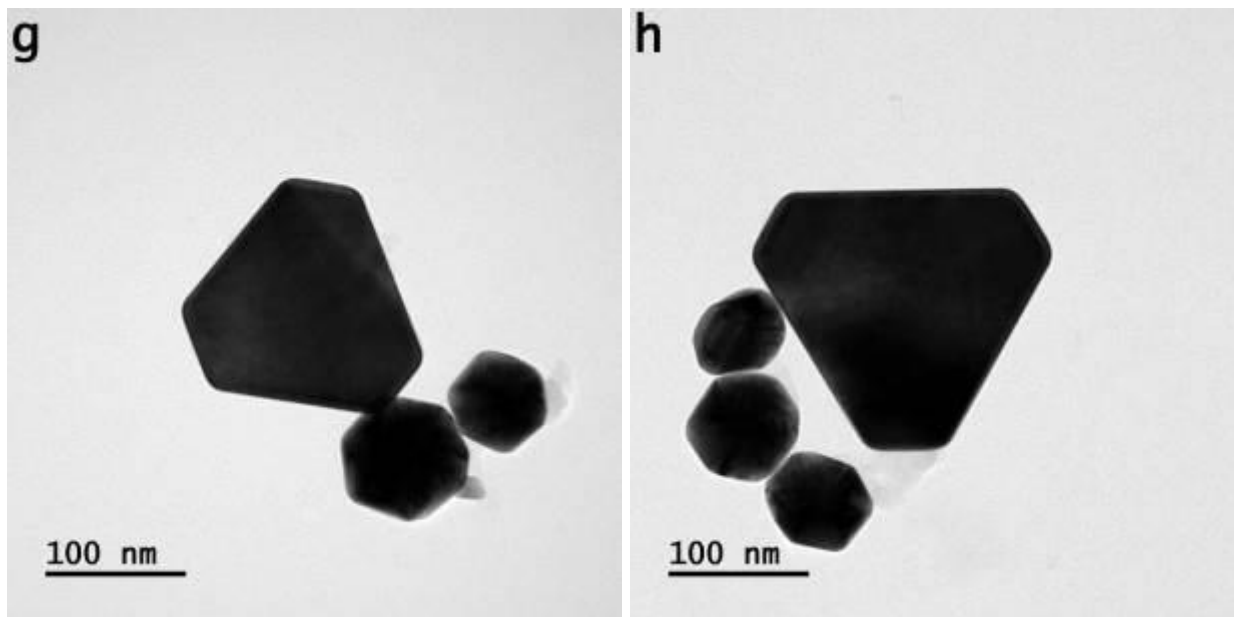
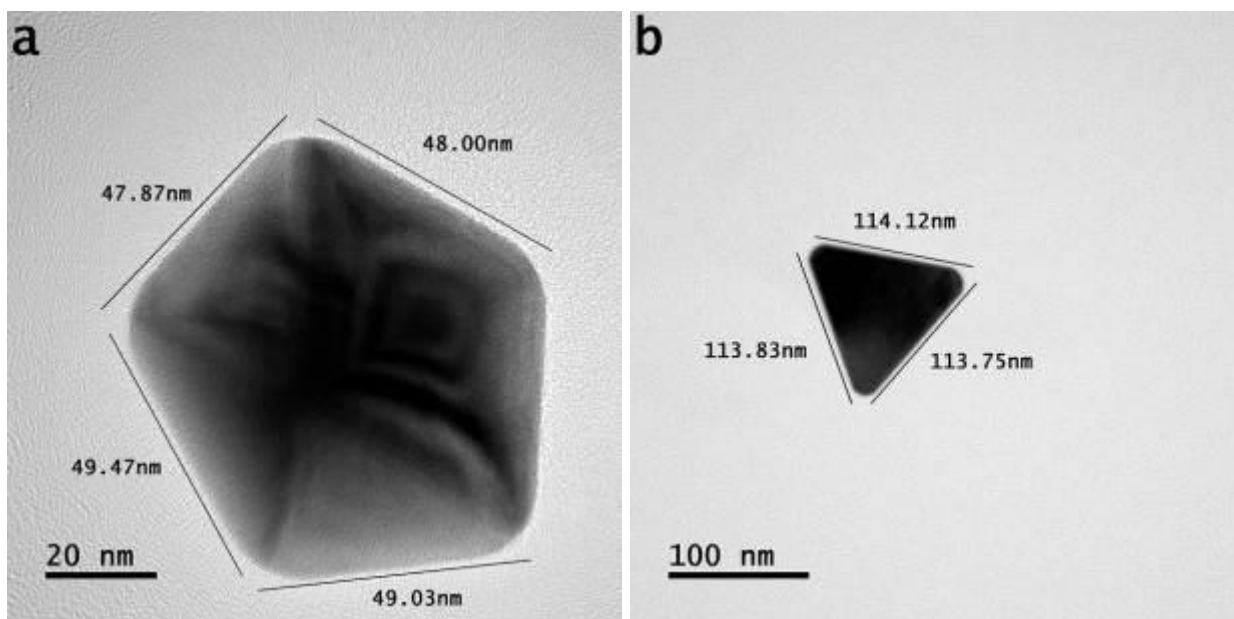
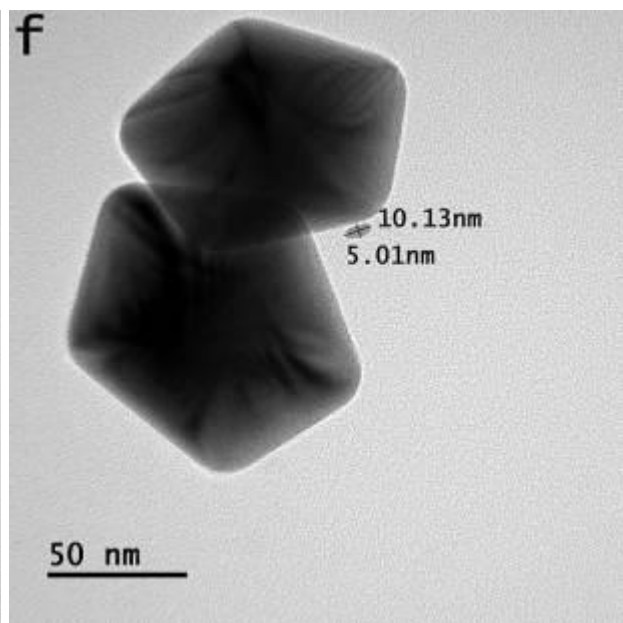
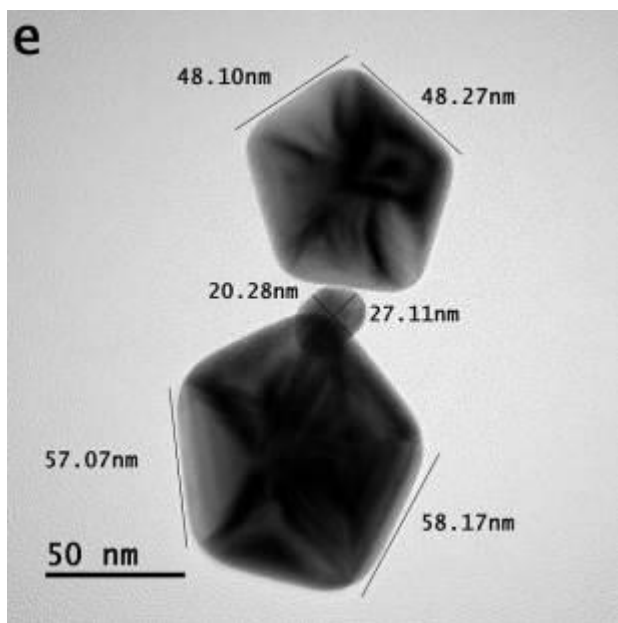
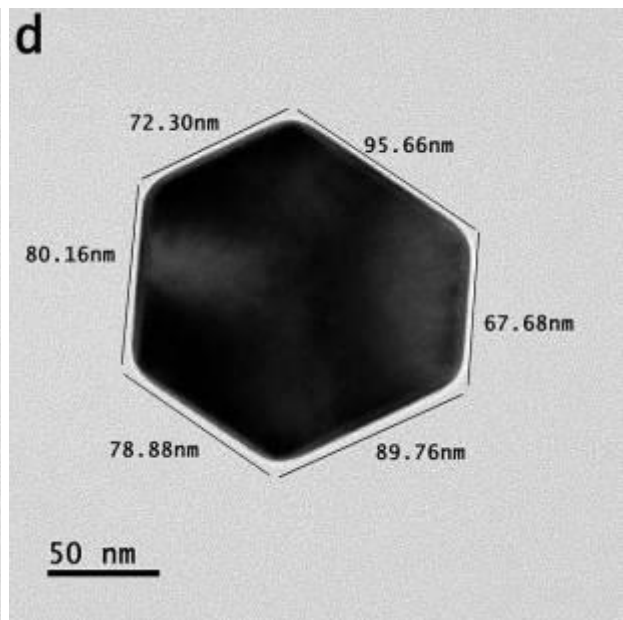
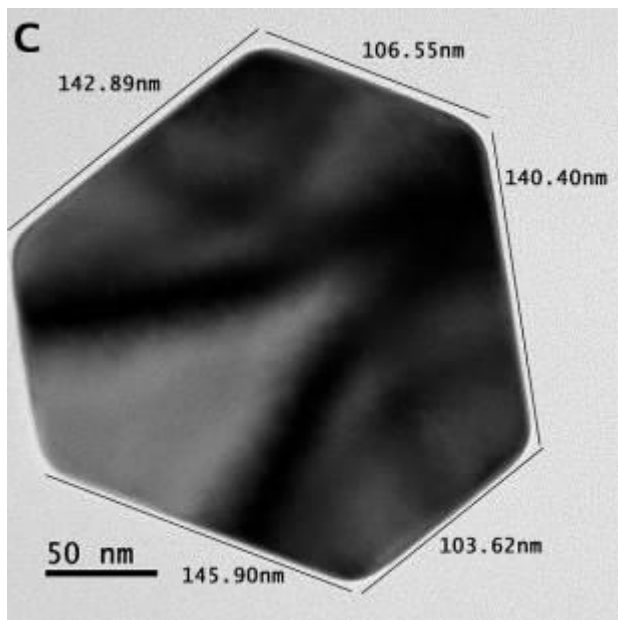


Figure S15: Bright field transmission microscope images of various nanoparticles and particles synthesized at precursor concentration 0.30 mM, process duration 15 minutes, pulse ON/OFF time 10 μ sec and negative pulse polarity.





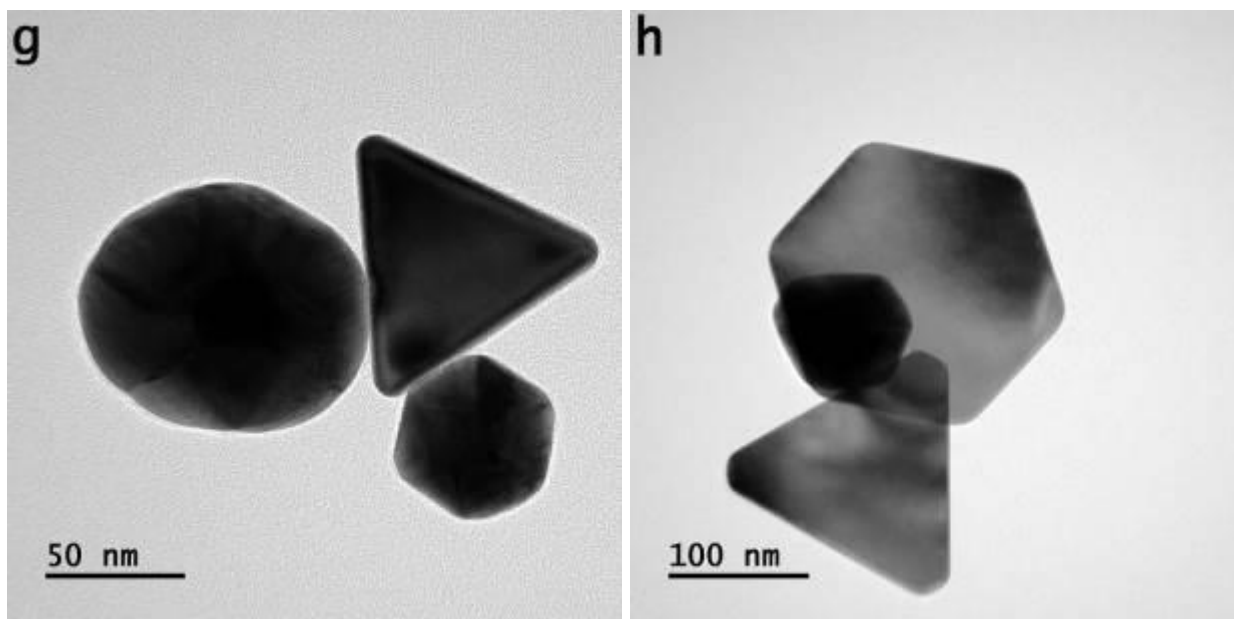
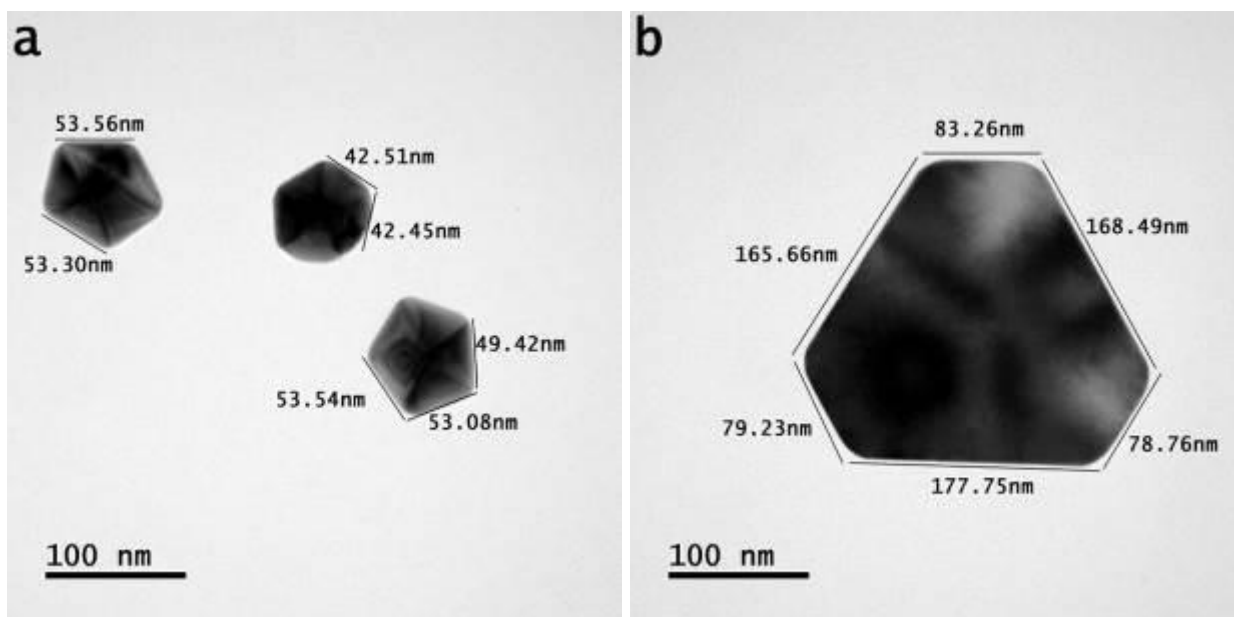
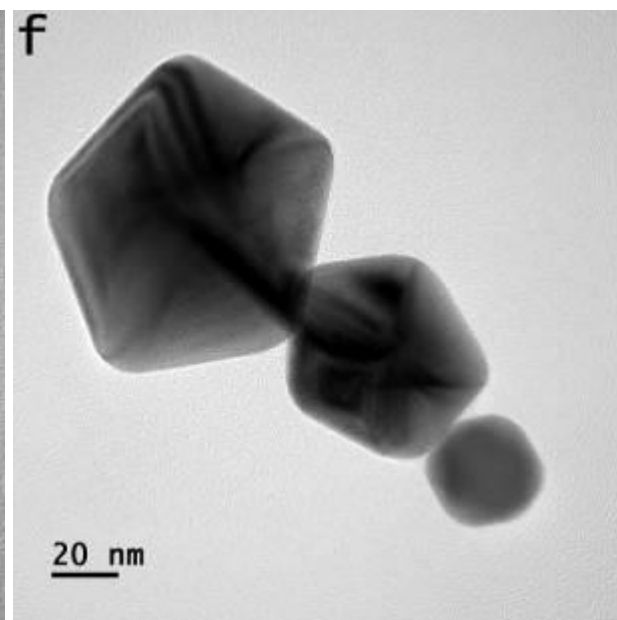
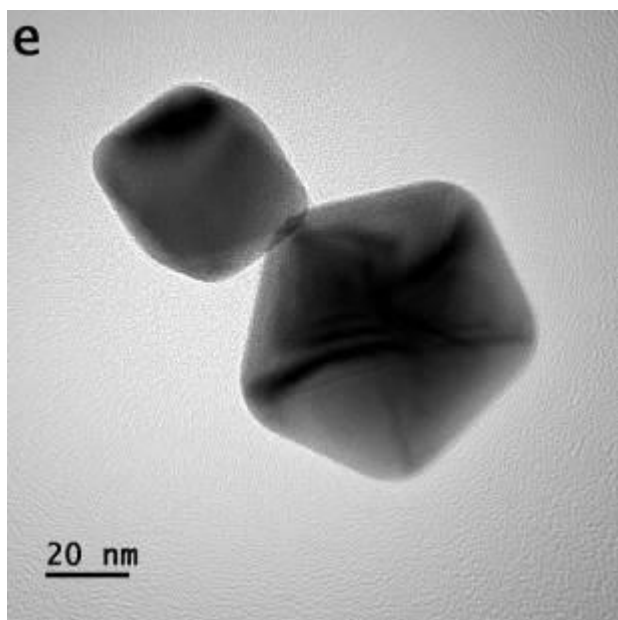
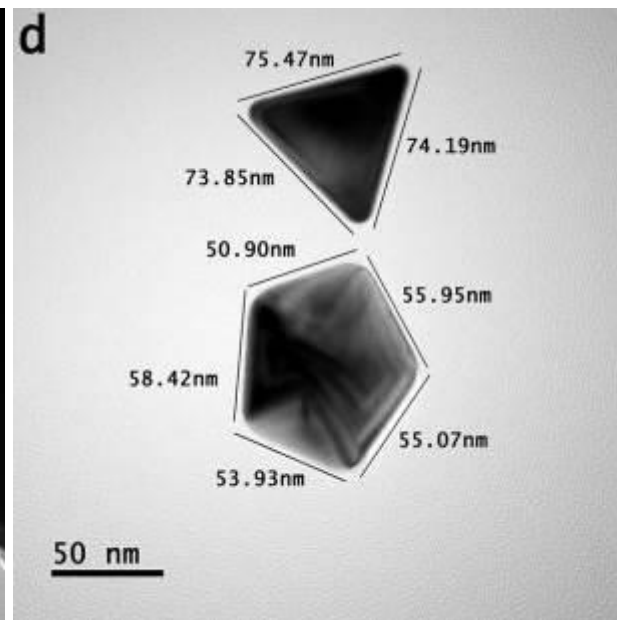
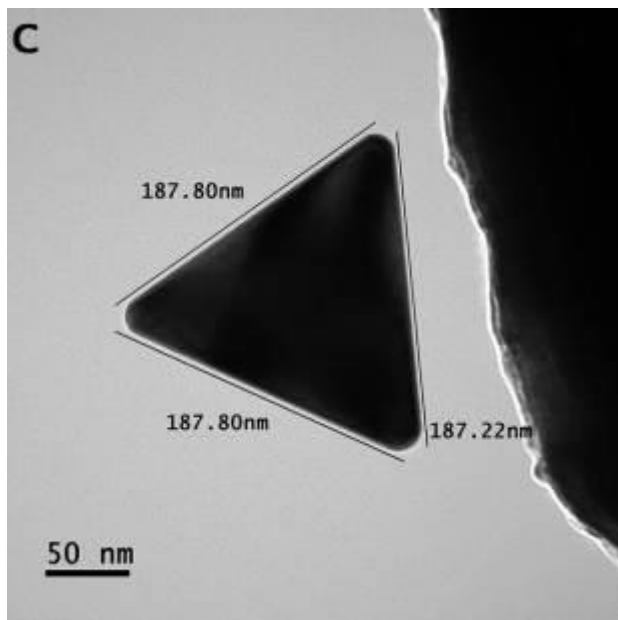


Figure S16: Bright field transmission microscope images of various nanoparticles and particles synthesized at precursor concentration 0.30 mM, process duration 15 minutes, pulse ON/OFF time 10 μ sec and positive pulse polarity.





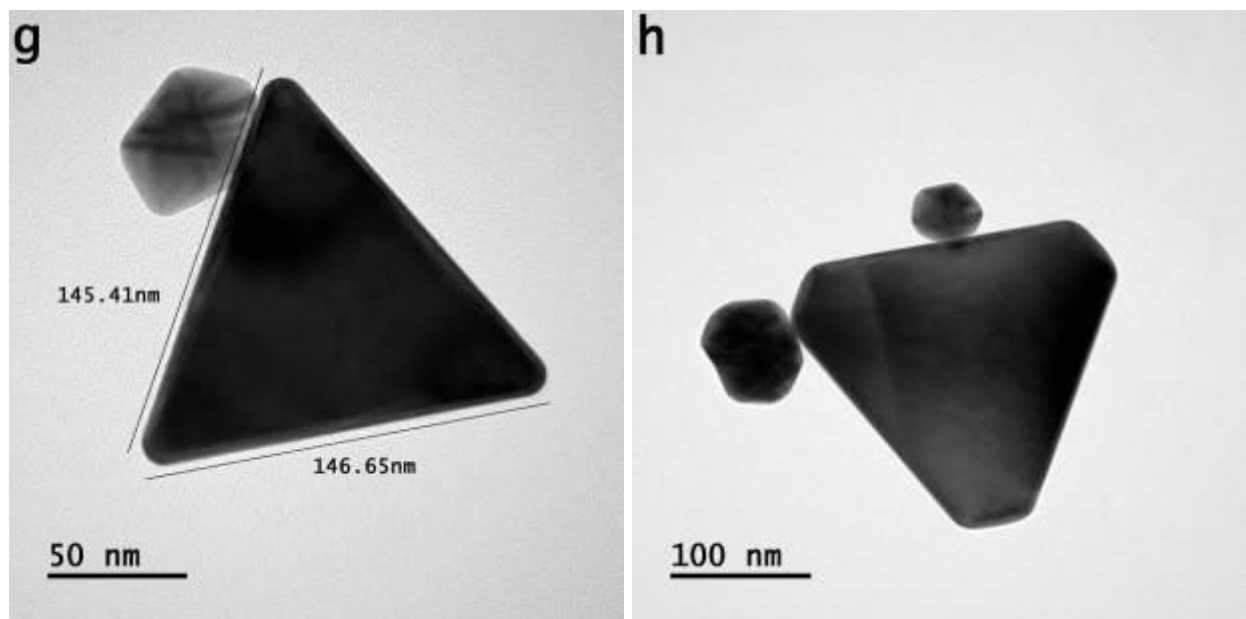


Figure S17: Bright field transmission microscope images of various nanoparticles and particles synthesized at precursor concentration 0.30 mM, process duration 15 minutes, pulse ON/OFF time: 10 μ sec and bipolar pulse polarity.

Table S1: Process parameters at different pulse ON/OFF time at 0.20 mM

Parameters	pulse ON/OFF time				
	$t_{on} = 5 \mu\text{sec}/ t_{off} = 30 \mu\text{sec}$	$t_{on} = 10 \mu\text{sec}/ t_{off} = 30 \mu\text{sec}$	$t_{on}/t_{off} = 15 \mu\text{sec}$	$t_{on} = 30 \mu\text{sec}/ t_{off} = 5 \mu\text{sec}$	$t_{on} = 30 \mu\text{sec}/ t_{off} = 15 \mu\text{sec}$
Pulse ON/OFF time					
Frequency (kHz)	28.57	25.00	33.33	28.57	22.22
Voltage (at start) measured in volts @ 40 times	80.0 volts	60.0 volts	44.0 volts	28.0 volts	38.0 volts
Voltage (at end) measured in volts @ 40 times	80.0 volts	51.0 volts	31.0 volts	21.0 volts	25.5 volts
Current (at start) measured in amps	1.00 amp	1.69 amp	1.70 amp	1.71 amp	1.70 amp
Current (at end) measured in amps	1.00 amp	1.70 amp	1.71 amp	1.72 amp	1.71 amp

Table S2: Process parameters at different pulse ON/OFF time at 0.40 mM

Parameters	pulse ON/OFF time				
	$t_{on}/t_{off} = 5 \mu\text{sec}$	$t_{on}/t_{off} = 15 \mu\text{sec}$	$t_{on}/t_{off} = 30 \mu\text{sec}$	$t_{on} = 15 \mu\text{sec}/ t_{off} = 5 \mu\text{sec}$	$t_{on} = 5 \mu\text{sec}/ t_{off} = 15 \mu\text{sec}$
Pulse ON/OFF time					
Frequency (kHz)	100.00	33.33	16.67	50 .00	50 .00
Voltage (at start) measured in volts @ 40 times	32.0 volts	32.0 volts	32.0 volts	28.5 volts	66.3 volts
Voltage (at end) measured in volts @ 40 times	31.8 volts	25.2 volts	23.2 volts	23.0 volts	66.3 volts
Current (at start) measured in amps	1.56 amp	1.58 amp	1.58 amp	1.58 amp	1.43 amp
Current (at end) measured in amps	1.56 amp	1.58 amp	1.58 amp	1.59 amp	1.38 amp